MODELLING OF THE MAGNETIC FIELD OF MAGNETOSPHERIC RING CURRENT AS A FUNCTION OF INTERPLANETARY MEDIUM PARAMETERS

Y. I. FELDSTEIN

Institute of Terrestrial Magnetism, Ionosphere and Radio Wave Propagation of the Academy of Sciences of the USSR, 142092, Troitsk, Moscow Region, U.S.S.R.

Abstract. The models are examined which are proposed elsewhere for describing the magnetic field dynamics in ring-current *DR* during magnetic storms on the basis of the magnetospheric energy balance equation. The equation parameters, the functions of injection F and decay τ, are assumed to depend on interplanetary medium parameters (F and τ during the storm main phase) and on ring-current intensity (τ during the recovery phase). The present-day models are shown to be able of describing the *DR* variations to within a good accuracy (the r.m.s. deviation $5 < \delta < 15$ nT, the correlation coefficient $0.85 < r < 1$). The models describe a fraction of the geomagnetic field variation during a magnetic storm controlled by the geoeffective characteristic of interplanetary medium and, therefore responds directly to the variation of the latter. The fraction forms the basis of the geomagnetic field variations in low and middle latitudes. The shorter-term variations of *DR* are affected by the injections into the inner magnetosphere during substorm intervals.

During magnetic storms, the auroral electrojets shift to subauroral latitudes. When determining the *AE* indices, the data from the auroral-zone stations must be supplemented with the data from subauroral observatories. Otherwise, erratic conclusions may be obtained concerning the character of the relationships of *DR* to *AE* or of *AE* to interplanetary medium parameters. Considering this circumstance, the auroral electrojet intensity during the main phase is closely related to the energy flux supplied to the ring current. It is this fact that gives rise simultaneously to the intensification of auroral electrojets and to the large-scale decrease of magnetic field in low latitudes.

The longitudinal asymmetry of magnetic field on the Earth's surface is closely associated with the geoeffective parameters of interplanetary medium, thereby making it possible to model-estimate the magnetic field variations during magnetic storms at given observatories. The inclusion of the field asymmetry due to the system of large-scale currents improves significantly the agreement between the predicted and model field variations at subauroral and midlatitude observatories. The first harmonic amplitude of field variation increases with decreasing latitude. This means that the long-period component of the D_{st}-variation asymmetry is due rather to the ring-current asymmetry, while the shorter-term fluctuations are produced by electrojets. The asymmetry correlates better with the *AL* indices (westward electrojet) than with the *AU* indices (eastward electrojet).

The total ion energy in the inner magnetosphere during the storm main phase is sufficient for the magnetic field observed on the Earth's surface to be generated. The energy flux to the ring current is $\sim 15\%$ of the ε-energy flux into the magnetosphere.

Table of Contents

1. Introduction
2. Basic relations
3. The ring-current decay parameter
4. The function F of injection into the ring current during magnetic storms
5. The results of modelling the hourly mean values of the storm-time ring current on the basis of present-day concepts
6. Magnetic activity dynamics during a magnetic storm
   6.1. Ring current and auroral electrojets
   6.2. Magnetic field of ring current at geomagnetic poles

Space Science Reviews **59:** 83–165, 1992.

6.3. Relationship of magnetospheric activity to the function of energy injection from solar wind
6.4. Polar electrojet during the magnetic storm
6.5. Penetration of the magnetospheric electric field into the equatorial ionosphere during the magnetic storm
6.6. The longitudinal asymmetry of magnetic field on the Earth's surface and its modelling
6.7. Ring current and the IMF B_y component
7. Ion energy in ring current relevant to ground-based magnetic disturbances
8. Conclusion

1. Introduction

The occurrence of electric currents on the magnetospheric surface (*DCF*) and in the region of the outer radiation belt (*DR*) is a consequence of the interaction of solar wind with the frozen-in magnetic field with the geomagnetic field. The *DCF* currents are generated when the solar wind compresses the magnetosphere and when the solar wind protons and electrons move in opposite directions on the magnetopause. The current system arising on the magnetopause enhances the geomagnetic field intensity inside the magnetosphere. The *DR* currents are due to a rapid increase in the number density of the energetic ions in the inner magnetosphere which form an ion belt and are in complicated oscillatory and rotational motions in the Earth's magnetic field. The resultant motions of charged particles are equivalent to a $\sim 10^6$ A intensity electric current shaped as a ring surrounding the Earth in which a fraction of the current in the near-Earth part flows eastwards, while its major fraction is westwards. The total effect of the ring current observed on the Earth's surface is that the horizontal component H of the Earth's magnetic field decreases, especially in low and middle latitudes. It is this decrease that is often used to identify the initial, main, and recovery phases of magnetic storms. During strong and persistent disturbances of the Earth's magnetic field, which are called magnetic storms, the *DR* current field intensity is much higher compared with the *DCF* fields, so the decrease in H is a characteristic feature of magnetic storms.

The results of some fine mass-spectrometry experiments on board GEOS-1 and 2, Prognoz 7 and 8, ISEE 1 and 2, and AMPTE–CCE were used to find the energetic-ion composition of the ring current which is present in the inner magnetosphere from $L \geq 2$ during magnetic storms. The ring-current belt consists of the ionospheric O^+, He^+, and H^+ ions and the solar wind ions penetrating into the magnetosphere. The energy densities of the particles and of the Earth's magnetic field prove to be comparable with each other in the ring current in some regions.

Chapman (1962) has traced the history of the evolution of our ideas about the storms on the Earth and paid main attention to the statistical laws governing the magnetic storm development and the equivalent current systems of the D_{st} and *DS* fractions of the magnetic storm field and discussed also the possible relationships of magnetic storms to polar magnetic substorms. Magnetic storm is one of the displays of magnetospheric storm, a complicated set of events embracing the entire magnetosphere of the Earth and reflected in the occurrence of, in practice, all geophysical events. The highest intensity of the disturbances is reached in high latitudes where they are observed to be magnetospheric substorms, in particular the polar magnetic disturbances.

Within the last quarter of century, mainly as a result of spacecraft studies of plasma and magnetic fields in the Earth's vicinities, the understanding of the reasons for ring-current generation in the Earth's inner magnetosphere has jumped high to its new stage. The model appeared which related quantitatively the *DR* variations and intensity to the interplanetary medium parameters, i.e., a decisive step was made on the way to diagnosing and predicting the given geophysical phenomenon. The modelling of this type has made it possible to infer helpful information about the electrodynamic processes in the Earth's magnetosphere, in particular about the magnetospheric energy balance, from the observed magnetic field variations.

The intensive studies of substorms which were assumed to elementary disturbance cells pushed studying the storms aside. The studies of substorms became numerous also because the researchers wished to rich a high resolution in time and space with a view to identifying the relationship of the field variations on the Earth to spacecraft measurement data. Another reason was that, according to Akasofu (1968), a magnetic storm is a superposition of strong substorms following each other rapidly, i.e., to present this schematically,

$$\text{a storm} = \text{compression of the magnetosphere} + \sum_i (\text{substorms})_i .$$

Kamide (1979a) made this relation more accurate by indicating that the contributions of weak and strong substorms to the storm magnetic field are of different values:

$$\text{a storm} = \text{compression of the magnetosphere} + \sum_i \alpha_i (\text{substorms})_i .$$

where α_i expresses the effectiveness of a particular substorm in generating the ring current. Kamide (1979b) says: "I believe that a geomagnetic storm *is* composed of successive substorms. This may be influenced too much by my experience in ground magnetic data. However, I even thought that is one of the definitions of storms!"

At the same time, the discussion at the AGU Chapman Conference on Magnetospheric storms and Related Plasma Processes (Los Alamos, October 9–13, 1978) has revealed another viewpoint concerning the relationship between substorms and storms. Said C. Russel: "A magnetic storm is *not* composed of successive substorms. A storm is something different. Substorms are only incidental, not fundamental, of the storm development. I defy you (i.e., Y. Kamide; my note) to predict the strength of ring current by the strength and duration of auroral electrojet activity. They are not correlated. Substorms occur during geomagnetic storms because the IMF is variable. However, if I were able to control the IMF, I am certain I could make a geomagnetic storm without a single substorm. During the same discussion, R. McPherron said: "I agree your (Y. Kamide's) statement that substorms and storms are mutually coupled, but I do not believe substorms cause the ring current. Enhanced convection is the cause of both. I also agree that you cannot have storms, large decrease in D_{st}, without substorms. However, there are time intervals of increase in the partial ring current prior to the first large substorm. Also, there are intervals after a large substorm expansion in which the ring current remains large or increases and there are no clearly defined expansion onsets

(convection bays). These facts suggest to me that storms are the results of enhanced convection rather than substorm expansion." This means that

$$\text{a storm} = \text{compression of the magnetosphere} + \text{convection} .$$

The decade which has elapsed since that conference should, in principle, have answered the question as to what is the real cause of a geomagnetic storm. The question must be answered by modelling the storm development, which is tantamount to modelling ring current, depending either on the solar wind electric field which gives rise to large-scale magnetospheric convection or on the intensity and duration of substorms each of which is an elementary storm.

A good agreement of the model calculation results with observation data will indicate that the model parameters of interplanetary medium or magnetospheric substorms define the occurrence of magnetic storms. The modelling will make it possible to find the determinant factors leading to generation and affecting the magnetic storm evolution.

2. Basic Relations

The ions moving in the Earth's magnetic field are main carriers of the ring-current energy. The ring-current plasma consists of the hydrogen, helium, oxygen, and nitrogen ions with energies from few keV to MeV (Roelof and Williams, 1988; Hamilton *et al.*, 1988). The general form of the energy balance equation is valid for the ring current (Akasofu and Chapman, 1972):

$$dE(t)/dt = U_{DR}(t) - E(t)/\tau , \tag{1}$$

where $E(t)$ is the total kinetic energy of ring-current particles; $U(t)$, erg s^{-1}, denotes the rate of energy supply to ring current; $E(t)/\tau$ is energy dissipation from ring current; τ represents the decay time which characterizes the rate of energy dissipation from ring current. The dissipation processes are due to (1) conversion of energetic ions into neutrals because of charge exchange with the geocoronal hydrogen (Tinsley, 1981), (2) direct particle precipitations to the atmosphere (Sharp *et al.*, 1976a, b), (3) convective motion (runaway) of ions on the day side as a result of intensity variations in the azimuthal electric field (Lyons and Williams, 1980), and (4) interactions of ions with ion-cyclotron waves (Cornwall *et al.*, 1970). If energy is not supplied to ring current, the energy accumulated in the latter relaxes with characteristic time τ:

$$E(t) = E_0 \, e^{-(t-t_0)/\tau} . \tag{2}$$

The total kinetic energy E of the ring-current particles defines unambiguously the DR magnetic field intensity by the relation

$$DR/B_0 = 2E/3E_M , \tag{3}$$

where $B_0 = 0.3$ G is the geomagnetic dipole field intensity at the Earth's equator; $E_M = 8 \times 10^{24}$ erg is the total magnetic energy of the geomagnetic dipole field outside

the Earth (Sckopke, 1966; Olbert *et al.*, 1968). This means that the ring current with particle energy 4×10^{20} erg produces an 1 nT (10^{-5} G) field on the Earth's surface.

Substituting E from (3) in (1), we get

$$dDR(t)/dt = F(t) - DR(t)/\tau , \tag{4}$$

where $F(t) = U_{DR}(t)/4 \times 10^{20}$ is the function of injection to ring current. In the further modelling, DR is expressed in nT, $dt = 1$ hour, $F(t)$ is in nT hr^{-1}, and τ is in hours in case of modelling hourly DR values. The modelling with a high time resolution necessitates introducing respective coefficients.

The DR values were calculated by the recurrent relation

$$DR_{i+1} = \frac{DR_i(2 - 1/\tau) + 2F_i}{2 + 1/\tau} . \tag{5}$$

The DR_{mod} intensity obtained by the expression (5) was compared with DR_{exp} characterizing the symmetric component of the ring-current field observed on the Earth's surface. The DR_{exp} value is usually inferred from the geomagnetic field D_{st} variation which is a sum of the current fields on the magnetopause (DCF) and DR:

$$D_{st} = DR_d + DCF_d - (DR + DCF)_q , \tag{6}$$

where the subscripts d and q relate to magnetically disturbed and magnetically quiet days, respectively. From (6) it follows that

$$DR = DR_d - DR_q = D_{st} - DCF_d + DCF_q . \tag{7}$$

Relation (7) permits DR_{exp} to be calculated from the known D_{st} variation which is inferred for each hour of UT from the observation data of the longitudinal chain of geomagnetic observatories. The given form of the relation for calculating DR_{exp} was proposed first by Feldstein *et al.* (1984) and was the used by Pudovkin *et al.* (1985a, b) and by Gonzalez *et al.* (1989a). Grafe (1988) has adopted a somewhat different expression to calculate DR. The DCF value during quiet and disturbed intervals is calculated using the empirical relations between solar wind pressure on the magnetosphere $p = nmv^2$ and the field DCF:

$$DCF = a\sqrt{p} = bv\sqrt{n} \times 10^{-1} , \tag{8}$$

where n is solar wind density; v is solar wind velocity; m is proton mass. The proportionality factor b in (8) varies from 0.2 to 0.3 nT $(\text{eV}^{-1}/\text{cm}^{-3})^{1/2}$, with v expressed in km s^{-1}, n in cm^3, and DCF in nT.

3. The Ring-Current Decay Parameter

The parameter τ is of importance to find with a view to both getting a deeper insight into the physics of the processes of particle loss from the ring current and estimating the rate and the integral value of energy input to ring current within a magnetic storm

interval:

$$U_{DR}(t) = 4 \times 10^{20} F(t) \text{ erg hr}^{-1}$$
$$\overline{U}_{DR} = \int_{t_1}^{t_2} U_{DR}(t)\, \mathrm{d}t = 4 \times 10^{20} \int_{t_1}^{t_2} (\mathrm{d}DR/\mathrm{d}t + DR/\tau)\, \mathrm{d}t \text{ erg}, \tag{9}$$

where the integration is from the storm onset (t_1) to end (t_2). As τ varies from 6.0 to 0.1 hr, the $\overline{U}_{DR}$ value may vary by more than an order (Akasofu and Yoshida, 1966). As noted elsewhere, it is not possible to make progress in understanding the relationship between the energy input rate–output rate of the magnetosphere unless the lifetime τ of ring-current particles can be estimated accurately (Akasofu, 1986). The value of τ depends essentially on the geocentric distance, ion composition, and ion energy of ring current (Smith *et al.*, 1981). Therefore, any quantitative study of the $\overline{U}_{DR}$ is practically useless unless the variation of τ is taken into account. In this connection, the dependences of the ring-current decay rate on magnetic storm intensity and phase, on solar cycle, and on other physical factors were studied by numerous researchers. The results obtained are summarized in Table I. At present the value of τ is often determined using the relation

$$DR = DR_0\, e^{-(t-t_0)/\tau}, \tag{10}$$

based on (4) on assumption that injection to ring current is absent and the ring current proper decays exponentially during the magnetic storm recovery phase. The values of τ may be inferred from (10) to be inverse to the factor of the linear term in the regression equation

$$\ln DR(t) = -\tau^{-1}(t - t_0) + \ln DR(t_0)$$

or they may be found by determining the value of $\tau = t - t_0$ at which

$$\ln \frac{DR(t_0)}{DR(t)} = 1\,.$$

The first attempt to infer the τ value from (10) were made using ground-based geomagnetic observation data disregarding the data on the interplanetary medium parameters which would made it possible to identify the time intervals without any additional injections during magnetic storm recovery phases and to exclude the *DCF* fraction from D_{st} variation. Akasofu *et al.* (1963) indicated that the ring-current decay rates were different during different intervals within the recovery phase of intensive magnetic storms, namely, the decay is sufficiently rapid in the initial stage ($\tau \sim 6$ hours) and proceeds more slowly in the final stage ($\tau \sim 30$–60 hours). The variations of τ inferred from the geomagnetic field D_{st} variation were treated to result from the presence of two ring currents, $DR1$ and $DR2$, one of which is more intensive, is located at smaller geocentric distances, and decays more rapidly than the more distant current.

Grafe and Best (1966) obtained a gradual increase of τ as the ring current decays,

TABLE I

Injection functions F in nT hr^{-1} and decay parameters of ring current τ in hours

No.	Author	Injection function	$\tau_{m.p.}$	$\tau_{r.p.}$	References
1	2	3	4	5	6
1	Akasofu *et al.*			$\tau = 6^h$ $\tau = 30$–60^h	*J. Geophys. Res.* **68**, 3345, 1963
2	Grafe and Best			$23 > \tau_{max} > 5^h$ $-100 > D_{st} > -650$ nT	*Pure Applied Geophys.* **64**, 59, 1966
3	Davis and Parthasarathy			$\tau = 10^h$ intensive storm τ = several days for weak storms	*J. Geophys. Res.* **72**, 5825, 1967
4	Kamide and Fukushima	$F \sim AE$	$\tau = 4^h$	$\tau = 40^h$ $\tau = 10^h$	*Rep. Ionosph. Space Res. Japan* **25**, 125, 1971
5	Shevnin			$4.5 > \tau > 1.5^h$ $-400 < D_{st}^{max} < -100$ nT	*Geomagnetizm i Aeronomiya* **13**, 122, 1973 **13**, 330, 1973
6	Siscoe and Crooker	$F \sim B_s v$			*Geophys. Res. Letters* **1**, 17, 1974
7	Kamide			$\tau = 1^h$ $\tau = \infty$	*J. Geophys. Res.* **79**, 49, 1974
8	Burton *et al.*	$F = \begin{cases} d(E_y - A) \text{ at } E_y > A; \\ 0 \quad \text{at } E_y < 0; \end{cases}$ $d = -1.5 \times 10^{-3}$ nT (s mV m^{-1})$^{-1}$ $= -5.4$ nT (hr mV m^{-1})$^{-1}$ $E_y = -VB_z \times 10^{-3}$ mV m^{-1}; $A = 0.5$ mV m^{-1}	$\tau = 7.7^h$		*J. Geophys. Res.* **80**, 4204, 1975
9	Bobrov	$F \sim (B_z - \sigma)v$			*Astron. Mag.* **54**, 1335, 1977
10	Perreault and Akasofu	$F \sim \varepsilon$	$\tau = 8^h$		*Geophys. J. R. Astron. Soc.* **54**, 547, 1978

Table I (continued)

No.	Author	Injection function	$\tau_{m.p.}$	$\tau_{r.p.}$	References
1	2	3	4	5	6
11	Bobrov	$F = \begin{cases} dvB_z \times 10^{-3} \text{ at } B_z + \sigma < 0,\ B_z < 0 \\ dv(B_z - \sigma)/2 \text{ at } B_z < 0,\ B_z + \sigma > 0 \\ dv(B_z - \sigma)/2 \text{ at } B_z > 0,\ B_z - \sigma < 0 \\ 0 \text{ at } B_z - \sigma > 0,\ B_z > 0 \end{cases}$ $d = 5.4$ nT (hr mV m^{-1})$^{-1}$	$10 < \tau < 15^h$		*Geomagnetizm i Aeronomiya* **81**, 1048, 1981
12	Akasofu	$F = -0.7\varepsilon = -0.945 \times 10^{17}$ nT hr^{-1} at ε in erg s^{-1}	$\tau = 20^h$ for $\varepsilon < 10^{18}$ erg s^{-1} $\tau = 2^h$ for $10^{18} \le \varepsilon < 10^{19}$ erg s^{-1} $\tau = 1^h$ for $\varepsilon \ge 10^{19}$ erg s^{-1}		*Planetary Space Sci.* **29**, 1151, 1981a
13	Akasofu		$\tau = 20^h$ for $\varepsilon < 10^{18}$ erg s^{-1} $\tau = 6^h$ for $10^{18} \le \varepsilon < 5 \times 10^{18}$ erg s^{-1} $\tau = 3^h$ for $5 \times 10^{18} \le \varepsilon < 10^{19}$ erg s^{-1} $\tau = 1^h$ for $10^{19} \le \varepsilon < 5 \times 10^{19}$ erg s^{-1} $\tau = 0.3^h$ for $5 \times 10^{19} \le \varepsilon < 10^{20}$ erg s^{-1} $\tau = 0.2^h$ for $\varepsilon \ge 10^{20}$ erg s^{-1} $\varepsilon = 2 \times 10^{14} B^2 v \sin^4 \theta/2$ erg s^{-1}		*Space Sci. Rev.* **28**, 121, 1981b
14	Murayama	$F_1 \approx B_s V$; $F_2 \approx B_s V^2$; $F_3 \sim \varepsilon$; $F_4 \sim B_s V (mnV^2)^{1/3}$	$\tau = 8^h$ or	$\tau = 12^h$	*Rev. Geophys. Space Phys.* **20**, 623, 1982
15	Tinsley and Akasofu		$\tau = 3^h$ or	$\tau = 25^h$	*Planetary Space Sci.* **30**, 733, 1982
16	Sizova and Shevnin			$20^h > \tau > 8^h$ $-300 < D_{st}^{max} < -100$ nT	*Geomagnetizm i Aeronomiya* **19**, 703, 1979
17	Feldstein *et al.*	$F = \begin{cases} d(E_y - A) \text{ at } E_y > A \\ 0 \text{ at } E_y < A \end{cases}$ at $d = -1.2 \times 10^{-3}$ nT (s mV m^{-1})$^{-1}$ $= -4.32$ nT (hr mV m^{-1})$^{-1}$ $E_y = -vB_z \times 10^{-3}$ mV m^{-1}; $A = -0.9$ mV m^{-1}	$\tau = 8.2^h$ at $\tau = 5.8^h$ at	$D_{st} > -55$ nT $D_{st} < -55$ nT	*Planetary Space Sci.* **32**, 975, 1984

Table I (continued)

No.	Author	Injection function	$\tau_{m.p.}$	$\tau_{r.p.}$	References
1	2	3	4	5	6
18	Sizova and Zaitseva	$F = \begin{cases} 4B_z V \times 10^{-3}\ \text{nT hr}^{-1} & \text{at } E_y < 0 \\ 0 & \text{at } E_y \geq 0 \end{cases}$	$\tau = 6^h$	$\tau = 3.6 + 0.09\,\lvert DR\rvert_{max}$ hour	*Geomagnetic Variations and Solar Wind*, p. 108, 1984
19	Pudovkin *et al.*	$F = -3.5 + 4.3V(0.5\sigma - B_z) \times 10^{-3}\ \text{nT hr}^{-1}$	$\tau = 4 \pm 2^h$	$17 > \tau > 7^h$ $-180 < DR_{max} < -30$ nT	*Planetary Space Sci.* **33**, 1097, 1985a
20	Pudovkin *et al.*	$F = \begin{cases} -3.5 + 4.3V(0.5\sigma - B_z) \times 10^{-3}\ \text{nT hr}^{-1} & \text{at } V(0.5\sigma - B_z) \geq 1.5 \times 10^3 \\ 3\ \text{nT hr}^{-1} & \text{at } 0 \leq V(0.5\sigma - B_z) < 1.5 \times 10^3 \\ 0 & \text{at } V(0.5\sigma - B_z) < 0 \end{cases}$	$\tau = 5 - e^{-\Delta t/8}$	$\tau = 6.6 + 0.07\,\lvert D_{max}\rvert$ hour	*Geomagnetizm i Aeronomiya* **25**, 812, 1985b
21	Murayama	$F \sim B_s^{1.09} V^{2.06} n^{0.38}$		$\frac{2}{5}(1.5e^{-t/\tau_1} + e^{-t/\tau_2}$ $\tau_1 = 2^h$ $\tau_2 = 21^h$	*Solar Wind-Magnet Coupling*, p. 119, 1986a
22	Pisarsky *et al.*	$d(E_y - A)$ at $E_y > A$ $0.5d(E_y - A)$ at $V < 300$ km s^{-1} 0 at $E_y \leq A$ $d = -6$ nT (hr mV m^{-1})$^{-1}$; $E_y = -B_z v \times 10^{-3}$ mV m^{-1} $A = -0.9$ mV m^{-1} $F = F(E_y) + \phi(v)$	storms with $\lvert DR\rvert_{max} < 180$ nT $8.2 > \tau > 4.5^h$ $-30 > DR \geq -180$ nT storms with $\lvert DR\rvert_{max} > 180$ nT $9 > \tau > 5.5^h$ $-30 > DR > -180$ nT	$\tau = 9^h$	*Geomagnetizm i Aeronomiya* **26**, 454, 1986a; **26**, 461, 1986b
23	Murayama	$F_1 \sim B_s^{1.09} v^{2.06} n^{0.38}$; $F_2 \sim B_s v^2 n^{0.4}$ $F_3 \sim B_s v n^{0.25}$ $F_4 \sim \varepsilon n^{0.05}$	$\tau = 1^h$	$\frac{2}{5}(1.5e^{-t/2} + e^{-t/21})$ $\frac{1}{3}(2e^{-t/2} + e^{-t/24})$ $\frac{1}{3}(2e^{-t/3} + e^{-t/24})$	Private communication, 1986b
24	Akasofu		$\tau = 20^h$ for $\varepsilon < 10^{18}$ erg s^{-1} $\tau = 2^h$ for $10^{18} \leq \varepsilon < 5 \times 10^{18}$ erg s^{-1} $\tau = 1^h$ for $5 \times 10^{18} \leq \varepsilon < 10^{19}$ erg s^{-1} $\tau = 0.5^h$ for $10^{19} \leq \varepsilon < 5 \times 10^{19}$ erg s^{-1} $\tau = 0.25^h$ for $\varepsilon \geq 5 \times 10^{19}$ erg s^{-1}		R. D. Zwickl *et al.*, *Magnetotail Physics*, p. 155, 1987

Table I (continued)

No.	Author	Injection function	$\tau_{m.p.}$	$\tau_{r.p.}$	References
1	2	3	4	5	6
25	Vasiliunas		$\tau = 20^h$ for $U_T < 10^{18}$ erg s^{-1} $\tau = 2^h$ for $10^{18} \le U_T < 3 \times 10^{18}$ erg s^{-1} $\tau = 1^h$ for $3 \times 10^{18} \le U_T < 10^{19}$ erg s^{-1} $\tau = 0.5^h$ for $10^{19} \le U_T < 3 \times 10^{19}$ erg s^{-1} $\tau = 0.25^h$ for $U_T \ge 3 \times 10^{19}$ erg s^{-1} $U_T = U_{DR} + U_j + U_A$		*Geophys. Res. Letters* **14**, 1183, 1987
26	Grafe	$F = -4.32(-B_z V \times 10^{-3} + 0.9)\, nT\, hr^{-1}$	$5 \le \tau \le 40^h$ $100 > \tau > 12^h$ $-50 < F < -5$ nT hr^{-1} $-90 > DR > -280$ nT		*Planetary Space Sci.* **36**, 765, 1988
27	Pudovkin *et al.*	$F = \begin{cases} -3.5 + 4.3v(0.5\sigma - B_z) \times 10^{-3}\ \text{nT hr}^{-1} \\ \text{at } V(0.5\sigma - B_z) \ge 1.5 \times 10^3 \\ 3\ \text{nT hr}^{-1} \text{ at } 0 \le V(0.5\sigma - B_z) < 1.5 \times 10^3 \\ 0 \quad \text{at } v(0.5\sigma - B_z) < 0 \end{cases}$	$\tau = 3.0 + 9.8e^{-F/4.5}$	$\tau = 6.6 + 0.07\,\lvert DR\rvert_{\max}$	*Gerlands Beitr. Geophys.* **97**, 523, 1988
28	Pisarsky *et al.*	$8.2 \times 10^{-3} v(B_z - 0.67\sigma) -$ $- 14.1 \times 10^{-3}(V - 300) +$ $+ 9.4$ nT hr^{-1} at $v(B_z - 0.67\sigma) < -1146$ (the injection interval) $-14.1 \times 10^{-3}(V - 300)$ nT hr^{-1} at $v(B_z - 0.67\sigma) > -1146$ (the decay interval)	weak and moderate storms ($DR_{max} > -160$ nT) $\tau = 1.6 + 13e^{0.08F}$ hr $\tau = 5.4 + 10e^{0.025DR}$ hr intensive storms ($DR_{max} < -160$ nT) $\tau = 2.4 + 13e^{0.07F}$ hr $\tau = 10.0 + 1.84e^{0.007DR}$ hr		*Stadia Geophys. Geod.* **33**, 61, 1989
29	Gonzalez *et al.*	$(mnv^2)^{-1/3} v B_T B_M K(S, \theta)$ ε, $(mnv^2)^{1/2} v B_z$, $(mnv^2)^{1/6} v B \sin^4(\theta/2)$	$\tau = 4^h$ for $D_{st} \ge -50$ nT $\tau = 0.5^h$ for $-50 > D_{st} \ge -120$ nT $\tau = 0.25^h$ for $D_{st} < -120$ nT		*J. Geophys. Res.* **94**, 8835, 1989

namely, $\tau = 23$ hours during the maximum D_{st} decrease in the storm main phase ($D_{st}^{\max} \sim -100$ nT) and $\tau = 5$ hours at $D_{st}^{\max} \sim -650$ nT. Kamide and Fukushima (1971) assumed both a rapid decay during the storm main phase ($\tau = 4$ hours) and a slow decay during the recovery phase ($\tau = 40$ hours), and $\tau = 10$ hours throughout the storm. However, most of the researchers assumed a constant τ-value from the onset to end of a storm (Kamide, 1974; Burton *et al.*, 1975; Perreault and Akasofu, 1978; Bobrov, 1981; Murayama, 1982).

Other types of the dependence of τ on $D_{st}^{\max}$ were presented elsewhere. For example, Shevnin (1979a, b) obtained an increase of τ from 1.5 to 4.5 hours as $D_{st}^{\max}$ varies from -100 nT to -400 nT, rather than a decrease of τ with increasing $|D_{st}|$, during the storm recovery phase. In case of weak and moderate magnetic storms, the values of τ proposed by Shevnin (1973a, b) is an order as low as those obtained by Grafe and Best (1966). In the later studies the values were corrected and raised to $\tau = 8$ hours for weak storms and $\tau \sim 13$ hours (Sizova and Shevnin, 1979) or $\tau \sim 20$ hours (Sizova and Shevnin, 1983) for strong storms.

The concept (Kamide and Fukushima, 1971) that the τ values are different during the main and recovery phases of a magnetic storm was extended by Akasofu (1981a, b), Tinsley and Akasofu (1982), and Pudovkin *et al.* (1985a). During the main phase, $\tau = 3$–4 hours or decreases with increasing ε, i.e., the energy flux inflowing to the magnetosphere.

During the recovery phase, $\tau \sim 20$–25 hours or increases with $|DR_{\max}|$. Somewhat different relations are used by Sizova and Zaitseva (1984) and by Pudovkin *et al.* (1985b) to describe the increase. At the same time, other researchers (Grafe, 1988; Pisarsky *et al.*, 1986a, 1989) obtained, on the contrary, that τ decreased with increasing *DR* and that the absolute values of τ were very different. The Akasofu concept concerning the dependence of τ on ε was developed also by Vasyliunas (1987) who related τ to the total energy dissipation inside the magnetosphere during magnetic storms, namely, τ decreases from 20 hours to 0.25 hour with increasing U_T.

A surprising discrepancy in the absolute τ values and even in the character of τ variations with *DR* intensity during storm recovery phase follows from comparing among the data presented elsewhere. Pisarsky *et al.* (1986a) discussed the following possible reasons for the discrepancy.

(1) The value of τ must be determined using the *DR* magnetic field values free of the *DCF* impurity. The example of the February 7–10, 1967 storm was used (Pisarsky *et al.*, 1986a) to demonstrate this statement. The value of τ for the storm was estimated by Tinsley and Akasofu (1982) from D_{st} variation to be 25.4 hours. The exclusion of the *DCF* field leads to $\tau = 44 \pm 2$ hours. At low D_{st} values the exclusion of *DCF* in finding *DR* leads to a pronounced increase of the τ values calculated by (10).

(2) The value of τ during recovery phase must be determined by (10) after selecting the time intervals when injection to ring current is absent. Otherwise, the τ values prove to be overestimated. The criteria IMF $B_z > 0$ nT and $AE < 100$ nT, or $\varepsilon \leq 10^{18}$ erg s^{-1}, for the mean-hourly *DR* values do not exclude short-term injections to ring current. Besides, a permanent injection to ring current may exist which maintains the *DR* value

at a certain level during the final stage of recovery phase and is controlled by solar wind velocity (Pisarsky *et al.*, 1989). Disregard of the additional injection leads to overestimated values of τ. The expression (4) may be used to obtain the approximate relation

$$T^{-1} = \tau^{-1} - F/(DR)\,,$$

where T is the value of the decay parameter inferred from (7); τ is the true value of the decay parameter; F is the injection function. A 2 nT hr^{-1} intensity injection raises the value of τ from 10 to 17 hours at $DR = -50$ nT, and from 10 to 12.5 hours at $DR = -100$ nT. Thus, the presence of injection during recovery phase leads to a seeming increase of τ, while a plateau in $DR(t)$ leads to $\tau \to \infty$. This effect demonstrates the variations in Figure 1 during the recovery phase of the March 24, 1969 strong

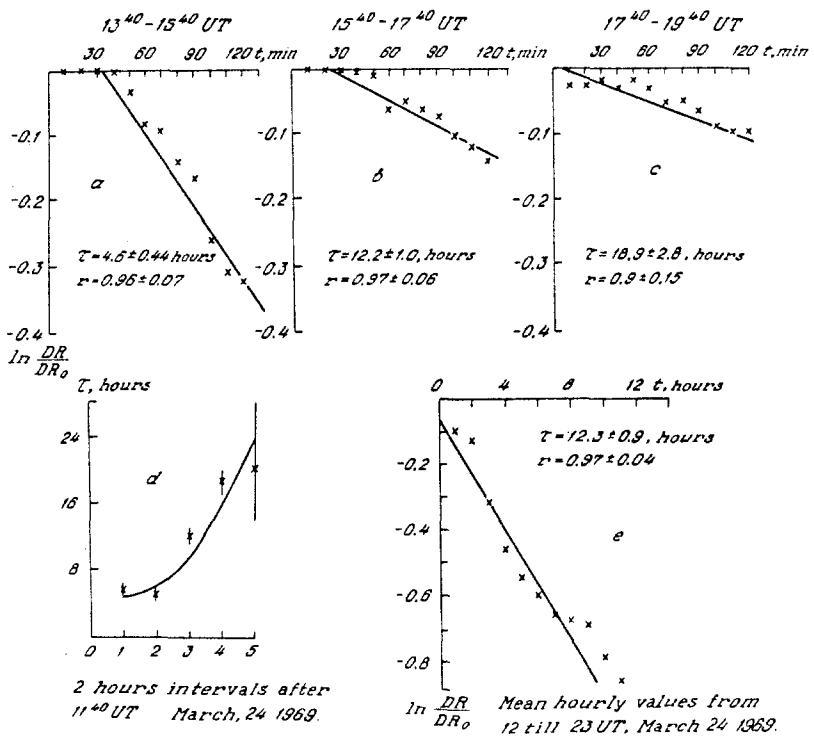

Fig. 1. The $\tau_{r.p.}$ values during the recovery phase of the March 24, 1969 strong magnetic storm in individual 2-hour intervals according to 10-min magnetic field values (a, b, c), for five consecutive 2-hour intervals from 11:40 to 21:40 UT (d), and according to the mean-hourly values from 12:00 to 23:00 UT (e).

magnetic storm from 11:40 UT to 21:40 UT when the IMF B_z component was $B_z \gg 0$. The DR values were calculated with a 10-min step using the data from a longitudinal chain of 11 low-latitude observatories; the value of τ was determined for successive 2-hour intervals, and proved to increase from 5.4 hours to ~ 20 hours as the ring current decayed. The value of τ inferred from the mean-hourly DR values for the

12:00–23:00 UT interval is 12.3 hours at the correlation coefficient $r = 0.97$ between the values of $\ln DR/DR_0$ and t. The fact that 12 values of DR from each of the 2-hour intervals were used makes it possible to regard the τ values obtained as sufficiently reliable. The resultant increase of τ in the course of ring-current decay may appear because the injection was disregarded (Feldstein *et al.*, 1984), as well as due to the motion of the energetic ion region location in the magnetosphere and to the variations of the ring-current ion composition (Hamilton *et al.*, 1988). A rapid increase of up to 100 hours as the ring-current decays was noted by Grafe (1988), which is qualitatively at variance with the data (Pudovkin *et al.*, 1985a, b, 1988). Grafe assumes that decay is sometimes not influenced by injection during recovery phase. The ring-current magnetic field on the Earth's surface during recovery phase is not influenced by injection. The injection, if any, fails to reach the ring-current region.

(3) Apart from the above-mentioned difficulties with finding τ from ground-based magnetic field variation data during storm recovery phases, great errors in the values of τ arise also when using mean-hourly values because of a small volume of input sampling in a particular disturbance. As a rule, the intervals for finding τ on the basis of hourly data are selected not to exceed 7 hours. Therefore, the factors in (10) for finding τ vary within very broad ranges. Figure 2 presents the values of τ for 13 time intervals with IMF $B_z > 0$ used by Pudovkin *et al.* (1985a). Despite scanty dots and their large spread, a trend may be traced in τ to increase with $|DR_{\max}|$. The numerals in Figure 2 indicate the number of hours used to calculate the values of τ in four intervals of January 20, 1968; January 15, 1972; February 22, 1973; and January 11, 1976. The vertical lines are the boundaries of a 95% confidence interval (the Student criterion). The τ variation ranges were $2.8 < \tau < \infty$, $6.1 < \tau < 18.8$, $6.7 < \tau < 16.8$, and $16.1 < \tau < 20.4$ hours, respectively. Considering the given variation ranges, the statement that τ increases with $|DR_{\max}|$ seems to be little convincing.

Thus, the determination of τ from ground-based geomagnetic observation data according to (10) fails to yield any sufficiently accurate values even if the data on the interplanetary medium parameters are used. The values obtained in each particular case depend strongly on the length of an interval selected, on the technique for excluding injection in the ring current and the DCF effects, and on the adopted measurement level for DR variations. When modelling the ring-current dynamics depending on interplanetary medium parameters, therefore, Pisarsky *et al.* (1986a) determined the values of τ by the method of minimizing the functional of discrepancy between the model-calculated and observed values of DR. The quadratic discrepancy of the observed and calculated DR values for 57 magnetic storm intervals inferred from the experimental mean-hourly values of solar wind parameters and of D_{st} index was used to be the effectiveness criterion. The effectiveness index was calculated as a function of the parameters of Equation (1) and 8 values of τ for different ranges of DR variations. In such a way, the optimization problem was solved in which the coordinates of the discrepancy functional minimum correspond to the parameters of the most effective model. The calculations were made by the method of stochastic optimization with adaptation (Vasiliev, 1980) in a region where all parameters are not limited and in a

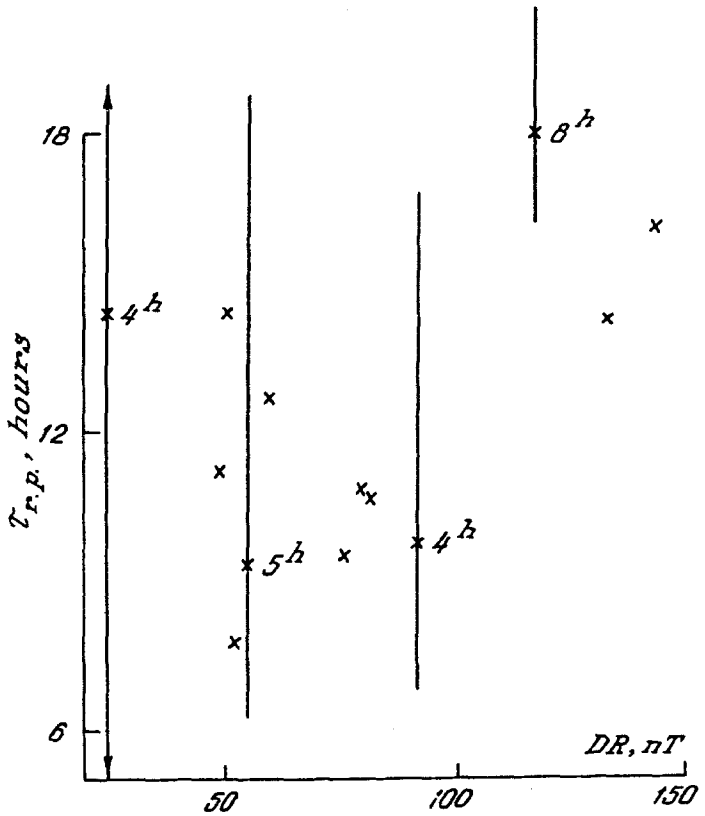

Fig. 2. The $\tau_{r.p.}$ values during the recovery phases of 13 magnetic storms in the $B_z > 0$ intervals indicated by Pudovkin *et al.* (1965a). The numerals for four storms indicate the number of hours used when calculating the τ-values. The vertical lines are the boundaries of the 95% confidence interval (the Student criterion).

region where some limitations are imposed on the parameters differing from τ. The dependence $\tau(DR)$ may take any form which can be described by piecewise-continuous function. The optimal models were selected among $\sim 25\,000$ different models. In all the optimal models, the dependence $\tau(DR)$ decreases monotonely, namely, the maximum τ values vary from 8 to 9 hours at $DR > -30$ nT, while the minimum τ values vary from 4.5 to 5.5 hours at $DR < -180$ nT.

The value of τ proved to be much higher during recovery phases of strong magnetic storms, i.e., the ring current decays more slowly compared with weak and moderate storms, thereby indicating that the ring current ion composition changes. Probably, the ratio of the ions numbers supplied to the magnetosphere from the solar wind and from the ionosphere changes during strong magnetic storms. The weak and strong storms differ from each other in not only the total energy of ring current, but also in the ion composition.

The ions which form the ring current may give rise to an enhancement of ion-cyclotron waves (Cornwall *et al.*, 1970; Solomon and Picon, 1981). The enhancement increment

is peaking near the plasmapause where the ratio of magnetic energy density of the Earth's magnetic field to plasma density is minimum. The plasma instability resulting in ring current decay is strongest after ion injection to the inner regions of radiation belt during magnetic storm, i.e., during the main phase. Calculating the pitch-angle diffusion of ions in resonance with ion-cyclotron waves has shown that the resonance ion lifetime is a few hours. The ion-wave interactions seem to define the τ value during the storm main phase, but must be allowed for also during the recovery phase when the processes of energetic ion charge exchange with neutral hydrogen constitute the principal mechanism of ion loss from ring current (Smith and Bewtra, 1978). The position of the region of the most intensive wave-particle interactions changes throughout a storm. During the main phase, the ions run away from lower L-shells in the region of the plasmapause having approached the Earth. After that the ion loss from ring current covers also the region of high L-shells as the plasmasphere gets filled with cold plasma during storm recovery phase.

The ion dissipation from ring current which leads to $\tau \sim 1$ hour is also possible in case of ion interactions with magnetosound oscillations. Chistoserdov (1983) examined the pitch-angle diffusion due to ring-current proton interactions with magnetosound oscillations at a doubled bounce frequency.

The τ values used in the modelling were examined only for a fraction of the studies listed in the table because the remaining studies used the principles employed in the works discussed. For example, Murayama (1986a) obtained $\tau_1 = 2$ hours and $\tau_2 = 21$ hours for 90 intervals during storm recovery phase, by analogy with two ring currents (Akasofu *et al.*, 1963); Pudovkin *et al.* (1988), and Pisarsky *et al.* (1989) specified the results of their earlier studies. Contrary to Vasiliunas (1987), τ during storm main phase was assumed to depend on the function of injection to ring current, rather than on the energy dissipated in the magnetosphere.

Gonzalez *et al.* (1989a) suggest that the following dependence of τ on D_{st} should be used for the storm main phase: τ decreases from 4 hours at $D_{st} > -50$ nT to 0.25 hour at $D_{st} < -120$ nT. Ochabova (1989) presents different values of τ for the main and recovery phases of magnetic storms.

Summarizing the results of numerous studies of the ring-current decay parameter τ using the ground-based geomagnetic field variation data obtained during magnetic storm, we can conclude that:

(1) the values of τ are very different during the main (injection period) and recovery (decay period) phases of a magnetic storm;

(2) during injection, the value of τ decreases with increasing injection to ring current. Under intensive injections, the values of τ may decrease to $\tau \sim 1$ hour;

(3) in the decay period during storm recovery phase, the value of τ is not constant, but increases with decreasing $|DR|$ in an individual storm;

(4) a trend exists for the τ values to be increased during strong storms compared with weak and moderate storms;

(5) the variations of τ during magnetic storms must be allowed for when studying the energy status of the magnetosphere, in particular during the intervals with different

rates of energy input and output in the magnetosphere. The fixed value $\tau \sim 6$–8 hours underestimates very much the ring-current injection rate U_{DR} during the main phase and overestimates U_{DR} during the recovery phase. Therefore, the studies of correlations between the solar wind parameters and the magnetospheric parameters will be very inaccurate unless the variations of τ are included.

4. The Function F of Injection into the Ring Current During Magnetic Storms

The following processes, which lead to plasma injection into the ring current, are discussed elsewhere:

(i) convective earthward motion of plasma sheet accompanied by the betatron and Fermi modes of ion acceleration;

(ii) acceleration of ionospheric ions by electric fields along geomagnetic field lines;

(iii) ion acceleration in the magnetospheric night sector by unsteady-state electric fields;

(iv) earthward motions of the inner boundary of outer radiation belt and of the ions which were stably trapped earlier in the radiation belt region.

According to (4) the *DR* variations on the Earth's surface is defined by the function of injection to the ring current $F(t)$. The $F(t)$ value can artificially be selected in such a way as to reproduce the parabolic form of the D_{st} variation for a typical magnetic storm (Akasofu and Yoshida, 1966). An important step in modelling *DR* was made by Burton *et al.* (1975) who related $F(t)$ in a simple way to the solar wind electric field. The injection into the ring current was assumed to be feasible only if the value of the azimuthal (dawn-dusk) electric field component in interplanetary medium is below 0.5 mV m^{-1}. The magnetosphere was treated to be a rectifier for the IMF B_z component. Plasma can be injected into the ring current only under southward IMF component. A linear relation between the time rate of D_{st} variation and the electric field on the magnetopause was predicted theoretically by Siscoe and Crooker (1974). The model proposed by Burton *et al.* (1975) can properly reproduce the complicated character of D_{st} variation during magnetic storm. A certain disagreement between the model and experimental data in the final stage of recovery phase may be ascribed to the disregard of the continual injection to the ring current and to the occurrence of the injection under northward IMF component. The inclusion of the injection removes also the difficulty faced with by Burton *et al.* (1975) who obtained that the intensity of steady-state ring current on the Earth's surface was + 5 nT. According to Perreault and Akasofu (1978), Akasofu (1981a), the injection to the ring current occurs not only in the interval with southward IMF B_z component, but exists in practice permanently, except the periods with strictly northward IMF; $F(t) = -0.7\varepsilon$, where $\varepsilon = 2 \times 10^{14} V \cdot B^2 \sin^4 \theta/2$; V and B are, respectively, the velocity and the magnetic field of solar wind; θ is angle between northward direction and solar wind magnetic field vector; ε is energy supplied from solar wind to the magnetospheric inside. Having solved the problem of solar wind streaming around the magnetosphere, Pudovkin and Semenov (1986) showed that the energy influx to the magnetosphere could actually be described by the above relation. Seventy percent of ε

is stored in the ring current, and as little as 30% of the energy influx is lost for other processes (Axford, 1967; Akasofu, 1977).

Bobrov (1977, 1981) has analyzed the solar wind parameters responsible for plasma injection to the ring-current region. The correlation between these parameters and the function $F(t)$ calculated using the data of ground-based magnetic field observations increases if the electric field is calculated allowing for not only the IMF B_z component, but also the IMF variability σ. Later on, the function F, allowing for σ, was used when modelling DR (Pudovkin *et al.*, 1985b, 1988; Pisarsky *et al.*, 1989).

Murayama (1982) modelled DR using the injection functions $F_1 \sim B_s V$, $F_2 \sim B_s V^2$, $F_3 \sim \varepsilon$, and $F_4 \sim B_s V(mnV^2)^{1/3}$, i.e., not only the velocity and the IMF but also the solar wind plasma density was used. Expediency of introducing solar wind pressure in the injection function was discussed by Gonzalez *et al.* (1989a, b). The correlation coefficient between the calculated and observed D_{st} values proved, on the average, to be 0.849, 0.899, 0.814, and 0.873 when, respectively, the functions F_1, F_2, F_3, and F_4 were used. Sixty intervals from 5 to 7 days were used. The functions F_3, F_1, and F_4 are discussed in terms of the relation for the power transferred from solar wind to the magnetosphere obtained by Vasiliunas *et al.* (1982) from considerations of scaling. A more detailed analysis of the form of the injection function F has shown (Murayama, 1986a) that $F \sim B_s^{1.09} V^{2.06} n^{0.38}$. The injection function was inferred from the DR variations for 90 time intervals including magnetic storm on assumption that $F \sim B_s^a v^b n^c$. The values of a, b, and c were inferred from the requirement that the observed and calculated DR values should be in the best agreement.

Later on, DR was modelled using the functions $F_1 \sim B_s^{1.09} v^{2.06} n^{0.38}$, $F_2 \sim B_s v^2 n^{0.4}$, $F_3 \sim B_s v n^{0.25}$, and $F_4 \sim \varepsilon n^{0.05}$ (Murayama, 1986b). The respective mean correlation coefficients between DR_{mod} and DR_{exp} for 135 time intervals are $r = 0.917, 0.917, 0.903$, and 0.871. The values of r for the functions F_1 and F_2 are the same; the worst correlation occurs when ε is used to characterize the injection. The regression coefficient A, which relates the ring-current intensity to injection and to decay, varies very significantly from storm to storm. The value of A was selected for each storm in such a way that the best agreement between DR_{mod} and DR_{exp} should be obtained. The variability of A was assumed to be due to the fact that the hourly values of solar wind parameters and of IMF (B_s, n, and v) used in the calculations are not always in a strict correspondence with the conditions in the region of merging on the magnetopause and to characterize, to an extent, the adequacy of a given function of injection to the ring current and the occurrence of noticeable seasonal variations of A (the value of A is 30% as high in equinox as in solstice).

The dependence of F on the solar wind electric field allowing for the IMF dispersion similar to that proposed earlier (Bobrov, 1981) was used by Pudovkin *et al.* (1985b, 1988) when modelling DR. The dependence on the interplanetary medium parameters similar to that proposed by Feldstein *et al.* (1984) was used by Grafe (1988) to calculate the injection function. Pisarsky *et al.* (1989) supplemented the injection function with a term depending on solar wind velocity and characterizing the additional injection to the ring current due to viscous interaction of the magnetosphere with interplanetary medium.

Basing on the data obtained during the main phases of ten intensive magnetic storms, Gonzalez *et al.* (1989a) assume that the best functions of injection to ring current are the functions proportional to ε, to $B_s v^2 n^{1/2}$ (Murayama, 1986a), to $(nv^2)^{1/6} vB \sin^4 \theta/2$ (Bargatze *et al.*, 1986), and to the generalized function R which characterizes the energy influx to the magnetosphere as a result of magnetic field merging on the magnetopause (Gonzalez, 1986). The last three functions include solar wind velocity with power-law exponent ranging from $-\frac{1}{3}$ to $\frac{1}{2}$.

Summarizing the results of the studies of the relationships of the function of injection to the ring current to interplanetary medium parameters, we may conclude that:

(i) as established in the fundamental study by Burton *et al.* (1975), the injection to the ring current is closely associated with the azimuthal component of the solar wind electric field;

(ii) not only the IMF B_z component, but also the IMF variability σ must be allowed for;

(iii) the injection function is affected by solar wind plasma density to a much lesser extent compared with the IMF and the solar wind velocity;

(iv) injection to the ring current does not stop when the IMF direction turns from southward to northward;

(v) permanent injection to the ring current takes place which sustains the existence of DR during magnetically-quiet intervals and may rise with varying the parameters of solar plasma, in particular with increasing its velocity.

5. The Results of Modelling the Hourly Mean Values of the Storm-Time Ring Current on the Basis of Present-Day Concepts

From the equation of ring-current energy balance (4) it follows that the storm-time variation of magnetic field DR is defined by the relation between the injection function $F(t)$ and the loss function DR/τ. We have $|F(t)| > |DR|/\tau$ during the main phase and an inverse relation during recovery phase. From the table it follows that the functional relationships of $F(t)$ to the interplanetary medium conditions and the values of the parameter τ as a function of storm phase, $F(t)$, or DR were determined by many researchers. The given problem belongs to many-parameter problems, so it is not surprising that the researchers proposed a broad range of relations. To determine the model parameters, therefore, Pisarsky *et al.* (1989) solved the problem of minimizing the functional of quadratic discrepancy between the observed DR values (denoted, henceforth, as DR_{exp}) and the model-calculated DR values (denoted, henceforth, as DR_{mod}). DR_{exxp} was inferred from the relation (7) at the hourly values of solar wind parameters from (King, 1977) and D_{st} from the IAGA Bulletin. The injection function was assumed to depend on the azimuthal component of solar wind electric field and its variability and on the viscous friction of solar wind on the magnetosphere which, in turn, depends on solar wind velocity:

$$F = A_1 v(B_z - A_2\sigma) + A_3(v - 300) + A_4\,, \tag{11}$$

where A_1, A_2, A_3, and A_4 are constant factors. The hourly values of the IMF components and the variance of the IMF modulus were taken to agree with the data of (King, 1977). The decay parameter was assumed to be a constant during the storm main phase and to vary freely during the recovery phase. The method of stochastic optimization with adaptation was used by Vasiliev (1980) to find the values of the factors in (9) and the values of τ during the recovery phase ($\tau_{r.p.}$) at $\tau_{m.p.} = 4.9$ hours for 96 intervals including the decreases in D_{st} by 60 and more nT (5352 hours in total).

Depending on a particular calculation version, the number of variables used in the minimization was ranging from 9 to 25. Solving the optimization problem in the spare of such a dimension is faced with calculational difficulties. Another feature of the examined problem is that any rapidly converging methods of gradient type cannot be used. These circumstances have forced the choice of the method of stochastic optimization with adaptation for selecting the values of the model parameters. The calculations were made by up to 2000–5000 iterations.

At the moments of the highest ring-current intensity, we have $F = DR_{max}/\tau_{m.p.}$. The $\tau_{m.p.}$ values were found by calculating the values of F on the basis of the relation (9) 1 hour before the DR_{max} moment for 45 storms in which the DR values at two neighbouring hours about DR_{max} differ by not more than 5%. The $\tau_{m.p.}$ value decreases with increasing $|F|$. The resultant new $\tau_{m.p.}$ values were used in a next iteration when finding the factors in (9). The factors A_i changed but insignificantly, so any further iteration had not to be made. As a result, the injection fucntion F_{mod} depending on the interplanetary medium parameters proves to be of the form

$$F_{mod} = 8.2 \times 10^{-3} v(B_z - 0.67\sigma) - 14.1(v - 300) + 9.4\,, \qquad (12)$$

where F_{mod} is expressed in nT hr^{-1}, v in km s^{-1}, B_z and σ in nT.

The representativity of the F_{mod} value calculated by (12) was estimated by selecting 227 two-hour intervals within main phases of 96 magnetic storms during which $|\Delta B_z|$ was < 2 nT and the value of $\sqrt{p}$ ($p = nmv^2$ is solar wind pressure) varied by not more than 10 (eV cm^{-3})$^{1/2}$, i.e., the DCF variation was below 2 nT. The values of $F_{exp} = \mathrm{d}DR/\mathrm{d}t + DR/\tau$ during the above-mentioned intervals were calculated making allowance for the dependences of τ on F_{mod}. The least-squares method was used to obtain a linear dependence of F_{exp} on F_{mod} for the 227 intervals (see Figure 3). The linear regression equation yielded the value of 1 for the coefficient of the relation of F_{exp} to F_{mod} and the correlation coefficient $r = 0.88 \pm 0.05$.

The F_{mod} value is calculated by the relation (12) for injection periods during the main and recovery phases of a magnetic storm. During the injection periods, $v(B_z - 0.67\sigma) < -1146$, i.e., the electromagnetic injection exceeds the viscous injection. The remaining portion of a geomagnetic storm is attributed to the decay period despite the process of injection into the ring current keeps proceeding with intensity $F_{mod} = -14.1 \times 10^{-3}\,(v - 300)$ subject that $v > 300$ km s^{-1}.

In (12), the F_{mod} term depending only on solar wind velocity v arises from the quasi-steady-state convection to the ring current due to the 'viscous' interaction of solar wind with the Earth's magnetosphere which enhances with increasing v. One of the

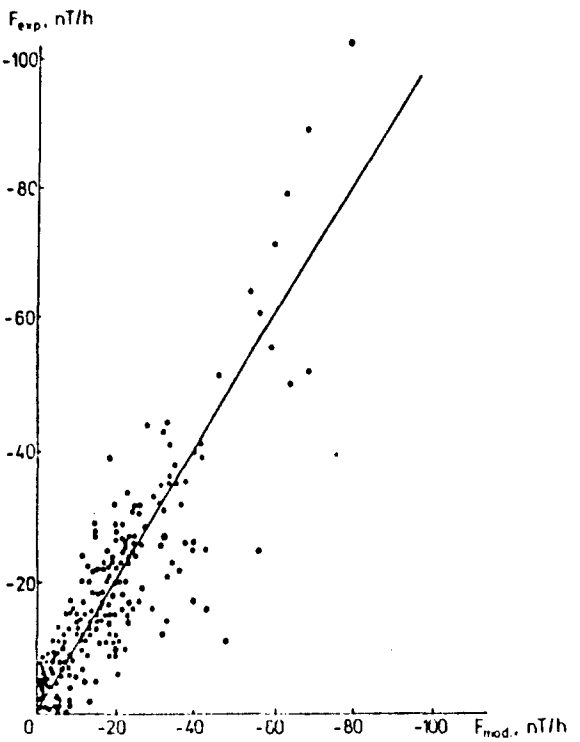

Fig. 3. Relationship between $F_{exp} = dDR/dt + DR/\tau$ and the $F_{mod} = 8.2 \times 10^{-3} v(B_z - 0.67\sigma) - 14.3 \times 10^{-3}(v - 300) + 9.4$ for 227 two-hour intervals during the injection period (the main phase) of a magnetic storm (Pisarsky *et al.*, 1989).

results of the quasi-steady-state injection is that the magnetic field intensity at low-latitude observatories exhibits an increase during magnetically quiet periods which enhances with increasing v. Indeed, an independent analysis (Rangarajan, 1984) made using the data of four Indian observatories has proved that the horizontal component of the Earth's magnetic field decreases actually with increasing v in the near-equator region at night-time hours of magnetically quiet days. The data (Rangarajan, 1984) displayed in Figure 4 show that the values of H at the equator decrease by 20 nT with increasing v from 300 to 500 km s^{-1}. The correlation coefficient $r = -0.6$ is not high, but appears still to be significant. The relation of the D_{st} values in high-velocity fluxes to v in the form $D_{st} = -\beta v + 43.7$ nT ($\beta = 0.1$ nT km^{-1} s^{-1}) was paid attention to by Shadrina and Plotnikov (1986). The data obtained at Kakioka and Tbilisi on magnetically quiet days with $D_{st} > 0$ were used by Porchkhidze *et al.* (1989) to find a trend in H to decrease with increasing v, namely, the value of H changes by 5–10 nT with changing v by 100 km s^{-1}. Assuming that the given variations characterize the quasi-steady-state ring current with $dDr/dt = 0$ and that the injection function during magnetically quiet intervals is $F = A(v - 300) \times 10^{-3}$, we obtain from (4):

$$A_3 \Delta V \times 10^{-3} = \Delta DR/\tau .$$

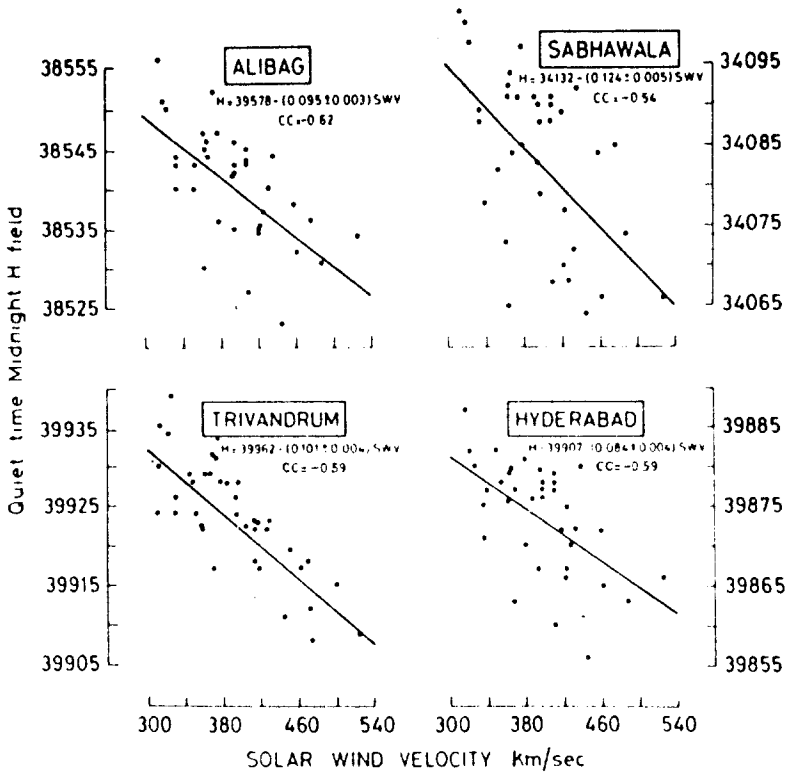

Fig. 4. Scatter plot of a quiet-day night time magnetic field at Trivandrum, Hyderabad, Alibag, and Sabhawala as a function of solar wind velocity. The straight line is the least-squares best fit to the data in each case (Rangarajan, 1984).

At $\Delta v = 100$ km s^{-1}, $\Delta DR \sim 10$ nT, and $\tau \sim 10$ hours, we have $A_3 \sim 10$ nT hr^{-1} km^{-1} s which are comparable in the order of magnitude with the value of A_3 in (12).

The F_{mod} value inferred from (12) was used to obtain new values of $\tau_{\text{m.p.}}$ for the moments of the highest intensity in 45 magnetic storms with one-hour delay of $DR_{\max}$ relative to F_{mod} (see Figure 5). The dependence of $\tau_{\text{m.p.}}$ on F_{mod} adopted in the model calculations of DR is in good agreement with the $\tau_{\text{m.p.}}$ values during the maxima of the main phases of 45 storms. The parameter $\tau_{\text{r.p.}}$ during the recovery phases (the decay interval) was found by the stochastic optimization method. During weak and moderate storms, the $\tau_{\text{r.p.}}$ value increases with decreasing $|DR|$ from 5.4 hours at $-150 \geq DR \geq -170$ nT to 10.2 hours at $-10 \geq DR \geq -30$ nT; the $\tau_{\text{r.p.}}$ value during strong storms with $D_{st} < -160$ nT depends very little on DR and is 10 hours at $DR = -300$ nT and 10.8 hours at $DR = -30$ nT.

Pisarsky *et al.* (1989) has tabulated the dependences $\tau_{\text{m.p.}}(F)$ and $\tau_{\text{r.p.}}(DR)$. The ring-current decay parameters may also be calculated using approximate interpolation relations. The relations were obtained for weak and moderate storms and proved to be $\tau_{\text{m.p.}} = 1.6 + 13e^{0.08F}$ and $\tau_{\text{r.p.}} = 5.4 + 10e^{0.025DR}$, and for intensive storms were found

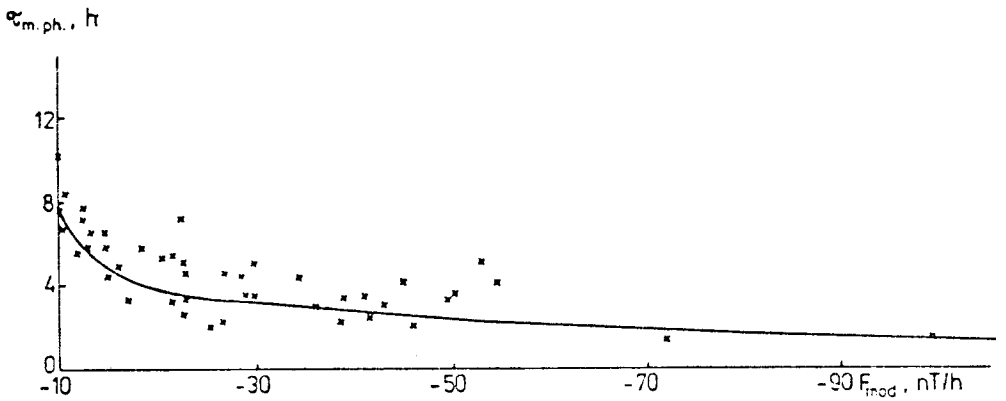

Fig. 5. Variations of the parameter τ due to F_{mod} during the epoch of maximum intensity of 45 magnetic storms with one-hour delay of $DR_{\max}$ relative to F_{mod} (Pisarsky *et al.*, 1989).

to be $\tau_{\text{m.p.}} = 2.4 + 13e^{0.07F}$ and $\tau_{\text{r.p.}} = 10.0 + 1.84e^{0.007DR}$. Here τ is expressed in hours, F in nT hr^{-1}, and DR in nT.

The model-calculated values of τ during the recovery phases of weak magnetic storms are in a sufficiently good agreement with the τ values found independently by other methods. Roelof *et al.* (1985) has inferred $\tau = 7.6$ hours from measuring the fluxes of high-energy neutral atoms produced in the ring-current region by energetic ions charge exchanges. During the measurements, the DR intensity decreased from -67 nT to -30 nT, which, according to the model (Pisarsky *et al.*, 1989), corresponds to $\tau \sim 8.5$ hours. Therefore, the model-calculated τ value agrees with the measured τ value within 11%.

Hamilton *et al.* (1988) estimated that $\tau = 9.3$ hours during the recovery phase of strong magnetic storm with $D_{st} < -300$ nT. This estimate agrees also within 10% with the adopted model value $\tau = 10$ hours.

The difference in the values of τ during the main and recovery phases of magnetic storms is due to the prevailing mechanisms of ring-current decay, namely, the interaction with hydromagnetic waves during injections (Cornwall *et al.*, 1970; Bespalov *et al.*, 1989) and the charge exchange with the geocoronal hydrogen during recovery phase (Smith and Bewtra, 1978).

We shall examine the results of modelling the ring-current magnetic field in terms of the models listed in the table by comparing among the resultant profiles of DR or D_{st} during particular magnetic storms. It should be reminded again that the methods for calculating D_{st}, together with the D_{st}-based ring-current intensity, characterize the ring-current symmetric part which is the same along a geomagnetic parallel. Figure 6(a) and 6(b) according to the pioneer work Burton *et al.* (1975) and the later work Feldstein *et al.* (1984). The values of D_{st} were determined at a 2.5-min resolution from the H-component at 11 mid- and low-latitude observatories. It is seen that the model-calculated and observed D_{st} values are in a sufficiently good agreement. The allowance for the permanent injection to the ring current (Feldstein *et al.*, 1984) yields an even

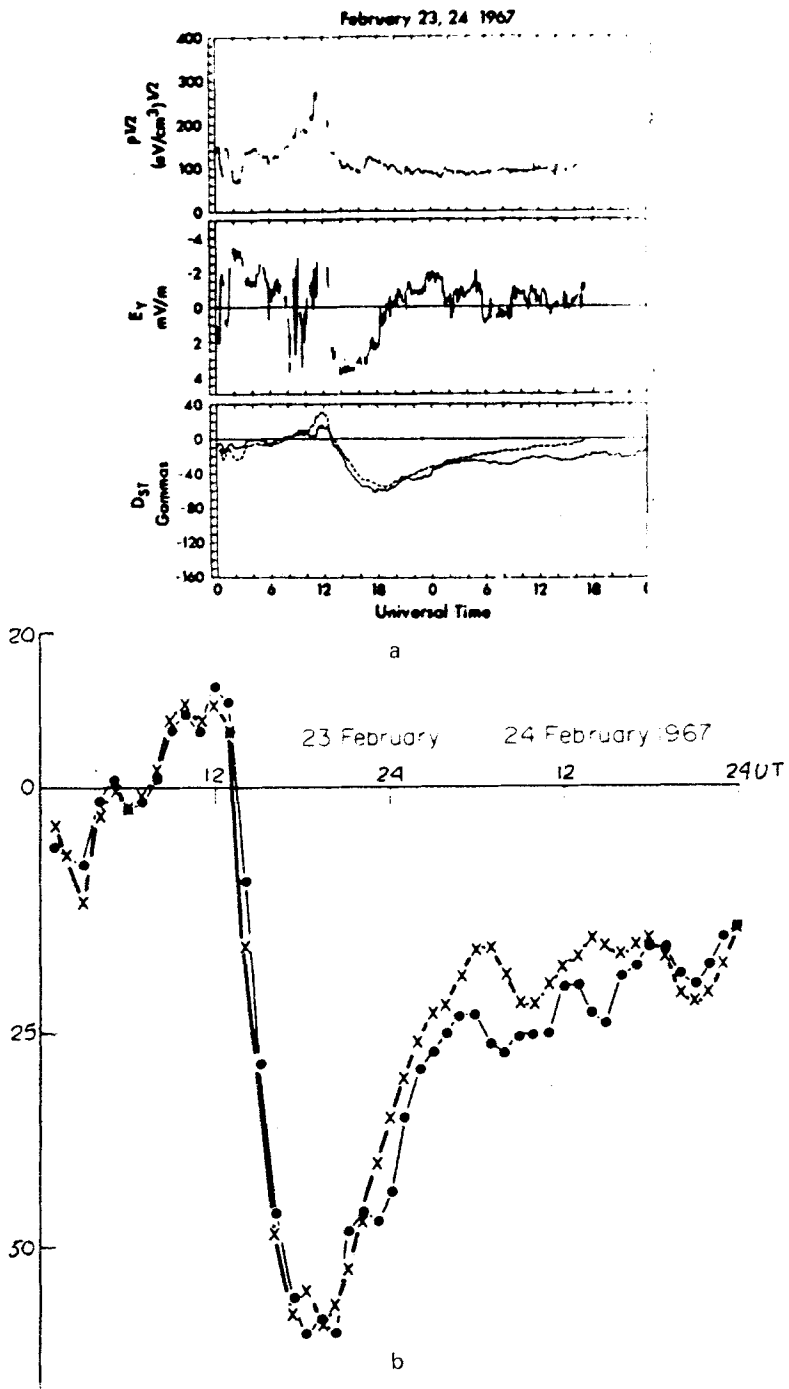

Fig. 6. (a) *From top to bottom*: the square root of the solar wind dynamic pressure, the dawn-to-dusk component of the interplanetary electric field, and the predicted (the dashed line) and observed (the solid line) D_{st} variation (Burton *et al.*, 1975). (b) The D_{st} variation during the same storm (Feldstein *et al.*, 1984). The crosses show the model D_{st} variation; the dots show the calculated D_{st} variations.

better agreement in the D_{st} value during the final stage of the recovery phase. The level of $D_{st} \sim -20$ nT observed in practice constantly after 09:00 UT on February 24, 1967 is the direct evidence for the occurrence of the permanent injection during the $B_z > 0$ intervals. The difference between the model-calculated and observed D_{st} values in Figure 6(a) will get increased even more if the modelling is continued after 18:00 UT on February 24.

The model (Akasofu, 1981a) describes the large-scale D_{st} variations, as follows from Figure 7 for the storm of March 31–April 2, 1973; however, the disagreements are

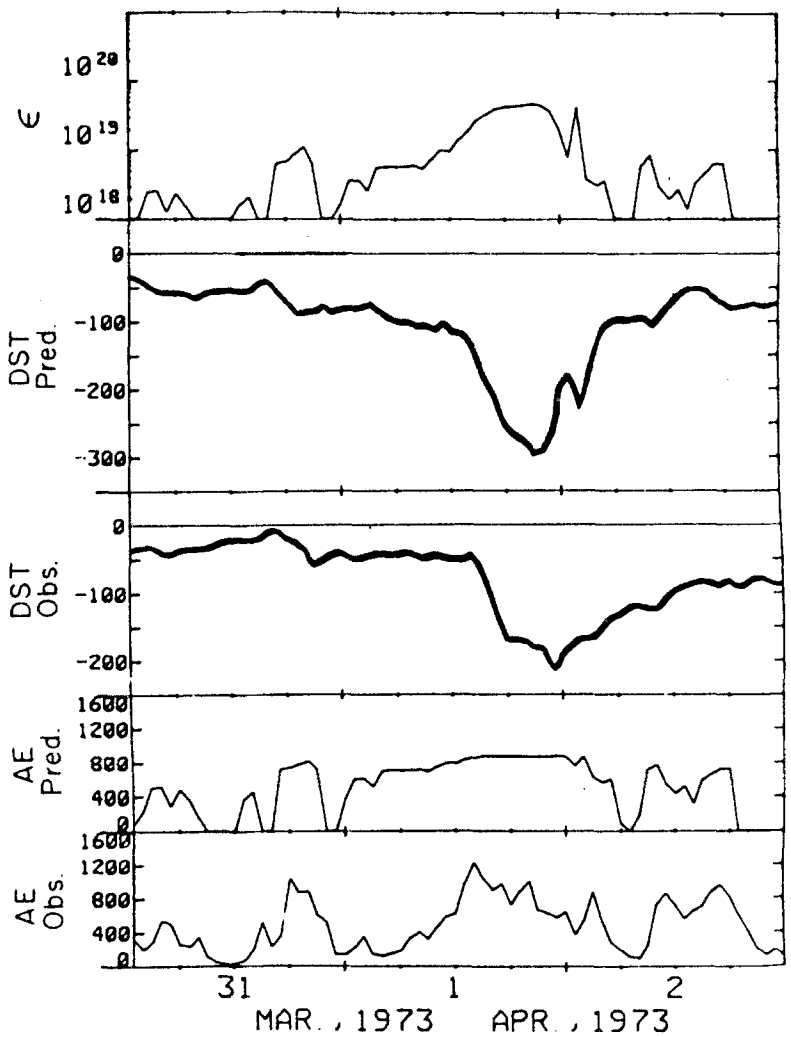

Fig. 7. Comparison of the predicted D_{st} (D_{stp}) and AE (AE_p) indices with the observed D_{st} and AE indices. *Fom top to bottom*: the solar wind-magnetosphere energy coupling function (ε), the predicted D_{st} index (D_{stp}), the observed D_{st} index, the predicted AE index (AE_p), and the observed AE index during the March 31–April 2, 1973 storm (Akasofu, 1981a).

sufficiently great in the D_{st} intensity and in the character of temporal variations. Unfortunately, the quantitative criteria of an agreement between the model-calculated and observed D_{st}-variations are not presented. A decrease in the AE index during the main phase of the storm with preservating the high values of the function ε is worth noting. The decrease arises from the displacement of the auroral electrojets to the subauroral zone due to ring-current development. A similar effect will be discussed below in more detail using the example of another storm.

The algorithm proposed by Bobrov (1981) cannot be regarded, in all senses, as a model for DR because the value of τ is not varied by any prescribed rules, but is, rather, selected for each individual storm to be such that the best agreement between the model-calculated and observed DR values would be obtained. The same can be said about the algorithm proposed by Murayama (1982), where the proportionality factor between the injection functions F_1, F_2, F_3, F_4 and the interplanetary medium parameters varies from one storm to another.

The results of modelling are difficult to compare quantitatively with each other using the published data directly because the criteria of an agreement between the model-calculated and observed $DR(D_{st})$ values are not always presented and, even if presented, appears to be incomplete and conflicting. Therefore, the potentialities of the present-day modelling of DR are demonstrated using the example of the August 27–29, 1978 magnetic storm which has been supported by a sufficiently detailed study of the interplanetary parameters in correlation with magnetic activity (Baker *et al.*, 1983; Gonzalez *et al.*, 1989a). Figure 8 borrowed from Murayama (1986b) shows the mean-hourly values of the solar wind density (D) and velocity (V), the modulus (B), and the IMF B_z component for the interval from August 26 to 30, 1978. Also presented are the results of modelling D_{st} for three forms of injection function F. The correlation coefficients r between $D_{st}^{\exp}$ and D_{st}^{mod} are very high. The coefficient A relating D_{st}^{mod} to injection function F for the given storm is $A = 0.2306$ at its mean value $A_{\mathrm{mean}} = 0.3017$ over 90 time intervals. From the high values of the correlation coefficient r it follows that none of the injection functions F has any quite evident advantage; D_{st}^{mod} describes $D_{st}^{\exp}$ sufficiently well for all functions F_i. Unfortunately, the values of the variance δ characterizing the r.m.s. deviation of D_{st}^{mod} from $D_{st}^{\exp}$ are not presented, although the deviation, together with r, constitute an important criterion to estimate the agreement between the model-calculated and observed values of D_{st}.

The DR_{mod} and $DR_{\exp}$ values are also compared between each other for the same storm in terms of different models. The $DR_{\exp}$ values were calculated according to (7), the time variations of DR_{mod} were inferred from (4) and (5). Use was made of the models proposed by Pisarsky *et al.* (1989), Pudovkin *et al.* (1988), Grafe (1988), and Akasofu (1981a, b), as well as of the modified models for interplanetary electric field (IEF), Murayama and Akasofu. The models were modified as follows. The functions, F, of injection to ring current were calculated using pairs of neighbouring hours during the main phases of 72 magnetic storms from 1969 to 1982. The conditions $|\Delta B_z| < 2$ nT and $|DCF| < 2$ nT were imposed on the pairs selected. These criteria were satisfied by 179 pairs of values. The last-squares method was used to calculate the linear regression

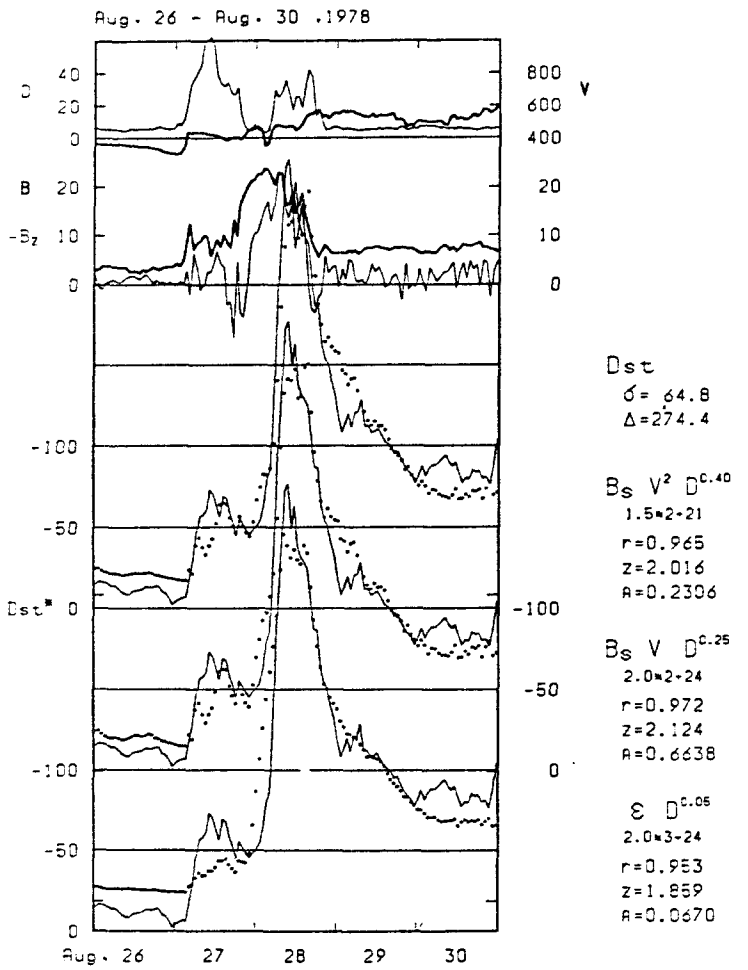

Fig. 8. The interplanetary medium parameters D (density), V (velocity), B (the IMF modulus), and B_z (the IMF north–south component) during the August 27–30, 1978 strong magnetic storm. The observed (the solid line) and model (the dots) D_{st} indices for different types of injection according to Murayama (1986b).

equations. As a result, we obtained

$$F = \begin{cases} 8.9 B_z v \times 10^{-3} + 7 \text{ nT hr}^{-1} & \text{at } B_z v \times 10^{-3} < -1 \text{ mV m}^{-1}, \\ -14.1(v - 300) \times 10^{-3} \text{ nT hr}^{-1} & \text{at } B_z v \times 10^{-3} > -1 \text{ mV m}^{-1}, \end{cases}$$

for the IEF model and

$$F = \begin{cases} -3.7 \times 10^{-6} B^{1.09} v^{2.06} n^{0.38} - 0.42 \text{ nT hr}^{-1} & \text{at } B_z < 0, \\ -14.1(v - 300) \times 10^{-3} \text{ nT hr}^{-1} & \text{at } B_z > 0, \end{cases}$$

for the modified Murayama model. The values of τ during the injection and decay intervals were taken from (Pisarsky *et al.*, 1989).

The modified injection functions determined by the above-mentioned method were also calculated for other functional dependences of F on the interplanetary medium parameters. In particular, the functions of Bargatze *et al.* (1986), the electric field on the magnetopause $vB_T \sin^2 \theta/2$, etc. were used. The modelling results obtained with the given injection functions are not presented because they proved to be worse than those obtained with the modified Murayama and IEF functions.

Several versions were used for the modified Akasofu function, namely, model A (Akasofu, 1981a), model $B1$ ($F = 0.7\varepsilon$) (Akasofu, 1981b), models $B2$ ($F = 0.5\varepsilon$) and $B3$ ($F = 0.33\varepsilon$) at the same values of τ as in model $B1$, model C at the value of τ according to Zwickl *et al.* (1987) for $F = 0.7\varepsilon$ (model $C1$) and $F = 0.45\varepsilon$ (model $C2$).

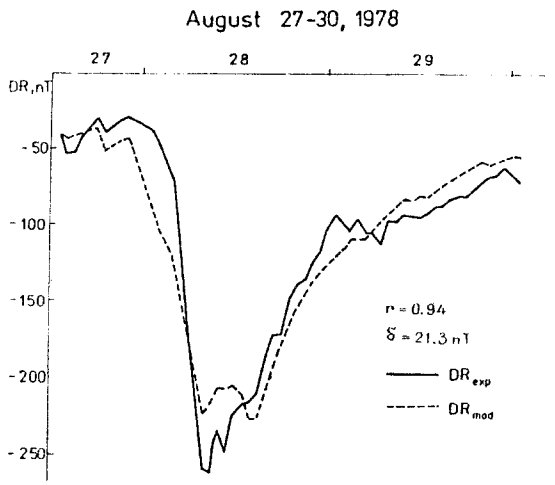

Fig. 9a.

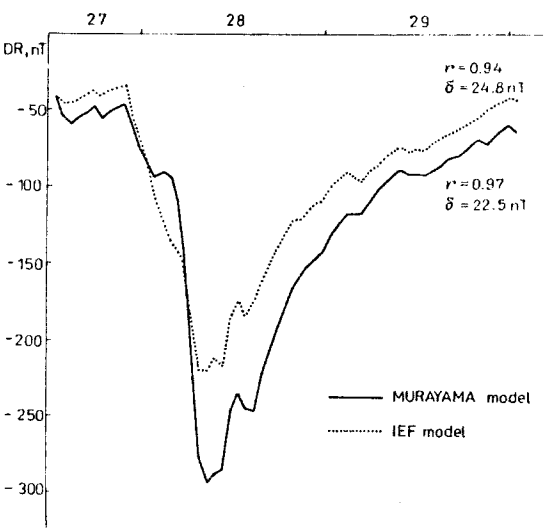

Fig. 9b.

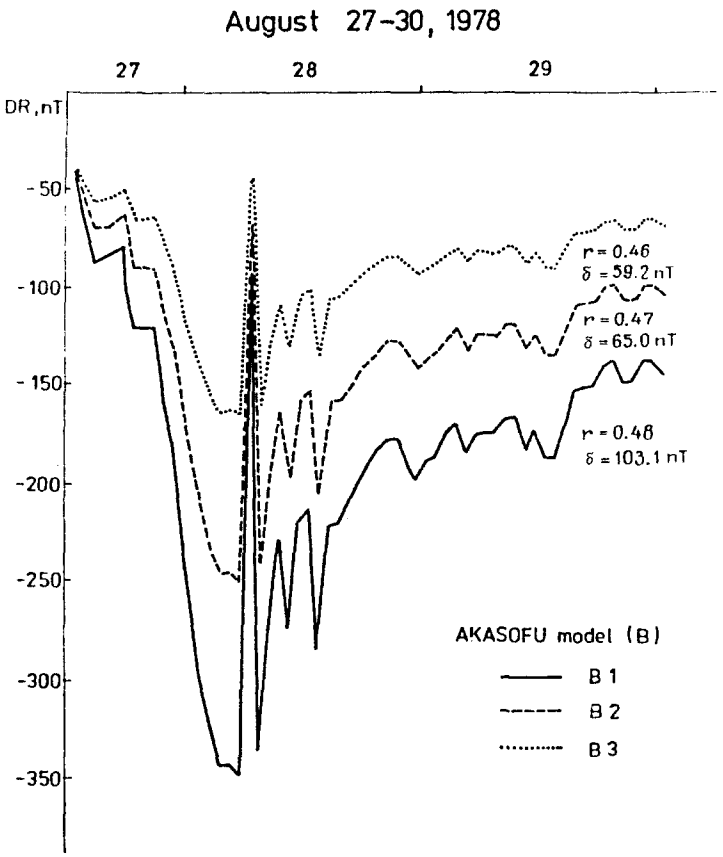

Fig. 9c.

TABLE II

Comparison DR_{mod} and DR_{exp} in different models

Models	Aug. 27–30, 1978		March 31–Apr. 3, 1979		March 22–23, 1979		Jan. 7–9, 1979	
	r	δ	r	δ	r	δ	r	δ
Pisarsky *et al.*	0.944	21.3	0.80	9.7	0.963	10.9	0.91	15.4
IEF	0.938	24.8	0.84	15.9	0.971	13.0	0.90	14.4
Murayama	0.973	22.5	0.90	11.1	0.953	11.1	0.91	15.0
Pudovkin *et al.*	0.928	32	0.88	7.7	0.923	18.3	0.81	23
Akasofu (mod. A)	0.589	92.0	0.76	30.5	0.817	81.0	0.84	29.8
Akasofu (mod. B1)	0.48	103.1	0.48	103.4	0.890	114.5	0.83	52.5
Akasofu (mod. B2)	0.48	65.0	0.46	60.4	0.890	67.8	0.84	23.1
Akasofu (mod. B3)	0.46	59.2	0.43	25.2	0.891	28.7	0.84	13.4
Akasofu (mod. C1)	0.44	64.2	0.40	16.6	0.699	37.1	0.69	17.2
Akasofu (mod. C2)	0.40	88.9	0.28	30.1	0.707	27.3	0.63	38.1
Grafe	0.94	33.6			0.75	29.0	0.22	55.4

In the Grafe (1988) model, the values of τ for the main and recovery phases of a magnetic storm were taken to agree with the results presented, respectively, in Figures 4 and 11 therein. It appears that $F = 0$ after the beginning of the storm recovery phase, i.e., the injection to ring current stops irrespectively of the IMF B_z component sign.

Figure 9 shows some of the modelling results for the August 27–29, 1978 storm; the values of r and δ for all the models have been summarized in Table II. The correlation coefficient for the Pudovkin *et al.* (1988) model is not presented in the work, but our calculations show to be sufficiently high. All the models, except the various versions of the Akasofu model, describe the character of the storm-time $DR(D_{st})$ variation, the fact that is indicated by the very high values $r > 0.9$. In the modified Murayama model, $r = 0.973$, i.e., is not lower than in the model presented in Figure 8. The r.m.s. deviation DR_{mod} from DR_{exp} is minimum in the Pisarsky *et al.* (1989) model and in the modified

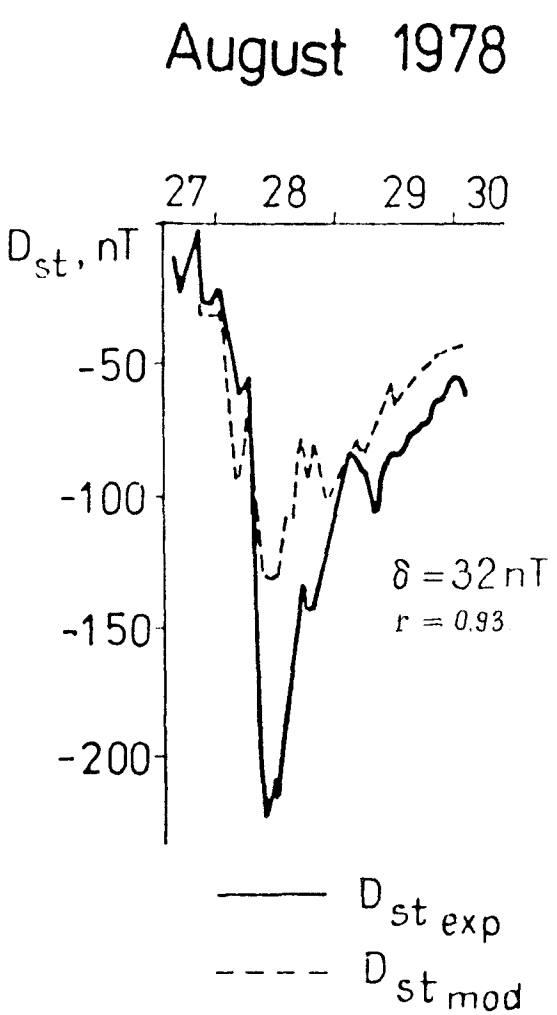

Fig. 9d.

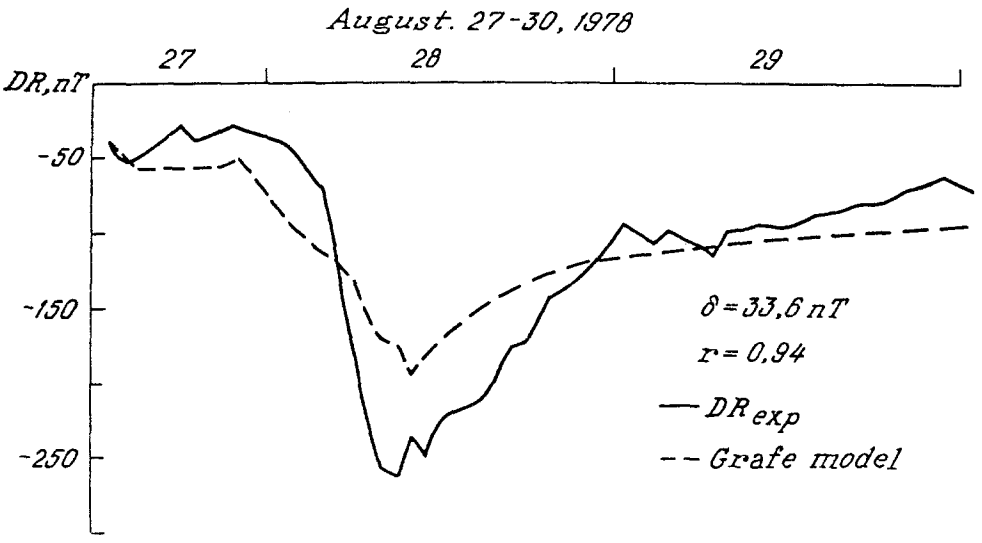

Fig. 9e.

Fig. 9. The ring-current intensity variations during the August 27–29, 1978 magnetic storm. (a) DR_{exp} and DR_{mod} according to Pisarsky *et al.* (1989). (b) DR_{mod} according to the modified IEF and Murayama models. (c) DR_{mod} according to the models (Akasofu, 1981b) $B1$, modified $B2$, and $B3$. (d) D_{st}^{exp} and D_{st}^{mod} according to Pudovkin *et al.* (1988). (e) DR_{exp} and DR_{mod} according to Grafe (1988).

Murayama model, is somewhat higher in the IEF model, and is much higher in the Pudovkin *et al.* (1988) and Grafe (1988) models. The Akasofu (1981a, b) models are characterized by not only low values of r but also high values of δ. The value of δ decreases with decreasing the energy flux fraction ε supplied from solar wind to ring current. At $F \sim 0.3\varepsilon$, however, the variance is also high.

The modelling results obtained for the August 27–30, 1978 storm prove, as a rule, to be the same in case of other storms. A good agreement between DR_{mod} and DR_{exp} in the modified Murayama model is indicative of a high effectiveness of the dependence of the function of energy injection to ring current on the interplanetary medium parameters as proposed by Murayama (1986a, b).

The effectiveness of the DR models was verified on the CDAW6 intervals in March–April, 1979 which were not included in the sampling of storms used by Pisarsky *et al.* (1989) to find the model parameters. The DR variations for the March 31–April 3, 1979 interval are shown in Figure 10, those for the March 22–23, interval are presented in Figure 11 and the relevant r and δ values are summarized in Table II. Similar to the storm of August 1978, the Pisarsky *et al.* (1989) model and the modified Murayama model describe best the DR intensity and variations for the March 22–23, 1979 storm, whereas the storm of March 31–April 3 is described best by the Pudovkin *et al.* model. The Akasofu model B also describes the DR variations, and the value of δ is much lower for $F = 0.33\varepsilon$ compared with $F = 0.7\varepsilon$.

The worst correlation between DR_{mod} and DR_{exp} occurs in the Grafe (1988) model

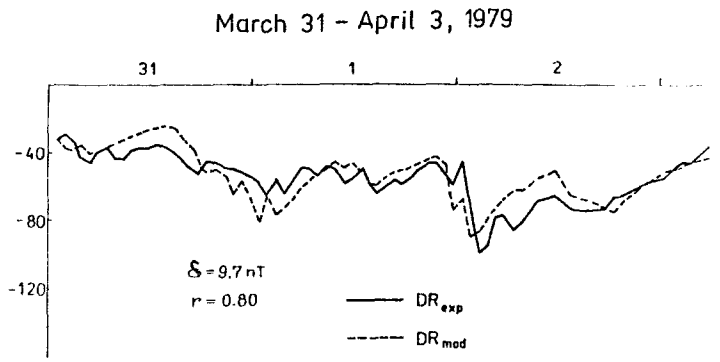

Fig. 10a.

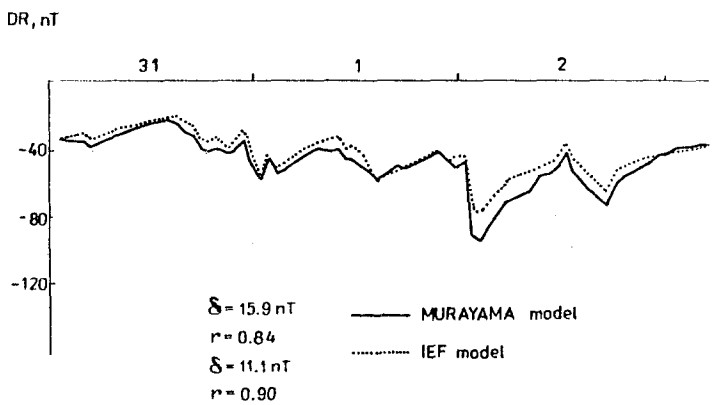

Fig. 10b.

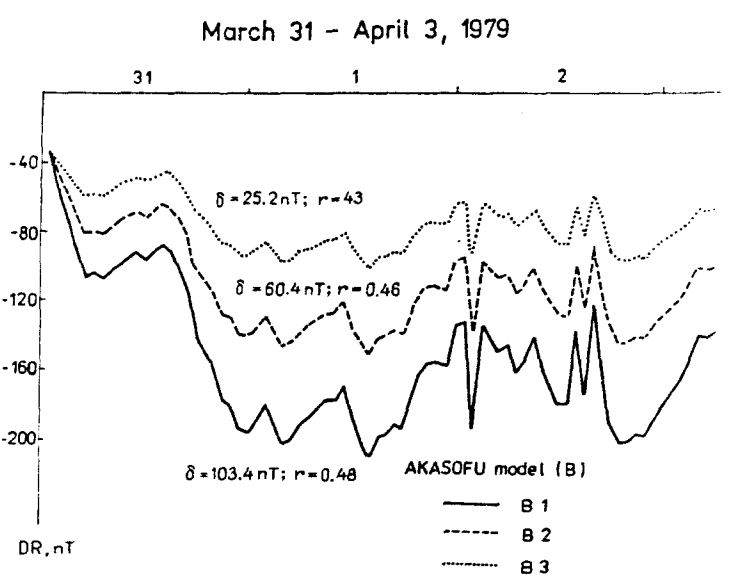

Fig. 10c.

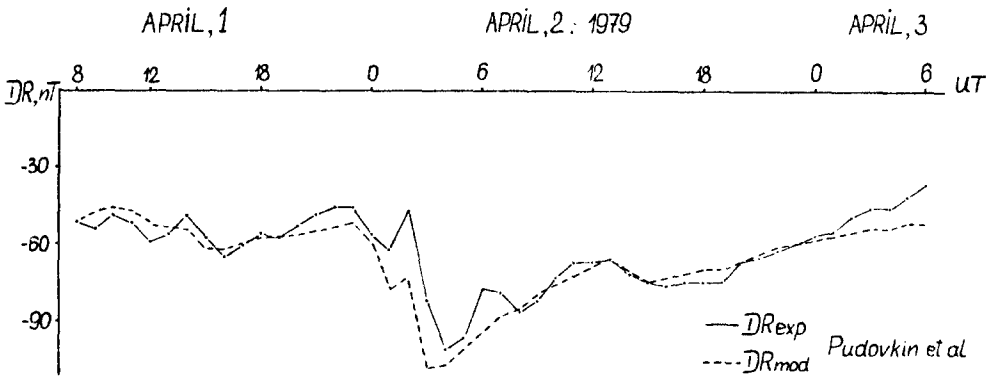

Fig. 10d.

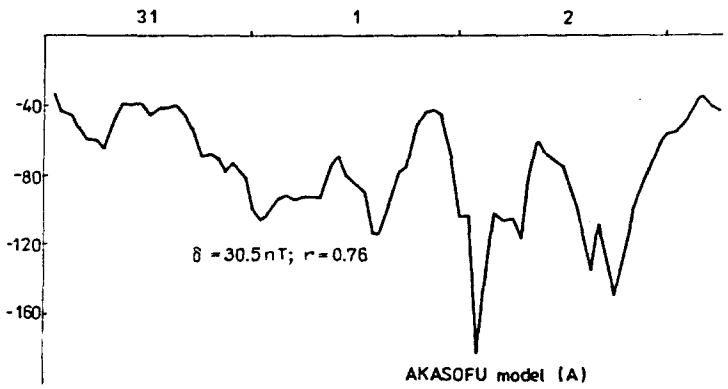

Fig. 10e.

Fig. 10. The ring-current intensity variations during the CDAW-6 interval from March 31 to April 3, 1979. (a, b, c, d) The same as in Figure 9. (e) The model (Akasofu, 1981a).

because the model was constructed on assumption that any additional injection to ring current is impossible during the storm recovery phase. The large variance for the March 22–23, 1979 storm is due in the model to a slow calculated attenuation of ring current ($\tau_{r.p.} = 150^h$) which disagrees with a much more rapid magnetic field decrease during the initial stage of the recovery phase found experimentally.

The CDAW6 intervals were studied in detail as regards the effect of interplanetary medium on generation of magnetospheric disturbances. In case of the March 22–23, 1979 interval, McPherron *et al.* (1984) used the technique of linear prediction filtering to calculate D_{st}. The technique is based on calculating the empirical response function which makes it possible to define the D_{st} index depending on solar wind parameters (Iyemori *et al.*, 1979). Figure 11(f) presents the experimental and predicted D_{st} values during the CDAW6 interval from March 22 to 23, 1979. The response functions inferred from the observations of 1967–1968 were used. The IEF makes it possible to find

$\sim 47\%$ of the D_{st} value. The relationship of D_{st} to the solar wind parameters does not seem to be described by a time-invariable linear function. The solar wind parameters define the function of injection to ring current, while the *DR* intensity is defined by the ratio of injection and energy loss from ring current. The comparison between the modelling results presented in Figure 11 shows that the technique of linear prediction filtering applied to the final stage of magnetic disturbance yields much worse results compared with the models based on solving the energy balance equation.

Observed and calculated on the base of different authors models magnetic field

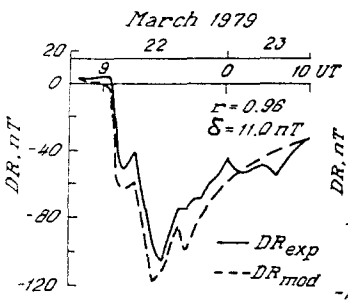

Fig. 11a.

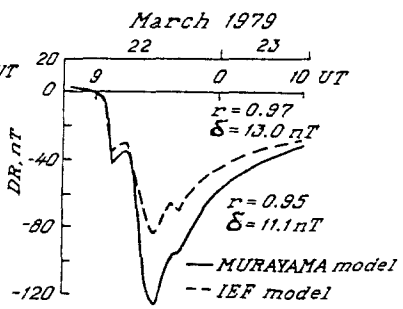

Fig. 11b.

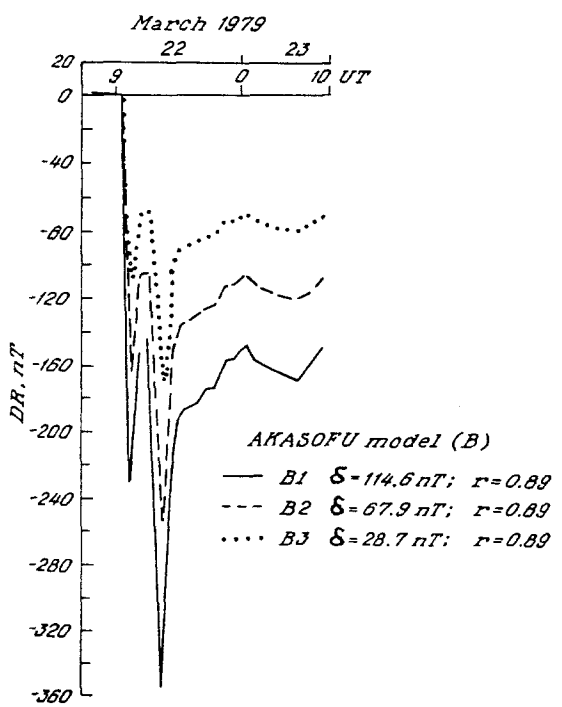

Fig. 11c.

variations during January 7–9, 1979 magnetic storm are shown in Figure 12. Table II contains values of r and δ. Grafe (1988) model is the worst for this storm.

Figure 13 presents the distribution of the number of magnetic storms with different values of r.m.s. deviations δ and of r between DR_{mod} and DR_{exp} calculated in terms of the Pisarsky *et al.* (1989) model. The modelling was made for 170 magnetic storms which occurred from 1967 to 1982. In case of most of the storms, the δ value is ranging between 5 and 15 nT, and the value of r between 0.85 and 1.0, thereby indicating a sufficiently good convergence of the model calculation results with observation data. The model proposed above must be assumed to adequately describe the fraction of the storm-time geomagnetic field variations which is controlled by the geoeffective characteristics of interplanetary medium and, therefore, responds directly to the variations of

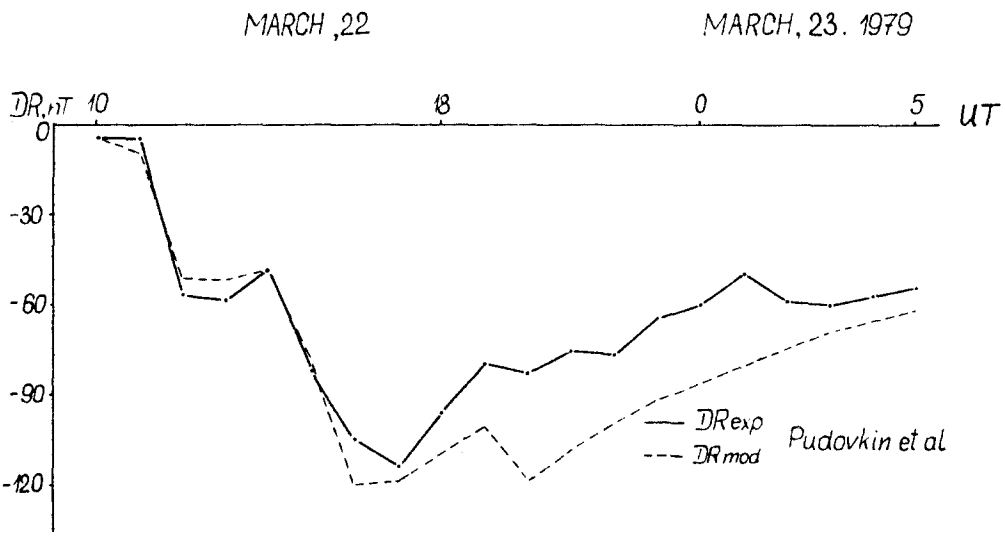

Fig. 11d.

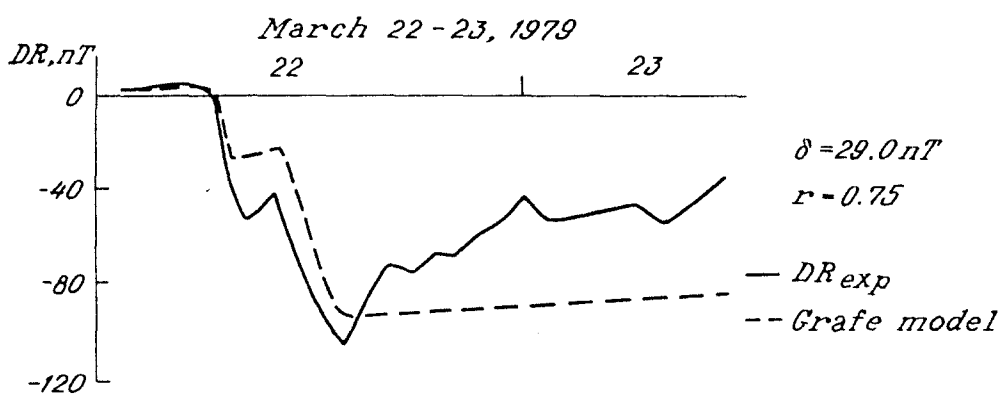

Fig. 11e.

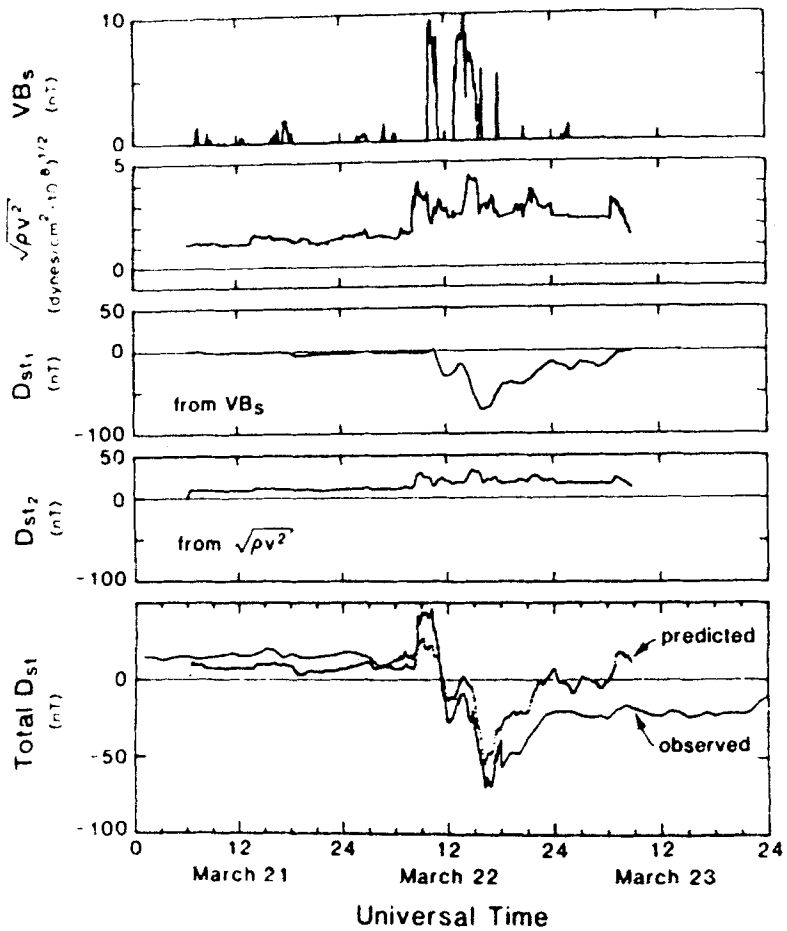

Fig. 11f.

Fig. 11. The same as in Figure 10(a–d) during the CDAW-6 interval from March 22 to 23, 1979. (e) DR_{exp} and DR_{mod} according to Grafe (1988). (f) D_{st} index during the first CDAW-6 interval. The two top panels present the input solar wind data: namely, the solar wind electric field and dynamic pressure. The middle panels display the D_{st} components predicted by each input. The bottom panel compares the total predicted D_{st} index with observation data (McPherron *et al.*, 1984).

the interplanetary medium parameters. The given fraction is the basis of the storm-time variation of the Earth's magnetic field in low and medium latitudes.

From the *DR* values calculated in terms of different models for particular magnetic storms it follows that the present-day models represent quite properly the intensity and time variations of *DR*. The modelling is made on the basis of the data on not only the IMF sign and intensity but also the interplanetary medium parameters (V and n). The question arises as to what of the model must be preferred. Any comprehensive analysis is difficult to make at present because the authors do not present the quantitative criteria for comparing between DR_{exp} and DR_{mod} in all cases (Burton *et al.*, 1975; Akasofu, 1981a), or give only the correlation coefficient r (Murayama, 1982, 1986b). The models

have been based on the hourly values of the field which smoothen shorter-term intensive variations. The high values of r indicate that the time variations are alike, but do not exclude that substantial differences in the intensities can occur. Probably, two criteria must indicate the modelling accuracy, namely, r and the r.m.s. deviation δ. Our experience has shown that the modelling is most accurate in terms of the Murayama (1986b) and Pisarsky *et al.* (1989) models or the modified Murayama model. The Pudovkin *et al.* (1989) model yields somewhat worse results. The comparison among

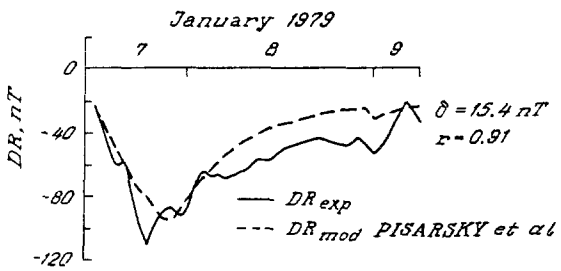

Fig. 12a.

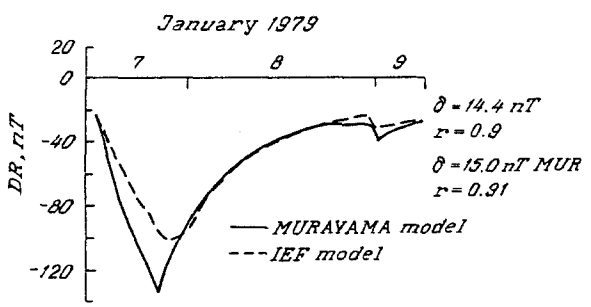

Fig. 12b.

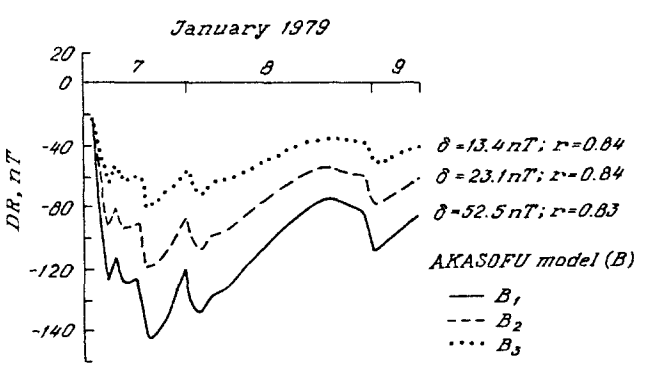

Fig. 12c.

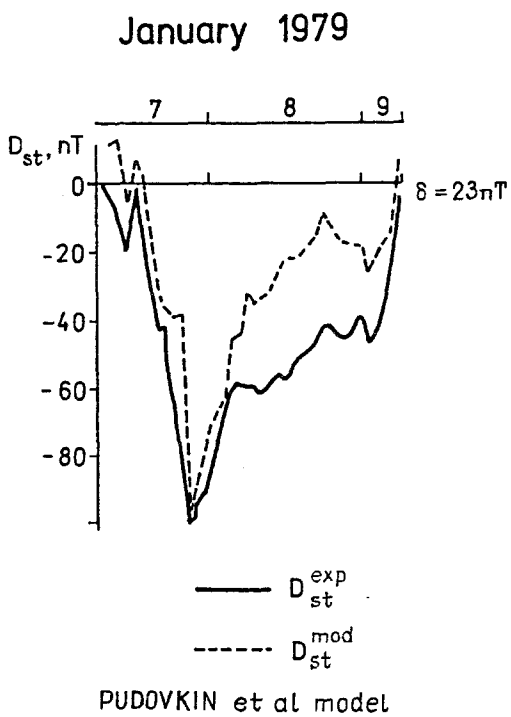

Fig. 12d.

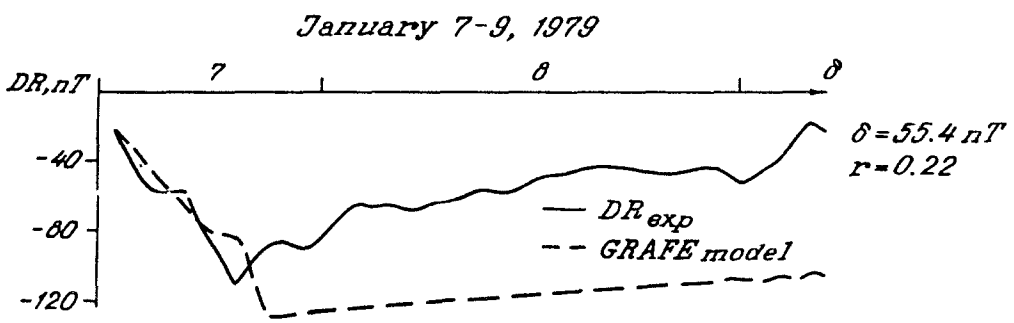

Fig. 12e.

Fig. 12. The same as in Figure 9 during the January 7–9, 1979 magnetic storm.

the values of δ obtained for a couple of dozens of storms in terms of the Pudovkin *et al.* (1988) and Pisarsky *et al.* (1989) models has shown that the mean values of δ prove to be 18 and 16 nT, respectively (see Table III). The difference does not seem to be substantial, but a consecutive improvement of the Pudovkin *et al.* (1988) model through four stages made the values of δ consecutively better, namely, 24, 20, 21, and 18 nT. So, the 2 nT decrease in δ is a further step in improving the ring-current modelling.

The use of a ε-dependent injection function F in modelling the ring current yields

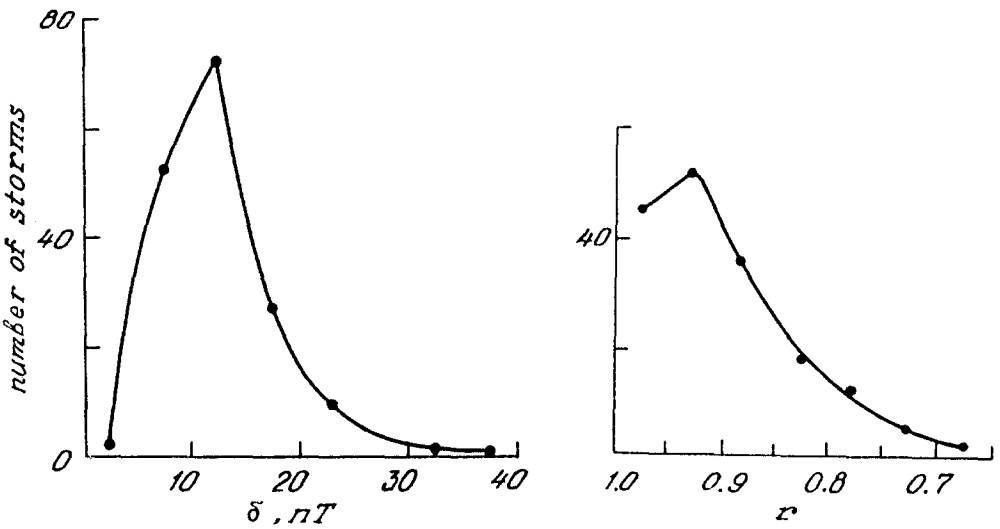

Fig. 13. The distribution of the number of magnetic storms at different values characterizing the r.m.s. deviation δ and the correlation coezfficient r of DR_{exp} and DR_{mod} calculated in terms of the model (Pisarsky *et al.*, 1989).

much higher values of δ and reduces the correlation between DR_{mod} and DR_{exp}. The values $F = 0.7\varepsilon$ adopted by Akasofu (1981a) made it necessary to use enormously high rates of ring-current decay (τ of up to 0.25 hours) for such a great injection to be compensated for. With such a high-decay rate, the energy loss from the ring current begins exceeding the energy input even during the main phase of a storm (Stern, 1984). At the same time, however, even such a rapid decay does not prevent the overestimated DR_{mod} values from occurring. Smaller values of δ are obtained with the injection function where the energy fraction supplied to DR is decreased down to $\frac{1}{3}$ of ε.

The modelling of DR may be used to make an attempt to answer the question put by Kamide (1979a), namely, whether the main phase decrease in the H component can be reproduced solely from information on substorm activity or on the IMF. The general DR enhancement during a magnetic storm is controlled by the large-scale electric field in solar wind, by its variability. The solar wind density has also a certain effect. The shorter-term DR variations are affected by the injections to the inner magnetosphere during substorm intervals. Considering the substantial effect of the IEF and of the IEF-controlled energy increase in the inner magnetosphere on the occurrence of the main phase of a magnetic storm, the storm may be represented by the following scheme:

	compression of	convection		substorm
storm =	the	+ (IEF-relevant	+	(pulsed .
	magnetosphere	DR energization)		injection)

The energy increase in DR related directly to the IEF may be due to the increased plasma convection from the magnetospheric tail and to the plasma acceleration (Harel *et al.*, 1981); to the approach to the Earth of the particles trapped earlier to the ring

TABLE III

Standard deviations δ of calculated D_{st}^{mod} from experimental data D_{st}^{exp} in different versions of Pudovkin *et al.* (1988) models

No.	Data and time (UT) of the beginning of the interval	Duration (hr)	Standard deviation δ				
			Pudovkin *et al.* (1988)				Pisarsky *et al.* (1989)
			1	2	3	4	
1	Feb. 7, 1967 11:00	85	25	19	16	8	9
2	Feb. 15, 1967 23:00	87	24	27	34	21	15
3	Feb. 23, 1967 02:00	46	19	18	11	10	9
4	Jan. 19, 1968 00:00	18	7	7	8	13	–
5	Feb. 10, 1968 11:00	61	24	19	17	20	15
6	Feb. 14, 1968 23:00	36	21	15	10	8	–
7	Feb. 27, 1968 11:00	26	8	9	6	6	–
8	Feb. 10, 1969 19:00	37	24	18	19	23	21
9	Mar. 7, 1970 13:00	41	49	51	54	25	32
10	Mar. 16, 1974 00:00	72	8	7	8	9	10
11	Apr. 18, 1974 00:00	27	15	8	8	11	10
12	July 3, 1974 18:00	71	27	20	21	17	27
13	Aug. 2, 1974 00:00	39	11	15	22	19	–
14	Jan. 13, 1975 03:00	61	9	18	24	22	–
15	Aug. 27, 1978 13:00	61	42	30	36	38	21
16	Jan. 7, 1979 07:00	47	22	21	19	23	13
17	Mar. 7, 1979 06:00	162	20	17	9	11	7
18	Apr. 25, 1979 05:00	163	26	16	15	11	13
19	July 26, 1979 16:00	27	11	8	8	13	12
20	Aug. 29, 1979 05:00	21	30	17	17	33	28
The mean $\bar{\delta}$			24	20	21	18	16

current (Lyons and Williams, 1980; Stern, 1984); to the enhancement of the ring current associated with large-scale field-aligned currents of zone 2 and its movement towards the Earth (Siscoe, 1982); and to the occurrence of ionospheric ions in the ring current (Gloecker *et al.*, 1985; Shelley *et al.*, 1985). The occurrence frequency of the ion fluxes moving from the ionosphere to the magnetosphere is characterized by the same latitude distribution as the aurora occurrence frequency (Ghielmetti *et al.*, 1978). A field-aligned electric field with a potential difference of up to 10 kV existing at altitudes of 1–2 R_E in the auroral latitudes accelerates the auroral particles (Reiff *et al.*, 1988). The ion fluxes entering the magnetosphere from the auroral zone during a storm suffer a stochastic acceleration and are transported to the inner magnetosphere where they are additionally accelerated under adiabatic motion. Cladis and Francis (1985) have concluded that the above mentioned mechanism of ionospheric ion pumping-up to $4 \leq L \leq 8$ yields an ion distribution fucntion in agreement with the ISEE1 measurements during the December 11, 1977 storm. It is contribution of the ionospheric and magnetospheric ions that defines the determinant role of the IEF in the generation of the ring current.

The contribution of substorms is associated with the unsteady-state injection resulting from the transformation of the energy accumualted earlier in the magnetospheric tail

(Mauk and Meng, 1987). The injection makes an additional, but not determinant, contribution to the ring-current evolution. This is indicated by a sufficiently good reproducibility of *DR* on the basis of the solar wind and IMF parameters. Probably, the injection occurs first from the magnetospheric tail to the outer magnetosphere and is then transferred to the Earth by convection. A similar result concerning an insignificant contribution of pulsed injection to ring current during substorm intervals was obtained by Liu *et al.* (1988) by analyzing the electric interaction among different regions in the solar wind-magnetosphere-ionosphere system. The relationships of magnetic storms to substorms noted elsewhere arises from the fact that the function F of injection to ring current is usually proportional to substorm intensity (to the *AE* index). Besides, the substorms proper, their occurrence and intensity, are controlled, to a great extent, by the solar wind parameters. The effectiveness of the substorm contribution to the ring-current field differs from case to case, for the *DR* variation is defined by not only the injection intensity $F(t)$ but also the decay term DR/τ. Even in the presence of injection can the *DR* intensity decrease or be preserved at a stationary level, depending on the relation between injection and decay.

From the modelling it follows that the dawn-dusk electric field must exceed an apparent threshold level in order to trigger the storm main phase of a given intensity. A definite IEF value is required for a magnetic storm with a prescribed intensity in the magnetic field decrease maximum to occur (Russel *et al.*, 1974). The injection to ring current occur also at lower IEF intensities, but the weak fields are accompanied, respectively, by small field decreases in low latitudes which are frequently difficult to attribute to magnetic storms.

Thus, there does not exist any threshold in the interplanetary medium parameters which has to be exceeded for the ring current to begin increasing. The ring current exists permanently and, in the absence of magnetic storms, is supported by the permanent injection thereto. Besides the lifetime of the ring-current particles increases during quiet conditions. The current begins increasing in connection with an increase of $F(t)$ without occurring any threshold, but the *DR* can reach its high intensities only when strong IEFs occur.

6. Magnetic Activity Dynamics During a Magnetic Storm

Magnetic storms are the greatest global phenomena including the ring current and quite a number of other geophysical events, such as magnetospheric substorms. In principle, therefore, they should have been the main object of studies in the field of solar-terrestrial physics. In recent years, however, main attention was paid to the magnetospheric substorms which were assumed to be elementary nucleation centers of mighty processes covering the entire magnetosphere. However, any magnetic storm is accompanied by the effects which define its occurrence differing from a mere sum of substorms.

The ring-current evolution in the inner magnetosphere gives rise to deformation of the geomagnetic field lines, thereby affecting also the position of the plasma domain boundaries in the magnetosphere (Akasofu and Chapman, 1972). As a result, the

characteristic features of auroral events can be found up to the middle latitudes. The various aspects of the magnetospheric activity dynamics will be examined below using the example of the March 23–24, 1969 magnetic storm which attracted repeatedly attention of different researchers (Akasofu, 1981c; Tinsley and Akasofu, 1982; Khorosheva, 1986; Sumaruk *et al.*, 1989).

The geomagnetic field variations were analyzed using the magnetograms of the worldwide network of 82 observatories. The deviations of three magnetic field components during the magnetic storm interval from the respective level during the interval from 12 00 UT on March 22 to 12:00 UT on March 23, 1969, which was taken to be a quiet interval, were found at each multiple 10-min UT moment. The resultant ΔH, ΔD, and ΔZ values of the field were transformed into the geomagnetic components ΔX, ΔY, and ΔZ by the relations

$$\begin{aligned} \Delta X &= \Delta H \cos(\psi + D) + \Delta D \sin(\psi + D), \\ \Delta Y &= -\Delta H \sin(\psi + D) + \Delta D \cos(\psi + D), \end{aligned} \tag{13}$$

where D is angle between magnetic and geographic meridians; ψ is angle between geographic and geomagnetic meridians. The hourly values of the components were obtained for each UT hour by averaging the 10-min values of a respective component.

The geomagnetic components ΔX were used to calculate the D_{st}-, AU-, AL-, and AE-indices of geomagnetic activity by selecting an appropriate network of magnetic observatories.

The interplanetary space parameters were defined by the solar wind ion velocity and number density and by the intensity of the IMF components. The IMF components were inferred from the plots of 81.92 mean values of the IMF modulus and of the latitudinal and longitudinal angles measured on IMPE (Explorer-35) in the solar-ecliptic coordinate system. The plots were used to obtain 10-min averages, whereupon the conventional technique (Russel, 1971) was used to calculate the values of three IMF components in the solar-ecliptic and solar-magnetospheric coordinates. Comparing the thus obtained IMPE values of IMF with the data of magnetic measurements on OGO-5 and HEOS for the same period has demonstrated that the IMF component vector variations are identical, but the IMF component intensities are slightly different. The present work makes use of a continuous series of IMF measurements on IMPE which was located within the region with coordinates $X_{SE} \sim 20\ R_E$, $Y_{SE} \sim 60\ R_E$, i.e., within solar wind far from bow shock. The 10-min bulk velocity (v) and number density (n) of solar wind protons were inferred from the OGO-5 measurements during the interval from 14:00 UT on March 23 to 08:30 UT on March 24, 1969 when the satellite entered the magnetosphere, and from the HEOS data obtained after 08:30 UT and presented in (King, 1977) as 3-hour values of v and n. OGO-5 measured also the values of v and n for α-particles. The values $n_\alpha < n$ by more than an order. Therefore, only the pressure of the solar wind proton flux on the magnetosphere is allowed for below when calculating the magnetic effects of the DCF currents.

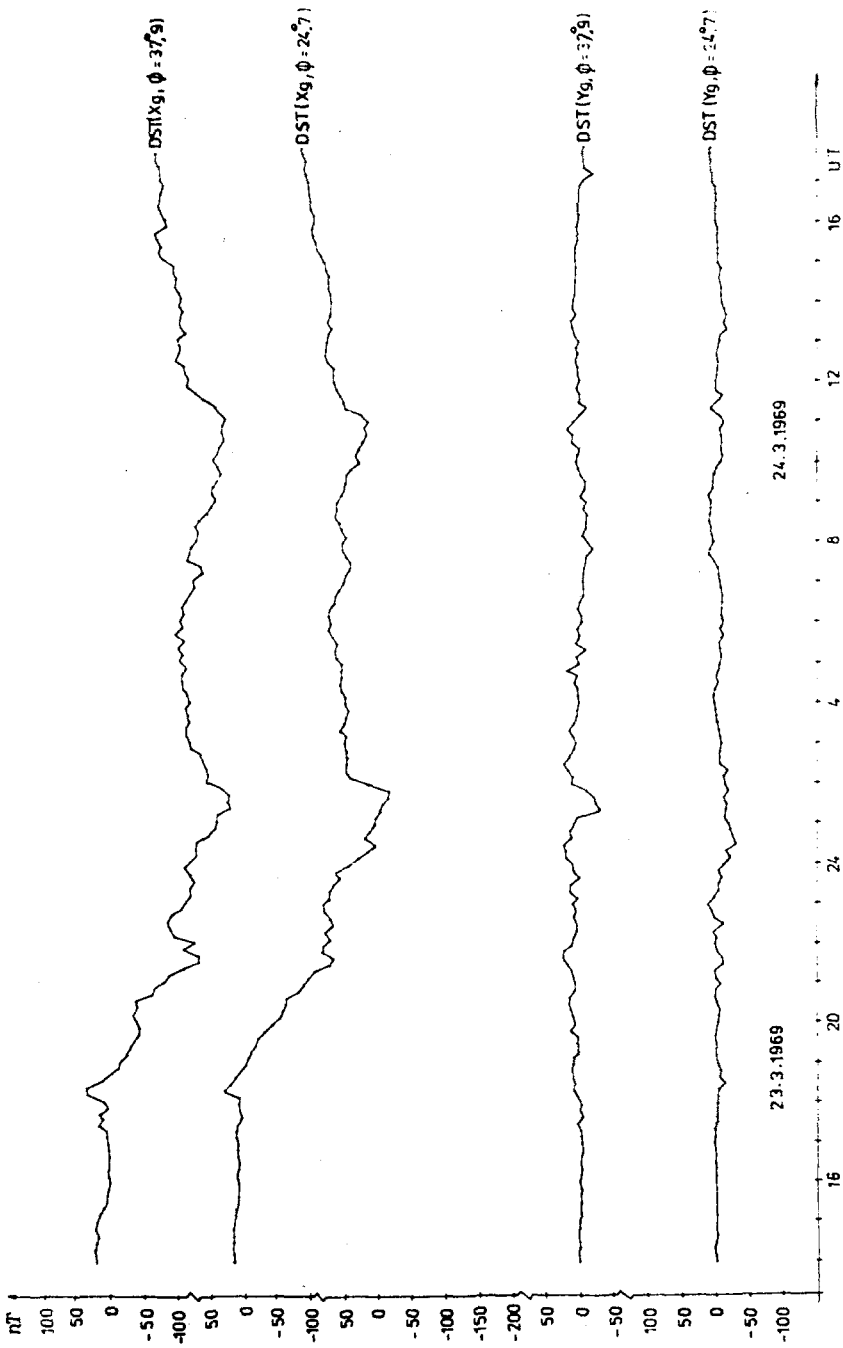

Fig. 14. D_{st} variation during the March 23–24, 1969 geomagnetic storm at the middle ($\phi = 37.9°$) and low ($\phi = 24.7°$) latitudes in the direction of geomagnetic pole (the upper two curves) and of geomagnetic east (the lower two curves).

6.1. RING CURRENT AND AURORAL ELECTROJETS

The 10-min values of the horizontal components (D and H) of geomagnetic field variations were used to calculate the D_{st} variations of the geomagnetic X- and Y-components at geomagnetic latitudes $\phi = 24.7°$ and $\phi = 37.9°$, as presented in Figure 14. The D_{st} variation reflects the variation of the intensity of the symmetric fraction of ring current during the storm. Indeed, the D_{st} variation is clearly traced in the X_g component, but is absent in the Y_g component. The $D_{st}(X_g)$ intensity increases equatorwards, just what must be the case for the magnetic field of symmetric ring current.

Figure 15 presents the D_{st} and DR variations inferred from the data of eleven low-latitude observatories arranged with a sufficient uniformity in longitude. The DR

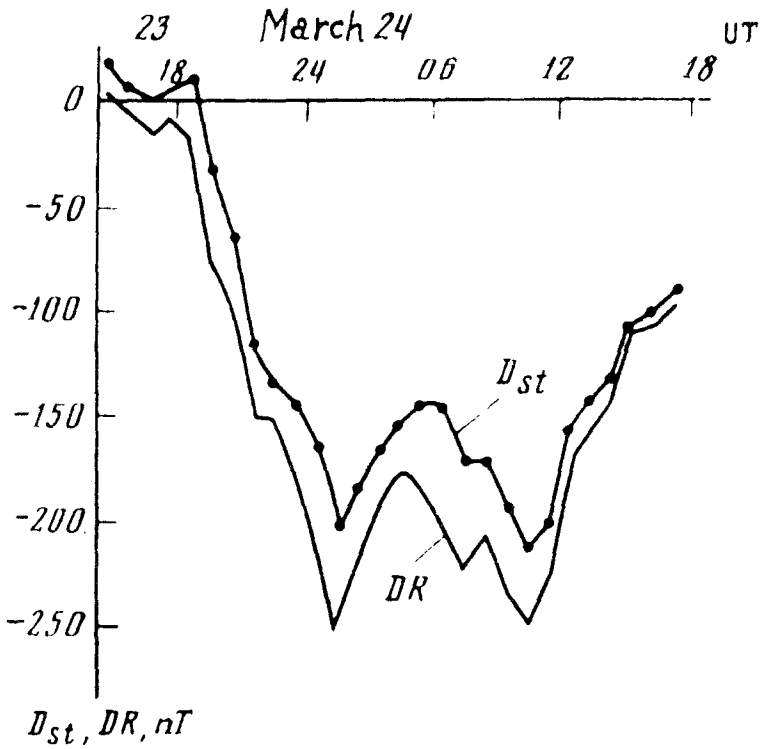

Fig. 15. The variations of D_{st} and DR magnetic field at geomagnetic equator during the March 23–24, 1969 strong magnetic storm (Sumaruk *et al.*, 1989).

values were calculated using (7). The DR evolution was accompanied by an intensification of magnetospheric substorms which are reflected as an enhancement of auroral electrojets. The standard AU, AL, and AE indices characterizing the auroral electrojet intensity are inferred nowadays from the magnetograms obtained at the longitudinal chain of magnetic observatories at $62° \leq \phi \leq 70°$.

The DR generation and the geomagnetic field line deformation give rise to an

equatorward displacement of auroral electrojets. As a result, the *AE* indices inferred solely from the data of auroral observatories stop reflecting the electrojet intensity. The use of the *X* and *Z* latitude profiles in the near-midnight – early dawn MLT sectors at different UT moments has made it possible to find the position of the westward convective electrojet center as a function of *DR* intensity. Figure 16 presents the position

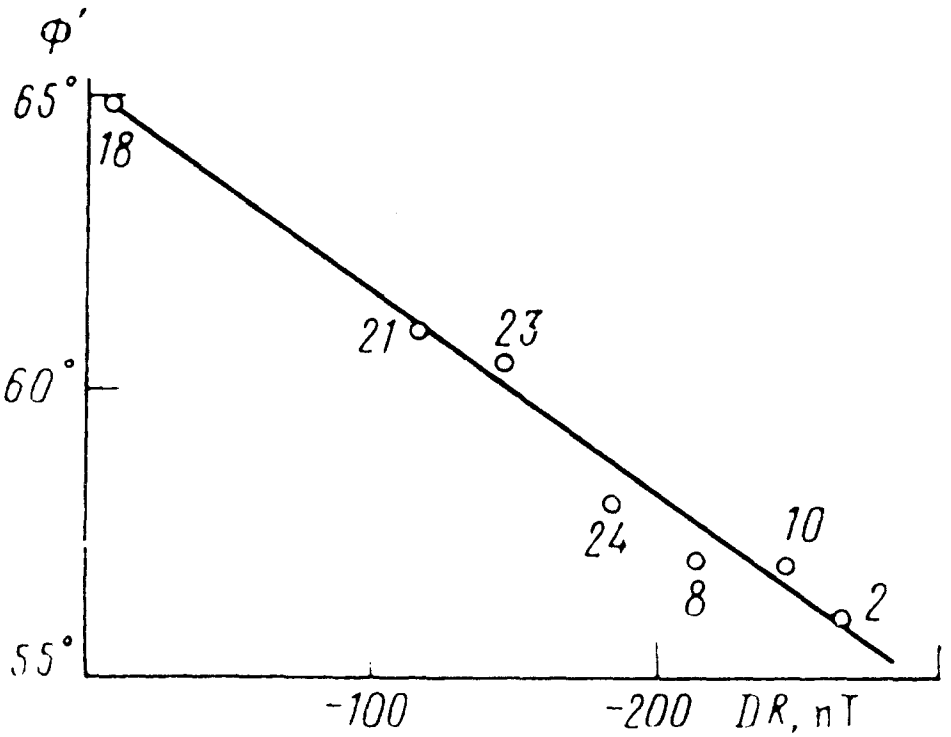

Fig. 16. The position of the westward convective electrojet center in the near-midnight–early dawn MLT sector as a function of *DR* intensity. The numerals at the dots are UT hours. The straight line has been obtained by the least-squares method according to Sumaruk *et al.* (1989).

of the convective electrojet center (the time moment before a pronounced substorm activization were selected when the electrojet get stratified and the separated fraction begins moving rapidly polewards) as a function of the *DR* intensity at the UT moments indicated by numerals at the points. The electrojet moves to lower latitudes as *DR* increases and its position is described by the relation

$$\phi = 65.2^\circ + 0.035DR \tag{14}$$

in the $0 > DR > -250$ nT interval, where *DR* is in nT.

At $DR < -100$ nT, therefore, the westward electrojet escapes from the belt of the auroral observatories used to find the *AE* indices. So, the data from subauroral observatories up to $\phi \sim 56^\circ$ must be used to estimate the auroral electrojet intensity if only the north–south component of geomagnetic field variations is used.

The equatorward shift of electrojet in the intervals of the maximum D_{st}-variation development during magnetic storm was analyzed by Khorosheva (1986). The results of the analysis have been summarized by the plot shown in Figure 17. The $\Lambda'_{\min}$ curve is the maximum equatorward shift of the westward electrojet as a function of $D_{st}^{\max}$. The

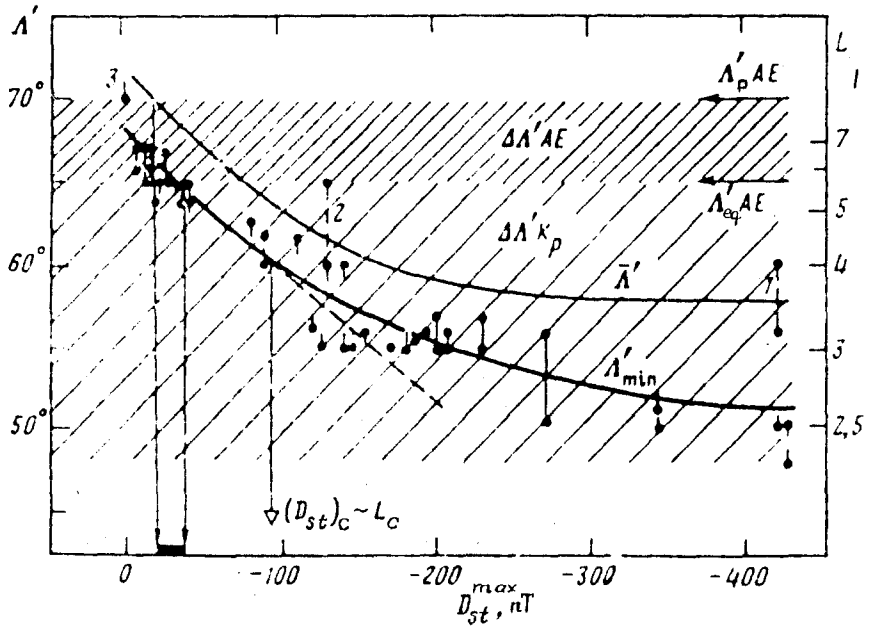

Fig. 17. The auroral electrojet latitudes Λ', versus the storm–maximum $D_{st}^{\max}$-variation ($\Lambda'_{\min}$ and $\bar{\Lambda}'$ are, respectively, the lowest and mean latitudes). The dots are the lowest latitudes where the electrojets are detected. The vertical bars at the dots are the directions to the electrojets inferred from the Z sign. The dots connected with vertical bar show the measurements at two stations. $\Delta\Lambda' AE$ is the latitude belt the data wherefrom are used to construct the standard $AE(12)$ index. $\Lambda'_p AE$ and $\Lambda'_{eq} AE$ are the poleward and equatorward boundaries of the belt $\Delta\Lambda' AE$. $\Delta\Lambda' K_p$ is the latitude belt the data wherefrom are used to construct the K_p-index. $(D_{st})_c$ is the critical D_{st} value at which the behaviour of the dependence $\Lambda'(D_{st})$ changes (Khorosheva, 1986).

Λ' curve is the storm-average position of the electrojet drawn over three reference points at $D_{st}^{\max} = -420$ nT (1), -130 nT (2), and 0 nT (3). As the ring-current intensity increases, the westward electrojet escapes from the latitude band where the observatories used to find the AE ($\Delta\Lambda' AE$) index shown in Figure 17 are located. Thus, the standard AE index ($AE(12)$ in the terminology of Akasofu *et al.* (1983)) gives a more or less reliable result for but a narrow disturbance interval which is indicated by arrows in the figure and is characterized by a D_{st} intensity of $\sim -(20–40)$ nT. The shift of the auroral electrojet to the subauroral latitudes was accompanied by occurrence of auroras on the latitudes. The night-time auroras are usually located on $\Phi' \geq 65°$. According to the data from the network of the meteorological stations which observe the auroras, they occurred on lower latitudes during the night from March 23 to 24, 1969. At 22:00 UT, rayed bands and arcs were observed to the north and at zenith of some stations on

$\Phi' \sim 56-59°$ over the West Siberia in the dawn sector. From 00:00 UT on March 24, auroral rays were observed near zenith at the stations of the European part of the USSR, for example at Vologda ($\Phi' = 55°$) and near the north horizon at Velikie Luki ($\Phi' \sim 53°$). The occurrence of auroras on the entire northern sector of the sky up to zenith near 12:00 UT on March 24 was reported by the far-east stations of the USSR on $\Phi' \sim 56-57°$. So, the occurrence region of the intensive discrete auroral forms, which were seen clearly on the sky by meteorological observers, extended up to $\Phi' \sim 56-57°$ during the *DR* intensification period near 00:00 UT and 10:00 UT. According to the relation (10), there are just the latitudes of the westward auroral electrojet in the night sector. Khorosheva (1987) noted that the stormtime-lowest latitudes of the auroral electrojet and of the auroral oval were approximately the same in the night sector of the magnetosphere.

The *AE* indices inferred from the data of the standard chain of auroral observatories supplemented some subauroral observatories are designated below as *AE'* and were estimated by a mean-hourly deviation of *H* from its quiet level at the network of auroral and subauroral observatories. Figure 18 demonstrates the difference in the intensity of

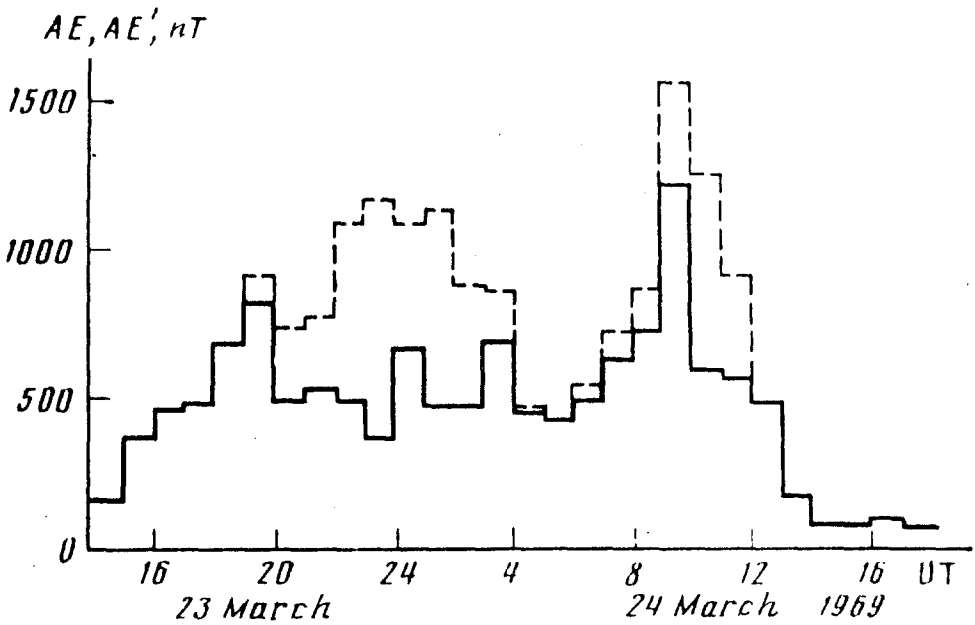

Fig. 18. The variation of the hourly values of *AE* (the straight line) and *AE'* (the dashed line) indices during the March 23–24, 1969 storm (Sumaruk *et al.*, 1989).

the *AE* indices characterizing the total amplitude of the eastward and westward auroral electrojets and infered from the data of only auroral observatories or of the latter supplemented by a network of subauroral observatories. The *AE* and *AE'* are the same during the interval from 14:00 to 19:00 UT on March 23, thereby indicating that the

disturbance maximum was located at the latitudes of the auroral belt. After that, the difference between AE and AE' increased rapidly because the auroral electrojets moved to subauroral latitudes. A pronounced difference is seen even in the character of time dependences of AE and AE', namely, AE' increases and is peaking at 23:00–02:00 UT and decreases afterwards by 04:00–06:00 UT, whereas AE fluctuates near $a \sim 500$ nT level from 16:00 to 06:00 UT.

The relationship of D_{st} to auroral electrojet intensity during the given storm was discussed by Akasofu (1981a) and Khorosheva (1986). Akasofu has concluded that a linear relation of AE to D_{st} exists at small D_{st} values and that the linear relation is violated as D_{st} increases (see Figure 19(a)). The dual character of the relationship of AE to D_{st}

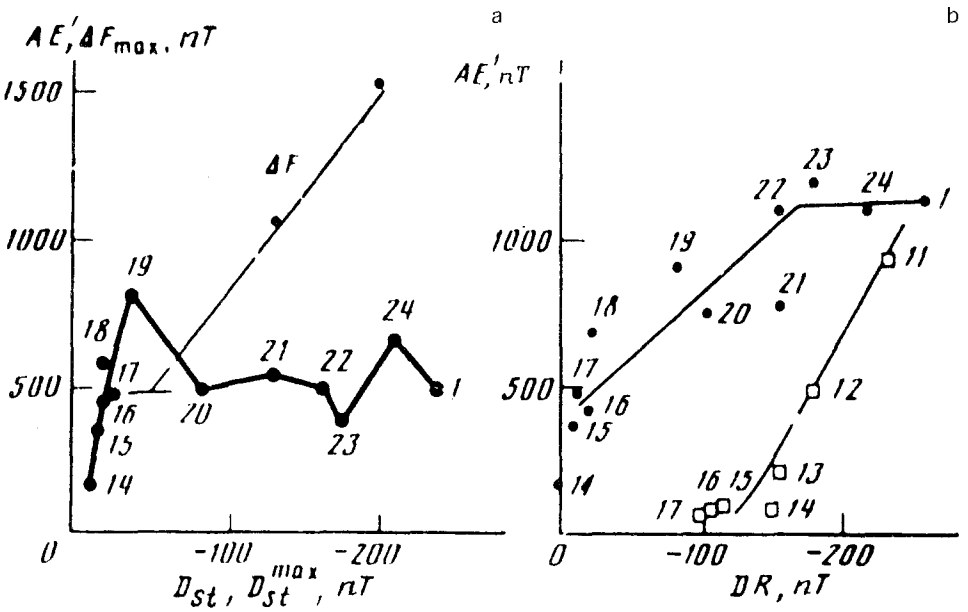

Fig. 19. The relationships among the hourly values of the intensity of auroral electrojets and of ring current. (a) AE and D_{st} during the March 23–24, 1969 storm (Akasofu, 1981c). The numerals at the dots are hours of UT. ΔF_{max} and D_{st}^{max} for the storm-maximum values during some storms (Khorosheva, 1986); ΔF_{max} is the total vector of magnetic field disturbance produced by westward electrojet. (b) AE' and DR during the same storm. The dots are for the main phase, the crosses are for the recovery phase. The numerals at the dots and at the crosses are UT hours.

is treated to be a consequence of the occurrence of two mechanisms for redistribution of the energy supplied to the magnetosphere from solar wind, namely, the energy at small D_{st} values is lost proportionally for current dissipation in the auroral ionosphere and the ring-current generation, while the energy at intensive D_{st} is lost predominantly for ring-current generation. Khorosheva assumes that the data on numerous storms indicate that in case of the maximum values throughout the storm, the total disturbance vector of geomagnetic field $F_{max} = [(\frac{2}{3}\Delta H)^2 + (\frac{3}{2}\Delta Z)^2]^{1/2}$ shows a linear relation to D_{st}^{max}. Figure 19(a) shows the respective dependence for westward electrojet. The

absence of any relationship of AE to D_{st} inferred by Akasofu (1981a) was explained in (Khorosheva, 1986) by the equatorward shift of electrojets from the latitude band where the auroral observatories are located. Figure 19(b) shows AE' as a function of DR during the same storm of March 23–24, 1969. The 14:00–01:00 UT interval corresponds to the storm main phase, while the 11:00–17:00 UT interval corresponds to the recovery phase. As a first approximation, a linear dependence $AE'(DR)$ can be adopted during the main phase from 14:00 to 22:00 UT; during the 22:00–01:00 UT interval, DR keeps increasing at a practically constant, but high, AE' value. During the recovery phase, DR decrease together with AE' (with the AE' decrease being more rapid).

The relationship between AE' and DR on Figure 19(b) is interpreted as follows. DR enhances with increasing AE' if the AE' values are calculated making allowance for subauroral stations. This is, however, but a trend from which marked deviation occur at individual hours. The deviation of the relationship of AE' to DR from a functional mode arises because DR is related to AE' through (4) with, as shown below, the injection function F being proportional to the AE' intensity. Depending on the relation between $F(AE')$ and DR/τ, the DR intensity may increase both with increasing AE' and at a fixed AE' level if the latter is sufficiently high. The character of the relationship between DR and AE' is defined by the fact that the DR variation is determined by the balance of energy supply and dissipation from ring current, while the AE' intensity is determined solely by a value proportional to F. The relationship between $DR_{\max}$ and $F_{\max-1}$ (the ring-current intensity in the maximum of the main phase and the injection at a previous hour) was noted statistically in the data on numerous storms (Sizova and Zaitsev, 1984; Grafe, 1988; Pisarsky *et al.*, 1989) with a fairly large spread of points. The spread is quite obvious to expect because DR is proportional to the energy accumulated in the magnetosphere (considering the prehistory), while F is proportional to the energy supplied to the magnetospheric inside during a given time interval. Even in the maximum of the main phase (when $dDR/dt \sim 0$), can any close relationship of DR to F hardly be expected because the ring-current decay parameter τ during the storm main phase is not constant, but depends on F and, therefore, varies from storm to storm at the moment of $DR_{\max}$. The DR intensity at the same AE' level during the storm recovery phase is determined, to a considerable extent, by the previous $DR_{\max}$ value. With the statistics gained for numerous storms and without dividing DR into the main phase and the recovery phase, the experimental points fill the entire field, thereby making it difficult to find the quantitative relations between D_{st} and AE', D_{st} and ε, D_{st} and B_z discussed by Akasofu (1981b) and Siscoe (1982).

6.2. Magnetic field of ring current at geomagnetic poles

The ring-current magnetic field appears in practice to be homogeneous on the Earth's surface. This means that, as a result of the effect of the field, the horizontal component of the Earth's magnetic field changes at the equator, while the vertical component changes at geomagnetic poles. Figure 20 shows the variations of ΔZ at Vostok and Thule, i.e., the stations located in the geomagnetic pole regions, during the magnetic storm main phase in deviations from March 22–23, 1969. The corrections for the

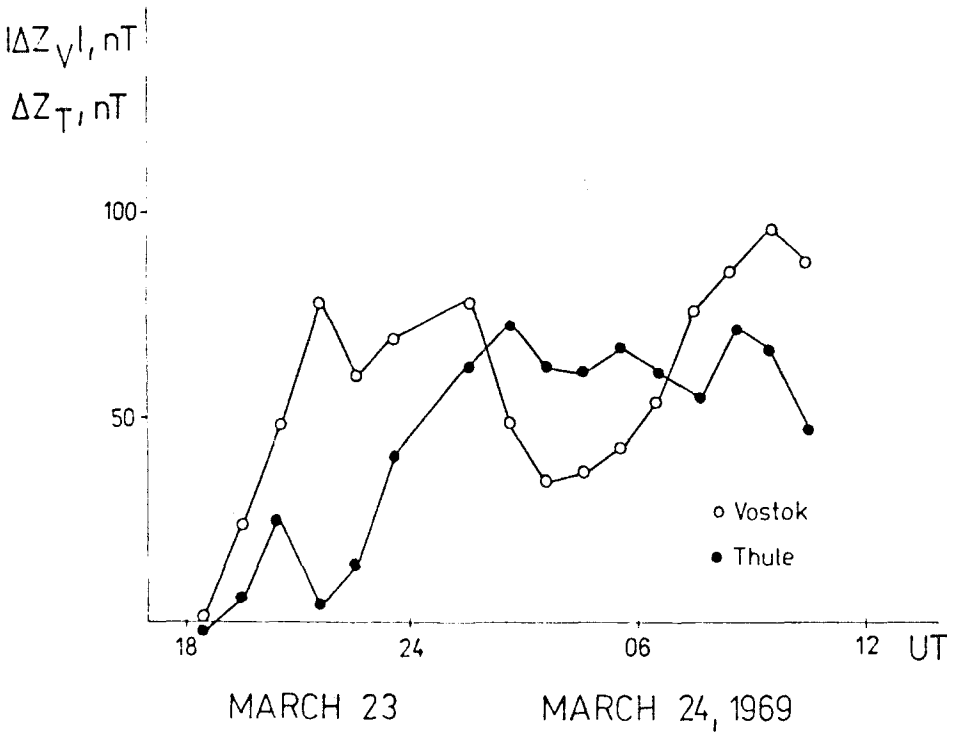

Fig. 20. The variation of the Earth's magnetic field vertical component ΔZ from an external source at Thule and Vostok in the vicinities of geomagnetic poles in Greenland and in the Antarctics during a magnetic storm. The corrections for the Z variations controlled by the IMF B_y have been made.

IMF B_z component-controlled variations of the Z-component (Sumaruk *et al.*, 1980) at the two observatories have been introduced. It is seen that, as a result of the ring-current development in the magnetosphere, the field modulus increases at poles and decreases at the equator in practice synchronously. The increase in the modulus agrees with the *DR* field direction at the geomagnetic poles. Rough estimates of the ΔZ values relevant to the *DR* field at the equator have yielded

$$\Delta Z^e = \Delta H^e_{\mathrm{eq}} = \tfrac{2}{3}\Delta H_{eq}\,, \qquad \Delta Z = \tfrac{1}{2}\Delta Z^e = \tfrac{1}{3}\Delta H_{eq} = \tfrac{1}{3}DR\,,$$

where ΔZ and ΔH_{eq} are intensities of the variations observed on the Earth's surface; ΔZ^e and ΔH^e_{eq} are the variation fractions due to external sources. The relation between ΔZ and ΔH_{eq} was derived making allowance for the fact that the fields of the external and internal sources on the Earth's surface are combined in H and are subtracted in Z-component. Thus, the ΔZ value at the geomagnetic poles must be ~ 80 nT in the *DR* development maximum of the given storm. It is the like values that were observed actually in the vicinities of the geomagnetic poles. At Thule, the ΔZ variations were somewhat delayed relative to the *DR* development commencement. The storm-time ΔZ disturbance vector direction at the observatory coincides with the direction of the magnetospheric ring-current field.

6.3. Relationship of Magnetospheric Activity to the Function of Energy Injection from Solar Wind

The auroral electrojets and the ring current get intensified during the magnetic storm because the energy flux from solar wind to the magnetosphere increases. The flux is controlled by the parameters of interplanetary plasma and of the IMF. The geoeffective characteristics are taken below to be the azimuthal component of solar wind electric field E_y (Burton *et al.*, 1975), the energy flux ε to the magnetosphere (Akasofu, 1981a, b), and the energy flux F to ring current (Pisarsky *et al.*, 1989). Figure 21 presents the

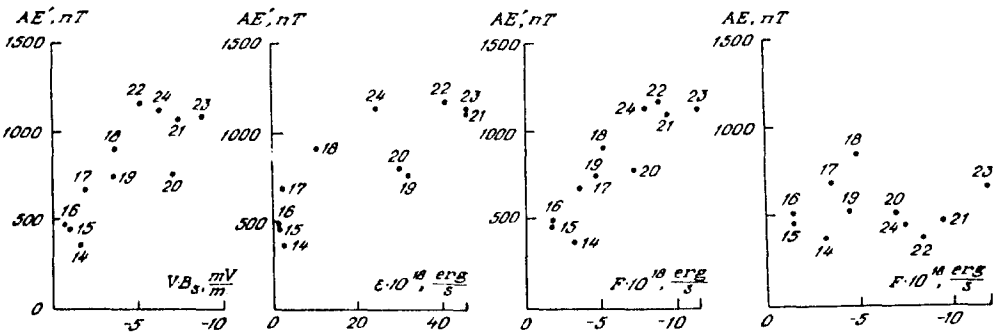

Fig. 21. Intensity of the hourly AE' indices of auroral electrojets relevant to different combinations of geoeffective parameters in solar wind which characterize the energy fluxes during the March 23–24, 1969 storm main phase. The solar wind parameters are 1 hour ahead of the AE' index. The numerals are UT hours. The right-hand side shows the same for the standard AE index.

dependences of the hourly AE' values on E_y, ε, and F, as well as on AE and F. The geoeffective characteristics are 1 hour ahead of AE' or AE.

All three characteristics are related directly to AE', namely, AE' increases with E_y, ε, or F. The AE' value is also small during the storm recovery phase when the three characteristics are nearly zero. The linear regression equations and the correlation coefficients r are

$$AE' = -86.6(B_s V) + 443\,, \quad r = 0.82 \pm 0.1 \quad \text{at} \quad |B_s V| \geq 1 \text{ mV m}^{-1}\,,$$

$$AE' = -13.0\varepsilon + 527\,, \quad r = 0.82 \pm 0.1 \quad \text{at} \quad \varepsilon \geq 2 \times 10^{18} \text{ erg s}^{-1}\,,$$

$$AE' = -81.9F + 326\,, \quad r = 0.9 \pm 0.08 \quad \text{at} \quad |F| \geq 10^{18} \text{ erg s}^{-1}\,.$$

Here, AE' is expressed in nT, $B_s V$ in mV m^{-1}, ε in 10^{18} erg s^{-1}, and F in 10^{18} erg s^{-1}.

In case of high correlations between AE' and all three geoeffective characteristics, the highest correlation occurs between AE' and F. This means that *the auroral electrojet intensity during the storm main phase is very closely related to the energy flux supplied to ring current.* It is not surprising, therefore, that a field decrease in low latitudes, which is commonly accepted to be a token of a magnetic storm, occurs simultaneously with intensive electrojets. This is why the substorms are closely associated with the ring-

current generation for hourly values and the concept has prevailed that magnetic storms are none other than intensive substorms following rapidly each other.

The relationship of AE' to F makes it possible to estimate the real hourly values of AE' indices during magnetic storm intervals if the interplanetaary medium parameters are measured during the intervals. In such cases, the data from the network of sub-auroral observatories, which contribute much to the AE' values because of the electrojet shift to lower latitudes as the ring current develops, must no longer be processed additionally. It should be noted that the absolute values of ε and F characterizing energy fluxes differ from each other by a factor of ~ 4 in Figure 21. Considering the fact that the injection function F used in the present study generates the outer and inner parts of the *DR* field, where ratio is 2, the difference between ε and F must rise up to a factor

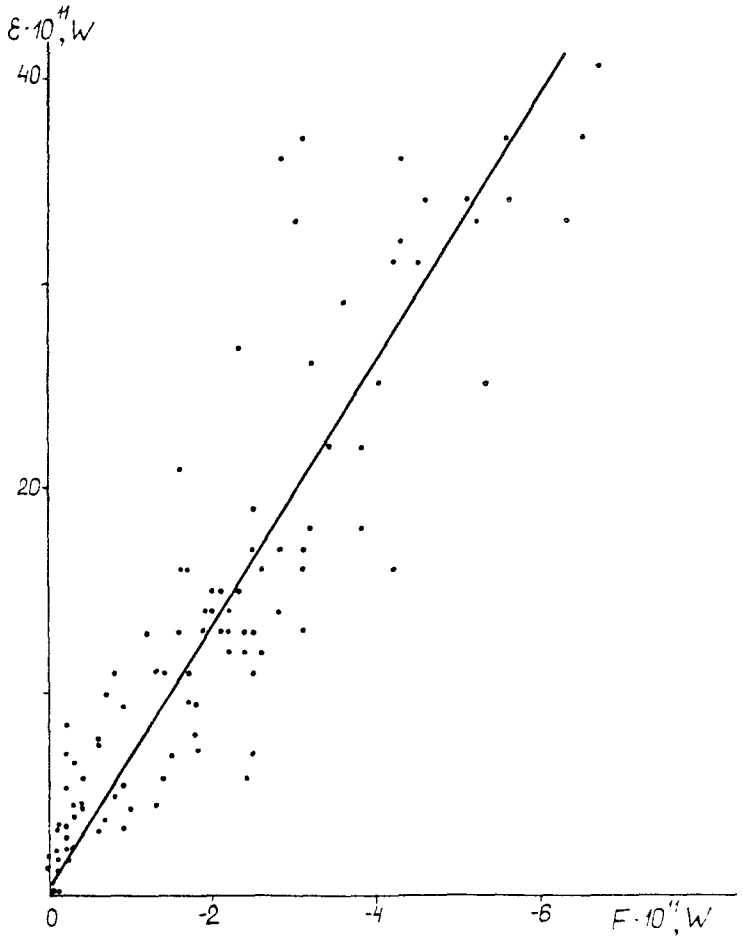

Fig. 22. Relationships among the hourly values of the function of energy injection to the magnetosphere, ε, and to the ring current, F, during the main phases of ten magnetic storms (the dots). The function F generates only the *DR* field from an external source. The solid line has been calculated by the least-squares method.

of ~ 6. More accurately, the relation between ε and F has been inferred from their hourly values shown in Figure 22 in the intervals of main phases of ten magnetic storms. The least-squares method was used to obtain the linear relation

$$\varepsilon = (6.6 \pm 0.3)F + (0.3 \pm 0.3),$$

where ε and F are expressed in 10^{11} W; the correlation coefficient of ε with F is $r = 0.9 \pm 0.05$. Approximately the same relations prove to be also valid for each individual storm. Thus, as little as 15% of ε is supplied to ring current. The difference between ε and F is undoubtedly due to the fact that ε characterizes the total energy flux from solar wind to the magnetosphere, while F defines the energy flux to ring current. This conclusion agrees with the results of modelling DR presented in Figures 9(c) and 10(c), where an ever decreasing difference between DR_{mod} and DR_{exp} (the minimum value of δ) was obtained when the injection function decreased from 0.7ε to 0.33ε. A certain difference between ε and F can also arise from the fact that the absolute value of ε is estimated, whereas F was calibrated using the particle energy in ring current on the basis of the Dessler–Parker–Sckopke (1966) theorem.

The injection to the ring current of only 15% of the total energy flux into the magnetosphere disagrees with the values suggested elsewhere (Akasofu, 1981a; Gonzalez *et al.*, 1989a). The disagreement arises from the differences in the values of τ during the main phase of a storm adopted in the calculations.

Figure 21 also presents the dependence of the standard AE index according to Allen *et al.* (1974) on F at the preceeding hour during the storm main phase. The use of only the auroral zone observatories not only results in an underestimated value of the AE index, but also gives rise to a marked spread of points in the plot. The absence of correlation between AE and F ($r = 0.08$) may even lead to the erroneous conclusion that the auroral electrojet intensity is irrelevant to the injection to ring current. The example of the given particular storm shows convincingly that the available series of AE indices have to be preliminarily analyzed thoroughly to verify their reliability when seeking for their possible relationships to the interplanetary medium parameters. The absence of any relation, or a weak relation, between them inferred in some studies may have merely arise from but insufficiently perfect methods for finding the indices characterizing the auroral electrojet intensity. The perfection of the methods improves pronouncedly the correlation of AE' to the interplanetary medium parameters (see Figure 21).

The low correlation (Gonzalez *et al.*, 1989a) of the AE index with the interplanetary medium parameters during main phases of several magnetic storms should probably be attributed to using the data of only auroral observatories to calculate the AE index.

6.4. Polar electrojet during the magnetic storm

Apart from the auroral electrojets which reaches their highest intensity in the night-time sector of the auroral oval, the polar electrojet exists on the latitudes of the daytime sector of the auroral oval. The polar electrojet is a concentration of the current lines of the current system, described by Friis-Christensen and Wilhjelm (1975) and by Feldstein (1976), which exists in the near pole region and is controlled by the azimuthal (B_y)

component of the IMF (Friis-Christensen *et al.*, 1972; Sumaruk and Feldstein, 1973).

The daytime sector of the auroral oval shifts equatorwards as magnetic disturbance increases (Starkov and Feldstein, 1967). According to the observations of soft auroral electron precipitations, the dayside cusp which, when mapped along magnetic field lines, outlines the daytime sector of the auroral oval shifts significantly equatorwards (Meng, 1983). The shift of the cusp during magnetic storms must also be reflected in the character of the Earth's magnetic field variations at the observatories located on the auroral oval latitudes, the fact that was observed actually during the March 23–24, 1969 storm.

As noted above, the auroral activity inferred from the AE' indices reached its maximum at 23:00–02:00 UT and at 08:00–11:00 UT; the ring-current intensity also reached its maximum during those intervals. The westward convective auroral electrojet in the night-time sector shifts equatorwards as DR develops; during the active phase of substorm, however, the electrojet expands rapidly polewards due to formation of the substorm auroral electrojet (the current wedge) and covers an interval of up to 15° in latitude. This circumstance affects the character of magnetic field variations on geomagnetic latitudes of 70°–75°. These are just the latitudes whereto the polar electrojet shifts in the dayside sector. All these factors give rise to an unusual character of the field variations at the magnetic observatories located at the given latitudes, namely, at Heiss Isl. ($\Phi' = 74.7°$, $\Lambda = 144.8°$) and at Cape Chelyuskin ($\Phi' = 71.3°$, $\Lambda = 177.2°$). The variations in the northward, ΔX, and vertical, ΔZ, components of the Earth's magnetic field at the two observatories are shown in Figure 23 at a 10-min time resolution.

The character of the ΔZ variations at Heiss Isl. is also peculiar. The ΔZ value was > 0 throughout the active phase of the storm from 21:00 UT on March 23 to $\sim$ 11:00 UT on March 24, 1969, being 300 nT before 06:00 UT on March 24 and falling afterwards monotonely to 0 nT at 13:00 UT. The positive ΔZ values at the high-latitude observatories of the northern hemisphere during the magnetic storm may be due to the enhancement of the ring-current field (Sumaruk *et al.*, 1980). At the same time, the ΔZ variations at Thule ($\Delta Z < 100$ nT), i.e., near the geomagnetic pole, indicate that the storm-time ΔZ variation intensity at $\Phi' \sim 75°$ cannot be quantitatively interpreted to result from the contribution of the ring-current field alone.

Two intensive disturbances at Heiss Isl. with $\Delta X < 0$ nT at 00:00–02:00 and 07:00–11:00 UT coincided with the intervals of increased values of $B_z < 0$ component of the IMF and with a drastic increase of auroral activity. The magnetic disturbances during those intervals were undoubtedly due to substorm evolution. At 00:00–02:00 UT, Heiss Isl. and Cape Chelyuskin were located in the dawn sector, while the ΔX and ΔZ variation sign indicated that the magnetic disturbance source was located equatorwards from the observatories, i.e., at $\Phi' < 71.5°$. At 07:00–11:00 UT, when the observatories shifted to day-dusk sector, the field source was located to the north of Cape Chelyuskin ($\Delta Z < 0$, $\Delta X < 0$), but to the south of Heiss Isl. ($\Delta Z > 0$, $\Delta X < 0$). Having been defined by the method (Loginov and Starkov, 1972), the position of the westward electrojet proved to be $\Phi' \sim 72.7°$ at 09:00–10:00 UT at $DR = -230$ nT.

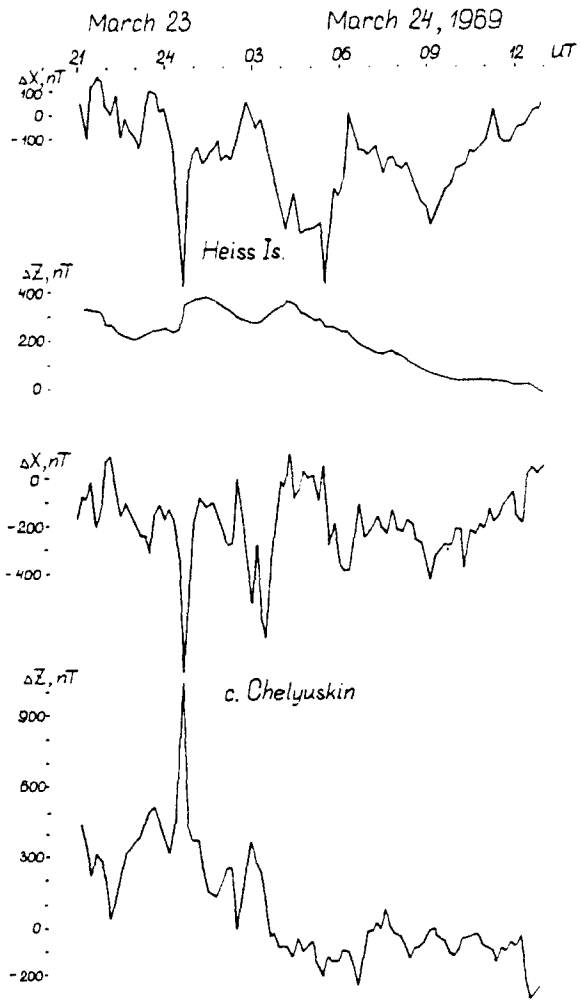

Fig. 23. Variations of the northward, ΔX, and vertical, ΔZ, components of the Earth's magnetic field in deviations from the quiet interval prior to magnetic storm at Heiss Isl. (*top*) and Cape Chelyuskin (*bottom*) during the magnetic storm.

At 03:00–06:00 UT the auroral activity intensity showed a noticeable decrease simultaneously with a decrease in the intensity of the IMF $B_z < 0$ component. During the same period, however, a baylike disturbance development with ΔX intensity of up to – 500 nT was recorded at Heiss Isl. and at Cape Chelyuskin. The disturbance cannot be due to auroral activity, for the magnetic field in the night-time sector (at Churchill and Baker Lake) at the same latitudes at 03:00–06:00 UT was close to its quiescent values. The baylike disturbance in the prenoon-daytime sector was most probably generated by the shift of the polar electrojet to the latitudes where Heiss Isl. and Cape Chelyuskin are located. At 03:00–06:00 UT on March 24, the IMF B_y intensity increased drastically and its mean-hourly values were – 19.2 nT, – 20.3 nT, and

– 16.9 nT, respectively. At negative IMF B_y values, according to (Friss-Christensen and Wilhjelm, 1975; Feldstein, 1976), the polar electrojet flows westwards, thereby reducing the northern component of the Earth's magnetic field ($\Delta X < 0$). The method (Loginov and Starkov, 1972) was used to obtain that the polar electrojet center of gravity was located at 03:00–03:30 UT equatorwards from Cape Chelyuskin at $\Phi' \sim 70.6°$ ($DR = -200$ nT) with the electrojet width of ~ 150 km. By 03:40–03:50 UT, the polar electrojet had shifted to the zenith at Cape Chelyuskin at $\Phi' \sim 71.5°$ ($DR = -190$ nT) and kept shifting monotonely polewards until 05:40 UT at $\Phi' \sim 73°$ with the current band width of ~ 300 km ($DR = -180$ nT). So, the peculiar character of magnetic variations at the auroral latitudes at daytime hours during an intensive magnetic storm was defined by the shift of the polar electrojet to $\Phi' \sim 70°$ where the current intensity and direction are controlled by the azimuthal component of the IMF. On the time interval of auroral activity decay, but a developed ring current with DR intensity of ~ – 200 nT, the polar electrojet width is ~ 2° of latitude. The peculiar character of the ΔZ variations at Heiss Isl. on March 23–24, 1969 (very high $\Delta Z > 0$ values with an intensity of hundreds of nT throughout a long time interval) is due to the consecutive positions of the stations in the dawn and day-time sectors under the auroral and polar electrojets.

6.5. Penetration of the Magnetospheric Electric Field into the Equatorial Ionosphere during the Magnetic Storm

In literature, the question has been being discussed for a long time where the current systems generated in the ionosphere during geomagnetic disturbances cover the entire region from the auroral zone to the equator, or they are confined within middle latitudes only. Nishida *et al.* (1966) have demonstrated that coherent fluctuations of magnetic field occur at the equator and in the near-pole region which cover large areas. The magnetograms obtained on individual days were used in (Feldstein *et al.*, 1967) to sertify the existence of the relationships of the irregular magnetic field fluctuations with intensities of few dozens of nT at the equatorial stations Huancayo (Peru) and Trivandrum (India) at near-noon hours to the occurrence of *DP*-type magnetic disturbances at the auroral observatories in night-time sector. Nishida (1968a, b) has established close relationships of global magnetic field fluctuations which cover the entire globe from poles to equator (*DP*2) to the variations of the IMF southward component. The *DP*2 is a signature of the magnetospheric convection intensity on the Earth's magnetic field and is described in terms of a two-vortex current system which enhances drastically at the magnetic equator (see also Gonzalez *et al.*, 1983). The enhancement arises from the peculiar character of ionospheric conductivity in the region where the magnetic field is tangent to the ionosphere, thereby proving without any doubt that the currents responsible for the *DP*2 field fluctuations are of ionospheric origin. The southward IMF B_z fluctuation is accompanied by an enhancement of the eastward current in the equatorial electrojet. According to (Nishida, 1971), the day-time *DP*2 amplitude increases at Huancayo (a 2° inclination) by a factor of ~ 4 compared with Fucuene (a 33° inclination). Since the distance between the two observatories is as small

as ~ 1500 km, the increase indicates that it is the ionospheric currents that are responsible for the total (or at least for a major fraction of) fluctuation field. The magnetograms from the observatories show that the equatorial enhancement of the fluctuations is in practice absent in case of substorms (*DP*1). This means that substorm-time low-latitude variations of magnetic field are irrelevant to the ionospheric currents. The given field can probably be generated by the currents flowing along magnetic field lines (Fukushima, 1969) or by the asymmetric ring current (Akasofu and Meng, 1969). The magnetic field fluctuations in the equatorial region of the day-time sector are in a high correlation with the eastward electrojet evolution in the auroral zone, thereby indicating that the auroral events are sometimes associated with equatorial events (Onwumechili *et al.*, 1973). However, the relationships between the equatorial and auroral regions are not always simple and unambiguous.

Later studies yielded conflicting results (Troshichev *et al.*, 1974; Rezhenov *et al.*, 1979). According to Troshichev *et al.* (1974), the two-vortex *DP*2 system relevant to the IMF B_z variations is confined within geomagnetic latitudes $\Phi \sim 50°$–$60°$. The field variations at $\Phi < 50°$ are described in terms of the zonal current systems, whereas their intensity varies with latitude as $\cos \Phi$. This behaviour is typical of the disturbances fields of extra-ionospheric origin (*DR* and *DCF*). The difference from the results obtained by Nishida *et al.* (1968a, b) for the spatial extension of the *DP*2 current system was accounted for by different selections of the reference level which was taken by Nishida *et al.* (1968a, b) to be the magnetic fluctuation base (i.e., the straight line connecting the onset and end of a fluctuation), and by Troshichev *et al.* (1974) to be the background field (i.e., the field observed on the exceptionally quiet days when magnetic activity reaches its minimum). Rezhenov *et al.* (1979) examined the effects in individual pulses (both negative and positive) in the IMF B_z component on the Earth's magnetic field variations. In such cases, the effect of the IMF on the geomagnetic variations in the polar cap and at the equator can be traced unambiguously. A negative (positive) pulse in the IMF B_z component generates ionospheric currents across the polar cap from night to day (from day to night) and an eastward (westward) current at the equator which enhances at the magnetic equator, just in agreement with the *DP*2 current system. The relationship between the disturbance intensities in the polar cap, ΔT_{pc} and at the equator ΔH_{eq} has been shown to be of the form $\Delta T_{pc} \approx 3.2 \Delta H_{eq}$.

Rastogi (1977) described storm-time variations of magnetic field and of vertical drift velocity at the equator. The *H*-component decrease at Huancayo is due to the westward ionospheric currents (returne electrojet). The ionospheric origin of the currents responsible for the field variations is confirmed by a pronounced decrease of the variation intensity when moving away from the electrojet. Rastogi and Patel (1975) and Ratel (1978) assumed that the electric field inverses are closely correlated with the change southward to northward direction of the IMF B_z. The east–west electric field, which generates the equatorial electrojet, is also responsible for the vertical drift in the *F* layer which can be measured to within a sufficient accuracy with the 50-MHz radar at Jicamarka (Peru) (Woodman and Hagfors, 1969). By studying in detail the feasibility of the relationship described by Rastogi and Patel (1975) and by Patel (1978) with the

Jicamarka radar, Fejer *et al.* (1979) found that any simple one-to-one correspondence had never occurred between the IMF B_z variations and the variations of zonal electric fields. There exist the cases of a good correlation and of the complete absence of any correlation. The effects in the equatorial ionosphere have been claimed to be irrelevant directly to the IMF, but to result from the variations of the large-scale magnetospheric convection and from the generation of the substorms initiated by the IMF variations. The statistical examination (Rastogi and Chendra, 1978) has shown that, as the southward IMF component decreases, the westward drift velocity of ionospheric inhomogeneities in the region of the auroral electrojet also decreases at all hours of a day.

Gonzalez *et al.* (1979, 1983) have described the close relationships among the electric fields in the ionospheric regions over the auroral zone and at the equator during magnetic disturbances. The rapid increases and decreases of the electric field of magnetospheric convection in the auroral zone may arise to instantaneous effects occurring at the magnetic equator. The data presented indicate that the convective field extends up to the equator until the screening by charges on the plasmapause compensates for the field in the inner magnetosphere. The electric field anomalies, which manifest themselves as inverses of the zonal components of the electric field, were observed during some substorms accompanied by generation of the ring current. The westward currents in the day-time electrojet were interpreted to be the day-side closing of the high-latitude field-aligned currents.

Reddy *et al.* (1979, 1980) emphasized the global character of the 20–40 min fluctuations in the Earth's magnetic field observed on very quiet days. Identical field fluctuations traced at the auroral-zone, mid-latitude, and equatorial observatories were accompanied by the same variations of the drift velocities of ionospheric inhomogeneities in the equatorial electrojet region. This means that the field fluctuations were due to the dynamo-region ionospheric currents which are of global character. The simultaneous occurrence and the relatively high intensity (up to ~ 10 nT) of field disturbances are indicative of a sufficiently close relationship between the auroral and equatorial dynamo regions during the fluctuations. However, the global current system of the baylike disturbance suffers strong variations even throughout an individual disturbance. Besides, additional local disturbances irrelevant to the occurrence of the electric field of planetary character are observed at the high-latitude observatories, thereby making it difficult to compare directly among the field variations at different latitudes. Reddy *et al.* (1981) made an attempt to separate the contributions of the ionospheric and magnetospheric currents to the magnetic field variations observed under the equatorial electrojet during magnetic storms. The ionospheric electric field was measured with a HF radar using the drift velocity of plasma inhomogeneities, while the SSC storm field variations at Thumba ($I = 0°56'$) were attributed to the enhancement of the eastward ionospheric electric field in the dynamo region. The enhancement was responsible for the major fraction of the ΔH increase at the electrojet latitudes. Large and rapid fluctuations of magnetospheric and ionospheric currents were observed during the storm initial phase prior to DR development. The asymmetric ring current

made the major contribution to the on-ground ΔH values during the storm main phase near the maximum decrease of the field when the $|\Delta H|$ values were 2 times as high as the D_{st}-variation intensity. The symmetric ring current made the major contribution to ΔH during the storm recovery phase, so ΔH was almost coincident with D_{st}. The day-time eastward electric field was weak at the electrojet latitudes because of the occurrence of the disturbance-associated westward electric field. During both main and recovery phases of the storm, the disturbance-associated westward electric field occurred in the dawn sector, and the eastward field in the late afternoon-dusk sector. During magnetic storms, the east-westward electric field of the equatorial electrojet varies in phase with the polar cusp latitude (Somayajulu *et al.*, 1985). The given variations are generated probably (1) by the variations of the polar cusp latitudes and the associated variations of the latitudinal position of the region of increased ionospheric conductivity and field-aligned currents. The electric field disturbances at the ionospheric dynamo altitudes on the cusp latitudes lead to electric field variations on global scale, the equatorial electrojet included; (2) by the magnetospheric electric field of a noticeable intensity produced by the enhanced storm-time magnetospheric convection and penetrating to the low-latitude ionosphere.

Somayajulu *et al.* (1987) examined in detail the feasibility for the magnetospheric convection electric field to low latitudes during the March 22, 1979 substorm. The eastward electric field was shown to penetrate to the equatorial ionosphere within but a restricted interval of ~ 30 min during the initial interval of the substorm. The solar wind electric field $E_y = -vB_z$ got positive at 10:08 UT because of the turn of B_z southwards. The E_y sign reversed somewhat before the drastic enhancement of the eastward electric field at the equator at 10:20 UT which coincided with the onset of a strong enhancement of the sunward equivalent electric currents in the polar cap (McPherron and Manka, 1985). The currents are indicative of an increase in the intensity of magnetospheric convection due to solar wind. Such an enhancement of the convection is typical of the creation phase of substorm and the occurrence of the $DP2$ field variation. The substorm active phase at 10:50 UT was accompanied by attenuation of the eastward electric field at the equator, although the value of E_y in solar wind was still negative for few dozens of minutes (until 11:20 UT) after the additional field of magnetospheric origin had attenuated at the equator. The occurrence of the eastward electric field detected by radars after the drift of ionospheric inhomogeneities was accompanied by a positive baylike magnetic disturbance of ~ 30 min duration detected at a magnetic observatory. The attenuation of the equatorial baylike magnetic disturbance, which was observed simultaneously with the attenuation of the ionospheric electric field, occurred against the background of ring-current development during the substorm active phase, as inferred from the monotone decrease of H at the equatorial station until 11:40 UT. On March 22, 1969, thus, the southward turn of the IMF at 10:08 UT resulted, within ~ 12 min, in an enhancement of planetary magnetospheric convection, in penetration of the electric field of magnetospheric origin to the equatorial ionosphere, in generation of a bay-like magnetic disturbance at the equatorial observatory, and in the onset of the substorm creation phase. The equatorial eastward electric field began

attenuating during the substorm active phase when the ring current began being generated in the magnetosphere, although the intensity and the sign of the solar wind electric field remained the same. In the given case, therefore, the ring-current generation resulted in such a rearrangement of the magnetosphere that the penetration of the magnetospheric electric vield to equatorial latitudes appeared to be hampered. This result, which was inferred from the data on but a single substorm, needs being confirmed additionally by the data on other disturbances. This is especially so, because the statistical data (Maynard *et al.*, 1988) from the *DE* satellite did not indicate any noticeable variations of the meridional electric fields due to magnetic activity.

Examine now the feasibility for the electric fields of magnetospheric origin to penetrate to equatorial latitudes during the March 23–24, 1969 storm. As follows from the above, such a penetration must be judged from either occurrence or absence of a drastic enhancement of the Earth's magnetic field variations at the observatories located near the magnetic inclination equator (Huancayo, Bangui, Annamalainagar) with respect to the observatories located further northwards at the same latitudes (Fucuene, Tamanrasset, Alibag).

The sudden commencement of the magnetic storm was detected by all the low- and mid-latitude observatories at 18:26 UT. Solar activity in that period was characterized by the passage of a complicated active region containing four sunspot groups across the central meridian. Class 2B and 3B flares occurred in the active region at 01:38 UT and 13:32 UT on March 21 (*Solar-Geophysical Data*). The flares were accompanied by strong radio bursts in the centimeter and meter bands and by the effect of sudden enhancement of absorption in the sunlit hemisphere. The very strong magnetic storm, whose sudden commencement was recorded on March 23, 1969, was probably associated by the solar flares of March 21. The geomagnetic activity increases at 00:00–01:00 UT and 09:00–10:00 UT on March 24 are just in correspondence with the arrival of the corpuscular fluxes from the given flares to the Earth. The sudden commencement of the March storm was analyzed in detail by Feldstein *et al.* (1974). The data from 66 observatories located in the northern hemisphere were used to calculate the value and direction of the disturbance vector in horizontal plane. The distribution of the vectors was generalized in the form of a current system. The *SC* current system consists of three vortices, namely, a night-early dawn vortex at $\Phi > 65°$, a night vortex at $20° < \Phi < 65°$, and a dusk vortex at $\Phi > 40°$. A homogeneous current flows in polar cap from 21:00 LT to 09:00 LT. Two night-time vortices are due to the electrojet at night hours at $\Phi \sim 55–60°$, which corresponds at the given longitudes to the corrected geomagnetic latitudes of 60°–65°. In such a way, there exists a high-intensity ionospheric fraction of the *SC* current system (Ivanov and Mikerina, 1970). Weak variations of the field were traced in the middle latitudes of the night side. The vector directions may be accounted for by the spreading of the westward electrojet current along the ionosphere across middle latitudes and by the distant effect of the field-aligned currents inflowing to the auroral oval at dawn hours and outflowing from the oval at dusk hours. The day-side current vortex with counterclockwise current is focused on $\sim 75°$ and is probably due to the continuous plasma injection across the

day-side cusp to the day side of the auroral oval. A drastic increase of the *SC* amplitude was observed at near-noon hours at the equatorial electrojet latitudes (Huancayo), in agreement with the results obtained by Obayashi and Jacobs (1957).

The OGO-5 measurements of plasma parameters indicate that the solar wind velocity increased by $\sim 100\ \mathrm{km\ s^{-1}}$ and that the proton number density increased by $\sim 2.8\ \mathrm{cm^{-3}}$ from 17:58 UT to 18:31 UT on March 23, 1969. The increases must be regarded as associated with the magnetic storm sudden commencement observed on the Earth's surface. The compression of the magnetosphere during *SC* can result immediately in generation of a magnetospheric substorm (Schieldge and Siscoe, 1970; Kawasaki *et al.*, 1971). Indeed the *SC* period coincided with a strong enhancement of the westward auroral electrojet intensity.

Figure 24 presents the magnetic field variations during the March 23–24, 1969 magnetic storm at three meridional chains of observatories in deviations from the values of the field during a respective interval on March 22–23 through West Siberia to India (a), through West Europe to Africa (b), and through North and South America (c). The magnetograms of observatories scaled in each 10 min interval from auroral latitudes to the equatorial electrojet are presented.

At the Indian stations Annamalainagar ($\Phi = 1.5°$) and Alibag ($\Phi = 9.4°$) located at

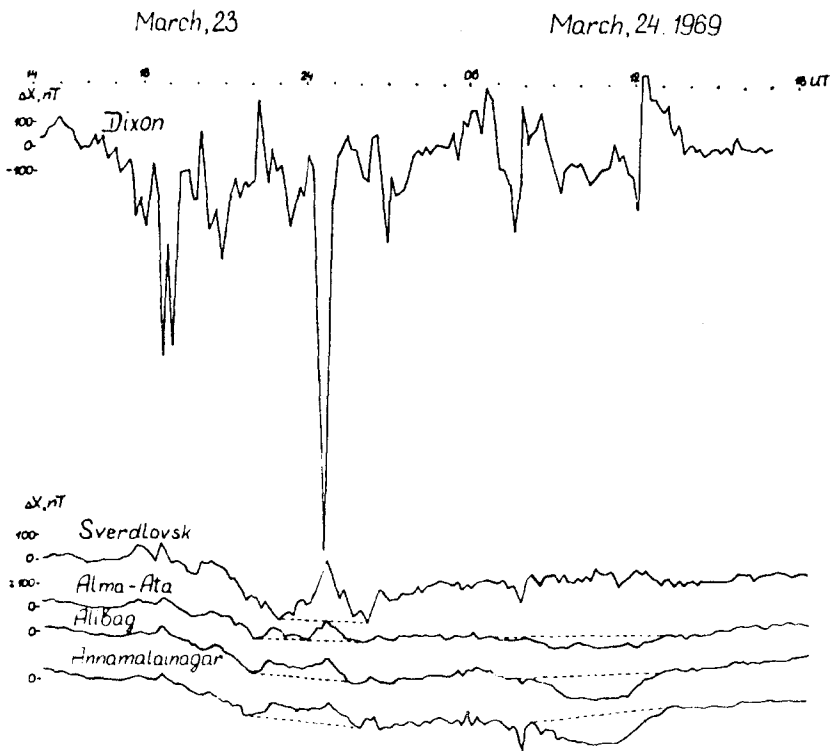

Fig. 24a.

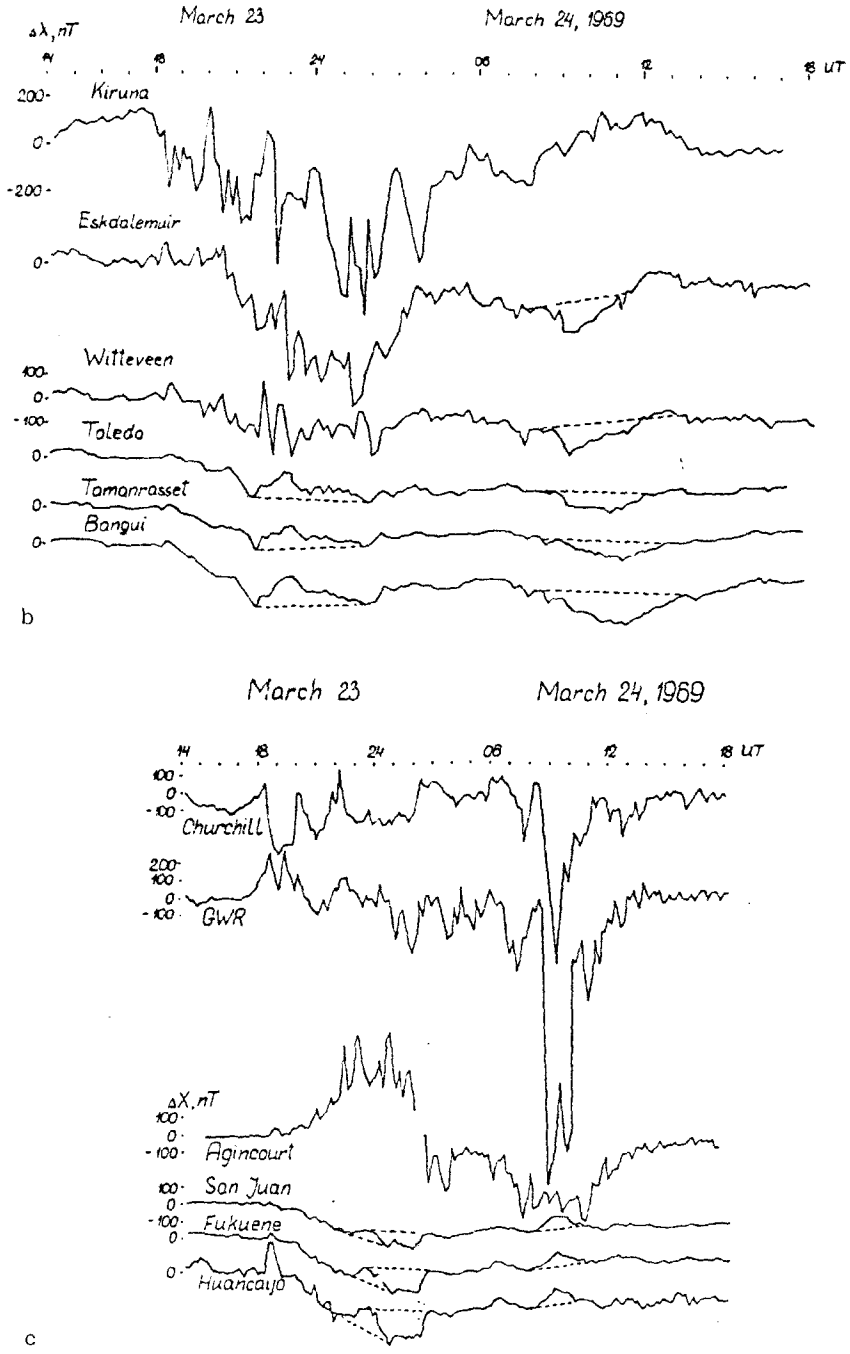

Fig. 24. Magnetic field variations during the March 23–24, 1969 storm in deviations from the quiet level at three meridional chains of observatories from auroral latitudes to inclination equator: (a) through West Siberia to India, (b) through West Europe to Africa, (c) through North and South America. The dashed line confines the magnetic field fluctuations during the extremal strong development of the intensity of ring current and auroral electrojets.

18:00–19:00 UT in the night-time sector, the storm sudden commencement (Figure 24(a)) manifests itself as a jump of a 30 nT intensity between 18:20 and 18:30 UT. The jump was clearly seen also at the midlatitude observatory Alma-Ata ($\Phi = 33.5°$). The variations did not appear to increase in the equatorial electrojet region. A certain enhancement of the jump was recorded at Sverdlovsk ($\Phi = 48.5°$), while the substorm which commenced after *SC* can be seen clearly in the magnetogram obtained at Dixon. Thus, the data obtained during the *SC* in the night-time sector show that a distant source, rather than ionospheric currents, is the source of the magnetic field variations at low latitudes. Asymmetric ring current began evolving after the *SC*, thereby giving rise to a synchronous decrease of the horizontal field component from the equator to middle latitudes. The auroral electrojet intensities inferred from the *AU*, *AL*, and *AE* data reach their extremal high values at 23:00–02:00 UT and at 08:00–11:00 UT. The mid- and high-latitude observatories of the Indian longitude sector recorded the anomalous fluctuations of the field during those intervals, namely an increase of ΔX at 23:00–02:00 UT (the dawn sector) and a decrease of ΔX at 08:00–13:00 UT (the day–afternoon sector). The fluctuations are confined in Figure 24(a) within the dashed lines. In the after-midnight sector, the field fluctuations in the low latitudes ($a \sim 50$–100 nT intensity) and in middle latitudes ($a \sim 250$ nT intensity) occur during an exceptionally intensive westward electrojet in the auroral zone (Dixon, $\Delta X \sim 1700$ nT). In the afternoon sector, the fluctuation intensity decreases from ~ 100 nT at the equatorial observatory to ~ 50 nT at middle latitudes. In the auroral zone the electrojet intensities are much lower compared with near-midnight hours. The fluctuation sign and the character of latitudinal variations make it possible to conclude that the field fluctuations at low and middle latitudes on the Indian meridian were due at 23:00–02:00 UT to the superposition of a three-dimensional current system field on the ring-current field, and at 08:00–13:00 UT to the ring-current field.

In the European–African meridional profile (Figure 24(b)), the main behavioural features of the low- and mid-latitude field variations are the same as those presented in Figure 24(a). The storm *SC* is characterized by $a \sim 20$–30 nT signal at the low-latitude observatories Bangue ($\Phi = 4.5°$) and Tamanrasset ($\Phi = 25.1°$), and at the mid-latitude observatory Toledo ($\Phi = 33.9°$). At higher latitudes, the jump enhances up to ~ 60 nT (Witteween, $\Phi = 53.9°$) and up to ~ 100 nT at Eskdalemuir ($\Phi = 58.2°$). The absence of any ΔX enhancement at the geomagnetic equator during *SC* and the character of latitudinal variations are also indicative of the absence of any noticeable contribution of the ionospheric source to ΔX at low latitudes in the dusk sector. The dashed lines confine the field fluctuations at 22:00–02:00 UT and at 08:00–13:00 UT. The field fluctuation is positive in the near-midnight sector and negative in the dawn-day sector, thereby defining the predominant contribution to the observed field variations from the three-dimensional current system in the former case and from the ring current in the latter case.

At the American chain of stations (Figure 24(c)), the magnetic field fluctuation intensity increased sharply up to ~ 180 nT in the equatorial electrojet region (Huancayo, $\Phi = -0.8°$) not only at the *SC* moment but also within $a \sim 20$ min interval. At Fucuene

($\Phi = 16.8°$), the field fluctuation intensity did not exceed 50 nT during the *SC*. The substorm beginning after the *SC* can be seen clearly in the magnetograms of the auroral observatories Churchill ($\Phi = 68.7°$) and Great Whale River ($\Phi = 66.4°$). At 22:00–02:00 UT, the magnetic field decrease at low-latitude observatories due to ring-current development is superposed with the complicated disturbances which may be treated, depending on the choice of the basis shown with the dashed line, to be either an increase or a decrease of the magnetic field. Probably, as the magnetospheric disturbance level increases at the given LT dusk hours at the observatories of the American chain, a noticeable contribution is made by the fields of the three-dimensional current system and of the asymmetric ring current. The disturbance increase at 08:00–11:00 UT manifests itself clearly as a westward electrojet intensity increase up to $\Delta X \sim -1600$ nT and as a positive magnetic field burst at the low- and mid-latitude observatories. The given profile located in the dawn sector differs by its field variation sign from two other meridional profiles with negative field fluctuations in the day-time and afternoon sectors. The weak latitude dependence and the fluctuation sign make it possible to attribute the burst to the field-aligned current effect.

The field variations ΔX shown in Figure 24 in deviations from the pre-storm quiet interval at the particular observatory may be presented to be a sum of field variations from the currents generated by different sources. In low latitudes, the sources are the currents on the magnetospheric surface (*DCF*), the ring current (*DR*), the currents along magnetic field lines (the field-aligned *FAC*), and the ionospheric currents (*IC*). We have, then,

$$\Delta X_{\text{obs}} = X^d_{\text{obs}} - X^q_{\text{obs}} = \Delta X_{DCF} + \Delta X_{DR} + \Delta X_{FAC} + \Delta X_{IC},$$

where the symbol Δ designates the difference in the values of the fields of different sources during disturbed and quiet intervals.

Figure 25 presents the field variations on the Earth's surface X at some observatories located at different longitudes in each 5-min interval from 17:30 to 19:30 UT when the AE' indices indicated the onset of the development of an intensive substorm. At Huancayo (ΔX_H), within 18:25–18:30 UT, i.e., during *SC*, the field intensity increased by 170 nT, remained at that level until 18:40 UT, and decreased monotonely afterwards to the quiet-day level until 19:05 UT. The ΔX_H value remained ~ 0 nT from 19:05 to 19:30 UT. The differences $\Delta X_H - \Delta X_F$ (the solid line) and $\Delta X_H - \Delta X_{SJ}$ (the dashed line) are presented under the ΔX_H curves, where ΔX_F and ΔX_{SJ} are field deviations at Fucuene and at San Juan from the quiet-day level. Presented even below are the differences $\Delta X_F - \Delta X_{SJ}$. Assuming that the current fields ΔX_{DCF}, ΔX_{DR}, and ΔX_{FAC} (distant sources) are approximately the same at the observatories located close to each other along a meridian, the differences $\Delta X_H - \Delta X_F$ and $\Delta X_H - \Delta X_{SJ}$ characterize the difference between the ionospheric-source current fields under, and at some distance from, the equatorial electrojet. From Figure 25 it follows that, during the *SC* interval, the increase of the field jump at the equator is 130 nT in excess of the jump at some distance from the equator. The excess rises up to 165 nT in 10 min and falls to zero in another 25 min. In this case, with respect to Fucuene ($\Phi = 16.8°$), the difference at

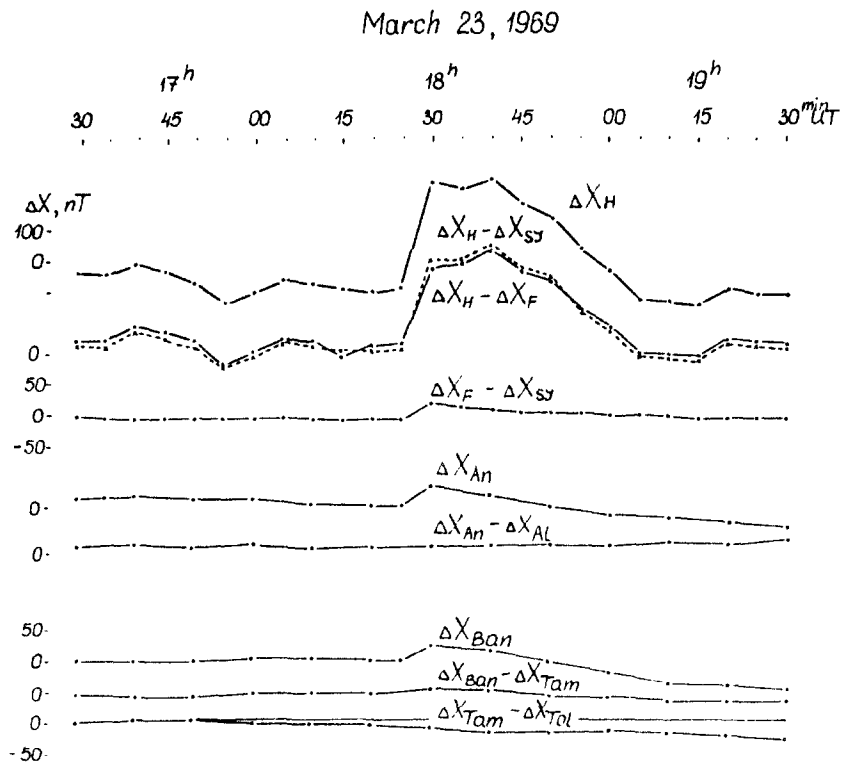

Fig. 25. Variations of the northward component of the Earth's magnetic field in deviations from the quiet level near *SC* of the magnetic storm at the observatories located at different longitudes in the region of the magnetic inclination equator.

18:30 UT is lower by 15 nT than with respect to San Juan ($\Phi = 29.4°$), i.e., the effect of the ionospheric source is still perceptible at $\Phi \sim 17°$. After 18:40 UT, the differences $\Delta X_H - \Delta X_F$ and $\Delta X_H - \Delta X_{SJ}$ were in practice the same, which is seen clearly from the $\Delta X_F - \Delta X_{SJ}$ curve. The *DCF* field cannot account for the pronounced increase of magnetic variations observed on the Earth's surface after the magnetic storm *SC* at the magnetic equator, for their significant value of ~ 150 nT within ~ 10 min, and for a monotonic decrease to 0 nT in another 25 min.

The lower part of Figure 25 presents the field variations on other meridians. During the *SC* period, the field jump intensity was about the same at Annamalainagar and at Alibag; besides no field variations were observed in the equatorial electrojet region. From the onset of the storm, the difference $\Delta X_{An} - \Delta X_{Al}$ was ~ 0 throughout the interval from 17:30 UT to 19:30 UT, but ΔX_{An} kept decreasing monotonely after 19:05 UT and was -35 nT at 19:30 UT. The same, i.e., almost identical, field variations in the beginning of the storm were also recorded at the observatories Bangue and Tamanrasset in the European sector; at Bangue, the monotone decrease to -48 nT took place by 19:30 UT. The decrease seems to characterize the development of the partial ring current in the near-midnight and dusk magnetospheric sectors which was not observed

at the early afternoon hours. The character of the field variations at Tamanrasset and Toledo (an increase of the differences $\Delta X_B - \Delta X_T$ and $\Delta X_B - \Delta X_{T_0}$ with latitude) is additional evidence for the ring-current contribution to the field variations. After the magnetic storm commencement accompanied by the commencement of an intensive substorm, thus, a rapid increase of the equatorial electrojet currents was observed at the early afternoon hours. Such an increase was never observed in the dusk and night-time sectors. The given magnetic field jump began to decrease monotonely in ~ 10 min; the decrease lasted for ~ 25 min. The field recovered to its initial level in the afternoon sector at the equator against the background of the development of the partial ring current in the night-time and dusk magnetospheric sectors. In the beginnig of the substorm, the electric field of the enhanced magnetospheric convection seems to penetrate to all latitudes up to the equator and to be accompanied by ionospheric current at all latitudes up to the equator. After that, the ring-current development provides for the screening of the inner magnetosphere against the magnetospheric electric fields, as a result of which the ionospheric currents generated by the fields disappear at low latitudes togehter with the respective fluctuations of the Earth's magnetic field. The disappearance is irrelevant to the attenuation of the magnetospheric substorm which lasted at a level of above 1000 nT in the *AE* index until 19:40 UT.

The obvious question arises whether some field sources, other than the magnetospheric substorm, can be responsible for the low-latitude field variaitons described above. The examination of the IMF variations inferred from the Explorer-35 data has made it possible to exclude the variations of the IMF B_z component as a source of the *DP*2 variations from 17:30 UT to 19:30 UT. Within that interval, $B_z < 0$ in the solar-magnetospheric coordinate system and the characteristic B_z fluctuations responsible for generation of *DP*2 magnetic disturbances were absent. The effect of a solar flare may constitute another source of the day-time field enhancement at the equator. A series of flares of different intensities was observed on March 23, 1969 (*Solar-Geophysical Data*) and lasted from 00:16 to 12:38 UT. The most intensive flare of class 3N occurred from 07:50 to 09:35 UT. Therefore, the magnetic effects at $\sim 18:30$ UT could not have been produced by wave emission from the solar flares which occurred much earlier on March 23.

The enhancement and the attenuation of the planetary ionospheric current system penetrating up to the equator seem to be defined by the characteristic evolution time of the three-dimensional current systems connecting the magnetosphere to the ionosphere. According to Lyatsky (1978), the characteristic enhancement time of the current in the electric circuit connecting the magnetopause to the equatorward boundary of polar cap is $\tau_1 \sim 15$ min. The evolution time of the current system at the equatorward boundary of the auroral zone relevant to the rearrangement of the inner boundary of the plasma sheet and to the screening of the inner magnetosphere against the magnetospheric electric fields is $\tau_2 \sim 40$ min. The given characteristic times agree with the observed times of increase (~ 10 min) and decrease (~ 25 min) of ΔX_H, i.e., the increase of ΔX_H is defined by the evolution of the current system of the zone 1 field-aligned currents while the subsequent decrease of ΔX_H is associated with generation of the current system of the zone 2 field-aligned currents.

The values of ΔX and of ΔX differences at pairs of observatories in different meridional profiles were obtained for 21:00–02:00 UT (in the same manner as in Figure 25). In the European and Indian profiles, the pronounced increase of the AE' index at 22:00–01:00 UT under a sufficiently developed DR does not result in any marked increase of the variations at the equator compared with middle latitudes (the differences $\Delta X_B - \Delta X_T$ and $\Delta X_{An} - \Delta X_{A.-A}$). During some intervals, however, the difference may prove to be significant. Although the main contribution to the field variation defined in the above described manner is probably made by the field of three-dimensional current system, which is also indicated by very high ΔX values (above 200 nT) at Sverdlovsk, the contribution of ionospheric currents to the low-latitude field variations is also actual during some intervals within strongly-disturbed periods.

The enhancement of the magnetospheric disturbance level at 08:00–11:00 UT manifested itself differently in the examined meridional profiles. At Huancayo and Fucuene, $\Delta X > 0$ of approximately the same intensity at 07:40–10:40 UT, together with $\Delta X_H - \Delta X_{SJ} \sim 0$, are indicative of the absence of any equatorial enhancement due to ionospheric currents. As a result of ring-current development, the westward convective electrojet shifted, within 07:40–10:40 UT, to the subauroral latitudes $\phi \sim 55°$. At the Indian observatories, the activity increase at 08:00–13:00 UT on March 24, 1969 was accompanied by a negative, rather than positive, burst. The comparison between the ΔX_{An} and ΔX_{Al} values shows that any equatorial increase of the field variation was absent. The field decay at the equatorial stations was much more intensive than at middle latitudes, which is indicated by the difference $\Delta X_{An} - \Delta X_{A.-A}$. The given behaviour of the field variations suggests that the ring-current contribution prevails at the low and middle latitudes of the near-noon sector. Thus, the response of the low-latitude magnetic field variations on the Earth's surface to the magnetic activity increase varies with LT sector, namely, the horizontal component increases in the early dawn sector and decreases in the day-time–early afternoon sector. The field variations are due to the three-dimensional current system in the first case, and to the ring current in the second case. In case of a developed ring current, the ionospheric currents do not contribute much to the low-latitude field variations throughout the magnetic storm either. Therefore, the conclusion (Tverskaya and Khorosheva, 1983) concerning the identification of the traces of auroral electrojets at low latitudes during intensive magnetic storms must be carefully treated.

Thus, the detailed analysis of the magnetic field variations at meridional chains of magnetic observatories during increased magnetic activity in the period of an intensive magnetic storm has shown that:

(1) the intensive magnetospheric substorm which began after SC is accompanied by an enhancement of the planetary ionospheric current system which penetrate up to the equator. The enhancement of the current in the equatorial electrojet occurs in the day-time sector only, lasts for ~ 35 min, and reaches ~ 0.25 A m^{-1} (which corresponds to a ~ 150 nT field). There variations must be related to the penetration of the magnetospheric convection electric fields to the equatorial latitudes during the initial stage of substorm development;

(2) within ~ 10 min after *SC*, the field fluctuation at low latitudes begins decreasing monotonely; the duration of the decrease is ~ 25 min. The field decay at the equator is accompanied by the development of partial ring current in the near-midnight-dusk sectors of LT. The given behavioural feature of the field must be related to the screening of the inner magnetosphere against the magnetospheric convection electric field by the development of the Alfvén layer and of an additional system of large-scale field-aligned currents at the inner boundary of plasma sheet;

(3) during the intervals with a developed ring current, magnetospheric substorms are not accompanied by penetration of ionospheric currents up to the equator. This fact can account for the disagreement among experimental data obtained elsewhere. In particular, the disagreement between the results obtained by Troshichev *et al.* (1975) and by Rezhenov *et al.* (1979) may have arizen from analyzing the disturbances without any developed ring current (Rezhenov *et al.*, 1979) and with the ring current (Troshichev *et al.*, 1975);

(4) the magnetospheric substorm intensification within a magnetic storm interval is accompanied by a positive field fluctuation in the early dawn–after-midnight sector and by a negative fluctuation in the day-time–afternoon sector. The given variations are due to the fields of three-dimensional current systems and of ring current, respectively.

6.6. The Longitudinal Asymmetry of Magnetic Field on the Earth's Surface and Its Modelling

The low-latitude magnetic field decrease during magnetic storms is not axially-symmetric, i.e., it is not identical along a geomagnetic parallel (Akasofu and Chapman, 1972). The analysis of the field H-component variations has shown that they are represented by the sum of the axially symmetric (planetary) component and the asymmetric component. During the early stages of the studies the asymmetric component was ascribed to the ionospheric electric currents which originate in auroral regions, while the symmetric component was described by the ring current surrounding the Earth which is the same in all longitudes. At present the ionospheric currents are assumed not to be the cause of the major portion of the asymmetry, at least during some of the periods. The fields of field-aligned currents and the ring-current asymmetry are responsible for the asymmetry, especially during the initial stage of the main phase of the magnetic storm. The asymmetry of the ring current proper arises from the jet-like plasma injection from the magnetospheric tail to the inner magnetospheric region. The injection occurs from a fairly narrow region in midnight sector, rather than along the entire inner boundary of the plasma sheet. The subsequent drift may carry the injected plasma away from the magnetosphere in daytime sector. Because of their restricted lifetime, a substantial fraction of ions are not in complete drift motions around the Earth. All the above factors facilitate maintaining the asymmetric distribution of plasma density along a longitude in the ring current. Thus, the ring current develops asymmetrical-hours, while the minimum decrease occurs at dawn hours. This character of the asymmetry is preserved throughout a storm. Figure 26 presents the quantitative asymmetry data inferred from the mean-hourly values of the component in the direction to the geo-

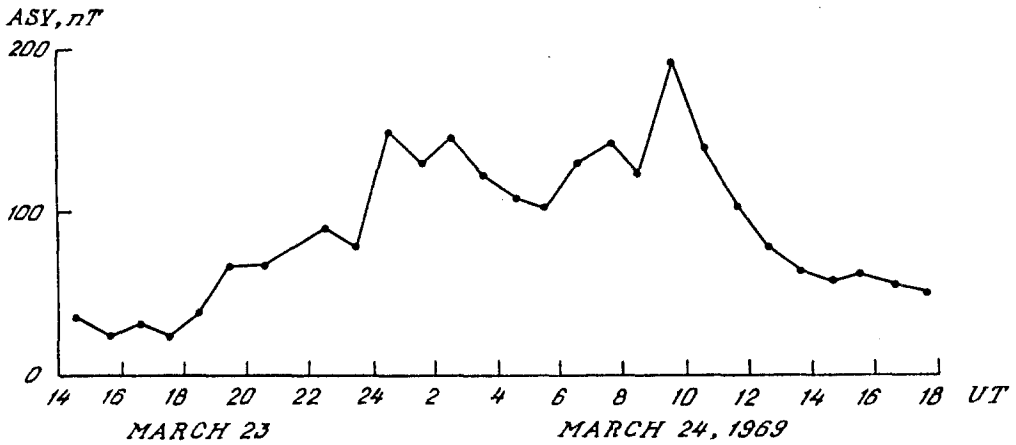

Fig. 26. The longitudinal asymmetry (ASY) of the hourly magnetic field values reduced to the equator in the direction of geomagnetic pole allowing for the current field asymmetry on the magnetopause. The data from 11 observatories were used.

magnetic pole ΔX allowing for the asymmetry in the DCF field. The asymmetry value (ASY) was determined to be a difference between the minimum and maximum field values for each hour of UT. The values of $\Delta X - DCF_x$ at each of 11 observatories were reduced to the equator by dividing by $\cos\phi$. As *DR* develops, the ASY increases from 30 nT in the beginning of the main phase to ~ 150 nT during the maximum of the main phase. During the recovery phase, the ASY decreases rapidly and is 50 nT at 16:00–18:00 UT. Under the same *DR* intensities, the magnetic field asymmetry during the main phase at 14:00–02:00 UT is higher by 15–25 nT compared with the recovery phase at 10:00–17:00 UT on March 24, 1969.

The UT-LT diagram shown in Figure 27 gives a generalized idea of the dynamics of the hourly $\Delta X - DCF_x$ and ASY values of magnetic field during a magnetic storm. The technique of plotting the diagram is the same as the method used by Clauer and McPherron (1980) to analyze the substorm effect on low-latitude field variations. The 50 nT isolines characterize the ring-current intensity and the effects of the fields of the ionospheric and field-aligned currents. The asymmetry is low in the beginning of the main phase. As $|\Delta X - DCF_x|$ increases, the asymmetry rises, thereby resulting in the isoline slope from the dawn 06:00–10:00 LT hours to the dusk 18:00–20:00 LT hours. The $|\Delta X - DCF_x|$ focus at dusk hours and minimum at dawn hours occur in the maximum of the main phase. The longitudinal field asymmetry reaches its maximum. In the recovery phase, the asymmetry decreases, while the maximum $\Delta X - DCF_x$ values are observed at near-noon hours, and the minimum $\Delta X - DCF_x$ values at late dusk and near-midnight hours.

The upper part of Figure 28 shows the hourly values of auroral electrojet intensity (the *AU* and *AL* indices) and amplitude of the first harmonic of *DS* variations of the field of observatories at $\phi \sim 25°$ and $\phi \sim 38°$. The lower part of Figure 28 present the same data smoothened over three neighbouring hours. It is seen that the smoothened

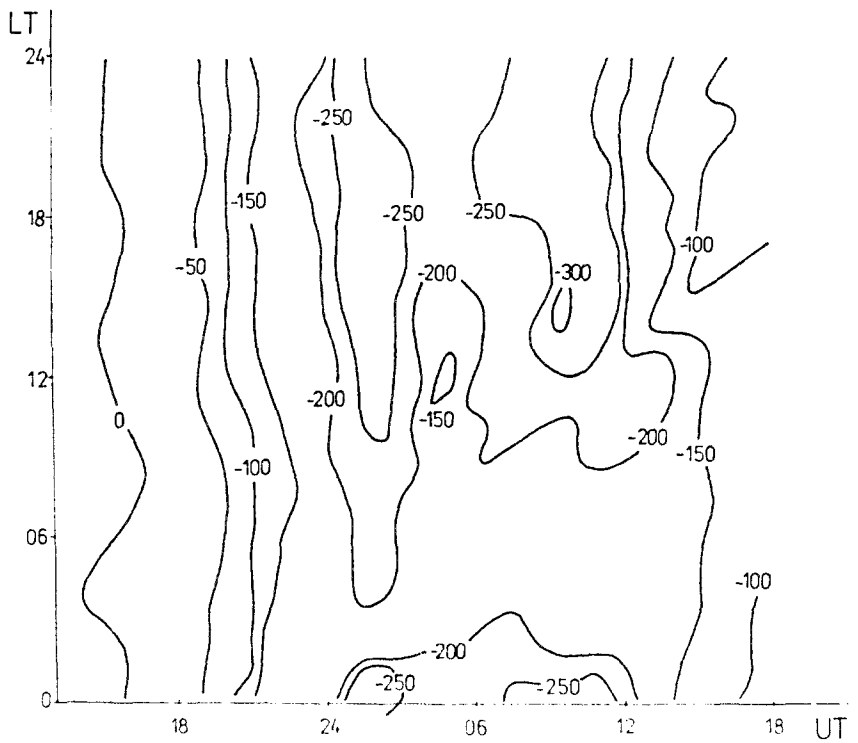

Fig. 27. The *UT–LT* diagram of hourly values of the geomagnetic field variations corrected for the DCF field at low latitudes during a magnetic storm.

$DS1$ values rise with decreasing latitude. From the data displayed it may be concluded that the long-period component of D_{st} asymmetry is due, to a great extent, to the ring-current asymmetry, while the shorter-term fluctuations arise from the effect of electrojets. Figure 28 presents the correlation coefficients r between AU, AL, and $DS1$ at different latitudes. The values of r are higher at $\phi \sim 38°$ than at $\phi \sim 25°$, the fact that is quite natural if the positions of electrojets in the auroral zone is allowed for. Besides, te AL-$DS1$ correlation is better than the correlation of AU with $DS1$. This fact discords with the opinion that the variations of the eastern electrojet are closely related to the ring-current evolution.

Figure 29 shows the dependences of the hourly values of the magnetic field asymmetry at the equator on the geoeffective characteristics of interplanetary medium. During the main phase, ASY rises with increasing the energy supplied to the magnetosphere; ASY $\sim$ 50 nT during the recovery phase arises from the permanent presence of large-scale field-aligned currents in the magnetosphere.

During the main phase of the magnetic storm, the equations of linear regression and of correlation coefficients for different geoeffective characteristics are as follows:

$$\mathrm{ASY} = -13.5(B_s V) + 13\,, \quad r = 0.91 \pm 0.06\,,$$

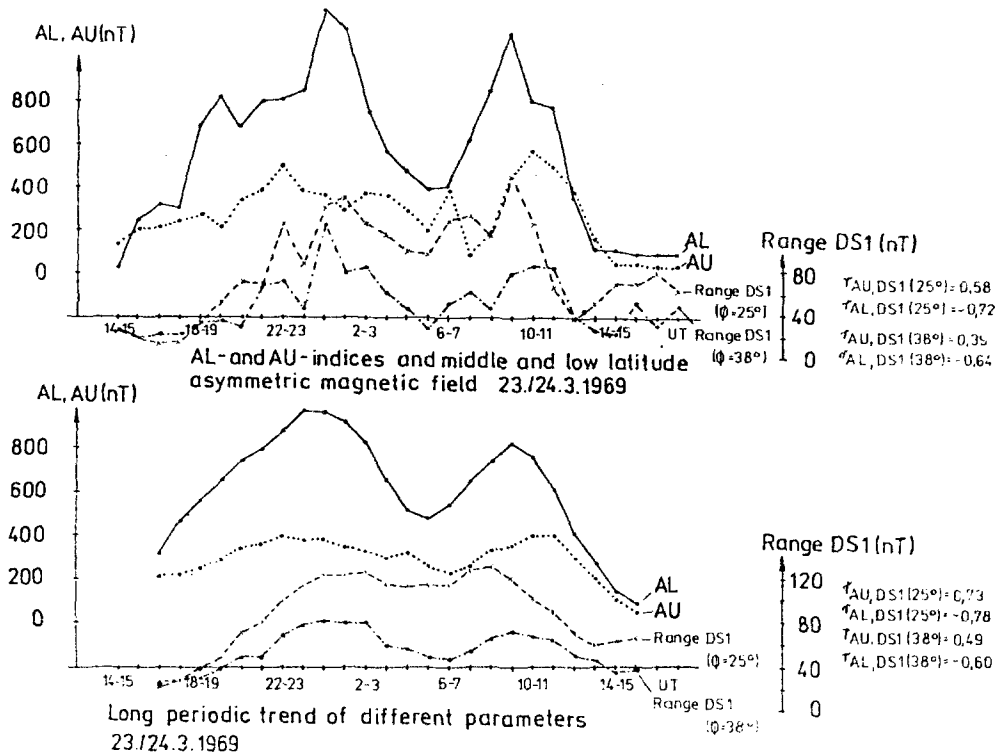

Fig. 28. Variations of the hourly values of the auroral AU and AL indices, the amplitudes of the first harmonic of magnetic field asymmetry in middle and low latitudes during geomagnetic storm (*top*). The lower panel shows the same data averaged over 3-hour moving data. Shown on the right are the respective correlation coefficients r.

$$\mathrm{ASY} = \quad 1.75\varepsilon + 32.3\,, \qquad r = 0.79 \pm 0.14\,,$$

$$\mathrm{ASY} = -11.7F + 1.43\,, \qquad r = 0.91 \pm 0.06\,.$$

Here, ASY is expressed in nT, B_sV in mV m^{-1}, E and F in 10^{11} W.

All three geoeffective characteristics of interplanetary medium are related sufficiently closely to the asymmetric development of the surface magnetic field during the main phase of the magnetic storm. Among the solar wind characteristics used, the lowest correlation is between ε and ASY. The high correlation of ASY with the geoeffective characteristics of interplanetary medium (B_sV and F) means a fairly close relationship of ASY to the AE' indices, i.e., to the large-scale ionospheric and, through them, the field-aligned currents inflowing to the ionosphere and outflowing from the latter to the magnetosphere in high latitudes.

The model (Pisarsky *et al.*, 1989) was used to calculate the DR_{mod} values characterizing the symmetric component of the ring-current field. In case of the given storm, the r.m.s. deviation of DR_{mod} from DR_{exp} is $\delta = 26.3$ nT; the correlation coefficient $r = 0.95$. DR_{mod} repeats DR_{exp} in Figure 15 with two extrema.

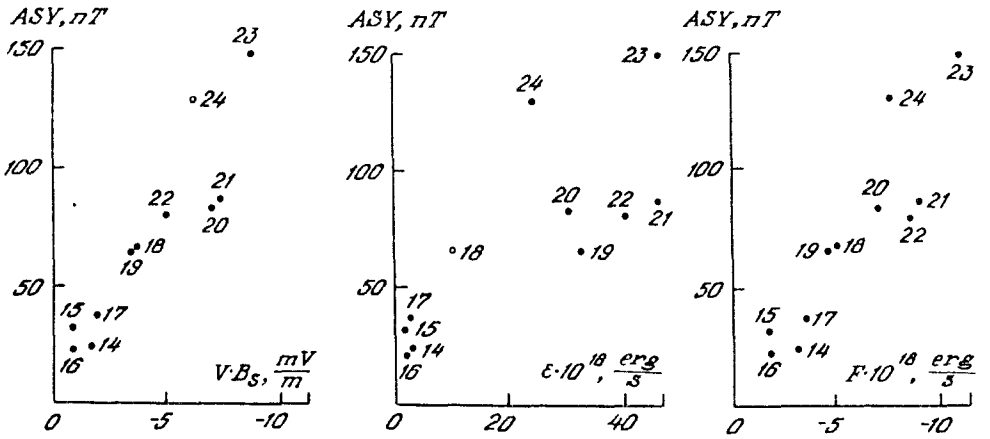

Fig. 29. The magnetic field asymmetry at the equator inferred from the hourly values during the magnetic storm main phase relevant to different geoeffective characteristics of solar wind. The solar wind parameters are 1 hour ahead of ASY. The numerals are UT hours.

The ground-based magnetic field variations at particular observatories must be modelled making allowance for both symmetric and asymmetric parts (Sun *et al.*, 1984) of the field. The magnetic effects of the high-latitude three-dimensional current system including both field-aligned and ionospheric currents and producing the field asymmetry in the subauroral and middle latitudes were calculated in terms of the model designed at IZMIRAN (Levitin *et al.*, 1984), but modified for a magnetic storm interval. The Levitin *et al.* (1984) model uses the prescribed values of the IMF B_z and B_y components to find the intensities of the transversal, $j_\perp$, and field-aligned, $j_\parallel$, currents throughout the high-latitude region $\phi \geq 60°$. Having known the values of the currents $j_\perp$ and $j_\parallel$, one can calculate the magnetic disturbance $\delta H(X, Y, Z)$ at a given point of the space on the basis of the Biot–Savart law. This method was suggested by Kisabeth (1979) and, as applied to our problem, was described by Dremukhina (1986).

The Levitin *et al.* (1984) model for the conditions of a magnetic storm was modified as follows: the field-aligned current system was shifted equatorwards by the value of the shift of the western electrojet center at an appropriate UT hour (see Figure 16). The threshold value $B_z = -10$ nT (the saturation effect) was used in the calculations at the hours when the southward B_s component of the IMF exceeded 10 nT.

Figure 30 presents the observed and $\delta H = D_{st}^{\text{mod}} + DP$ model-calculated magnetic disturbances at observatories Lvow ($\phi = 46°$) and Victoria ($\phi = 53.9°$) during the storm of March 23–24, 1969. The model calculations reflect sufficiently well the structural features of the actual geomagnetic disturbance. The correlation coefficients r and the variance δ of the observed and model-calculated δH values are $r = 0.91$, $\delta = 65$ nT at Victoria and $r = 0.93$, $\delta = 24.3$ nT at Lvow. If the magnetic effects of the field-aligned and ionospheric currents are disregarded, the respective values are $r = 0.55$, $\delta = 103$ nT at Victoria and $r = 0.9$, $\delta = 29.6$ nT at Lvow. Thus, the allowance for the magnetic effects of field-aligned currents and auroral electrojets at the subauroral and middle-

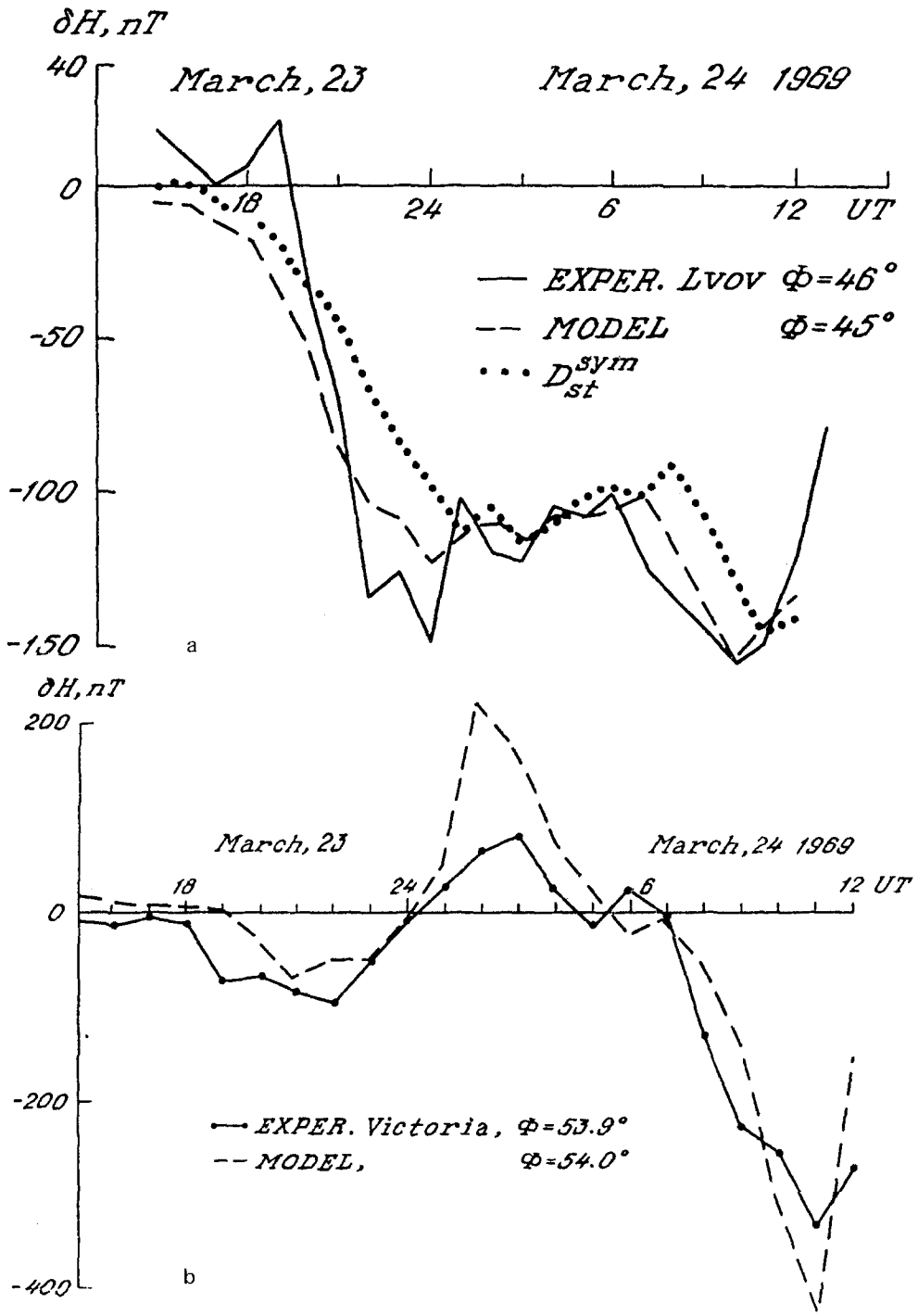

Fig. 30a–b. The observed and model-calculated (Levitin *et al.*, 1984; Dremuhina, 1986; Pisarsky *et al.*, 1989) geomagnetic field variations in the direction of geomagnetic pole at geomagnetic latitudes $\phi = 45°$ (Lwov, $\phi = 46°$) and $\phi = 54°$ (Victoria, $\phi = 53.9°$).

latitude observatories improves substantially the convergence of the model-calculated and experimental values of the magnetic variations fields. Some of the observatories, however, exhibit noticeable amplitude differences in the modelled and observed H values which reach up to 30% of the magnetic disturbance amplitude at individual UT hours. This fact is indicative of the effect of pulsed magnetic field disturbances relevant to substorms on the field variations which are disregarded in the model calculations. However, despite the amplitude disagreements at individual UT horus, the model describes sufficiently well the large-scale space-time structure of the storm-time geomagnetic variation field. This circumstance may indicate again that the pulsed plasma injection to the magnetosphere from the magnetospheric tail makes but an additional, rather than basic, contribution to the magnetic field variations. The field variations in low and middle latitudes are defined by the large-scale current systems controlled by the solar wind parameters and by the IMF components.

6.7. Ring current and the IMF B_y component

Kovalevsky *et al.* (1986) noted the occurrence of the magnetic substorms during which the D_{st} values and the IMF B_y component vary in the same manner, with $|D_{st}|$ increasing at IMF $B_y > 0$ and decreasing at IMF $B_y < 0$. The geoeffective parameters $B_s v$, ε, and F are defined by the B_z component of the IMF. Let us check the IMF B_y effect on the ring-current evolution using the March 23–24, 1969 storm as an example. Figure 31 presents the hourly values of $E_y = B_s v$, $E_z = B_y v$, and DR of the given storm. After 12:00 UT on March 24 the N–S component of the IMF turns northwards ($B_z > 0$) and $E_y = 0$ because the electric field becomes ineffective in the DR generation. From the figure it follows that E_y is closely related to DR, namely, high values of $|E_y|$ are accompanied by an increase of $|DR|$, while the $|DR|$ value decreases with decreasing $|E_y|$.

The storm recovery phase began after the IMF B_z had turned stably northwards. During the storm, DR did not exhibit any relation to the E_z component of electric field. The $|DR|$ maximum at 01:00–02:00 UT on March 24 was observed in 1 hour after the $|E_z|$ minimum, whereas the $|DR|$ minimum at 04:00–05:00 UT coincided with the $|E_z|$ maximum, while the decrease in $|E_z|$ was accompanied by the increase in $|DR|$ value. The E_z sign reversal coincided with a progressing enhancement of $|DR|$. The first $|DR|$ maximum occurred during $E_z < 0$ interval, and the second $|DR|$ maximum during $E_z > 0$ interval. Thus, the DR evolution during that particular storm was controlled by E_y (hence, by the IMF B_z), rather than by E_z (i.e., by the IMF B_y) component of electric field in solar wind. Another characteristic feature, namely, the $|DR|$ enhancement during the storm main phase occurred at $B_y < 0$, in contrast to the storm examined by Kovalevsky *et al.* (1986).

Kovalevsky *et al.* (1986) presented a list of seven magnetic storms when the correlation coefficients r between D_{st} and the IMF B_y component (or $E_z = -B_y v$) were $\gtrsim 0.5$. During the first tree storms, $r(D_{st}, B_y) \gg r(D_{st}, B_z)$; during the remaining storms, the difference was small. The ring-current evolution during the seven storms is assumed to be controlled, to a great extent, by the azimuthal component of the IMF. Table IV

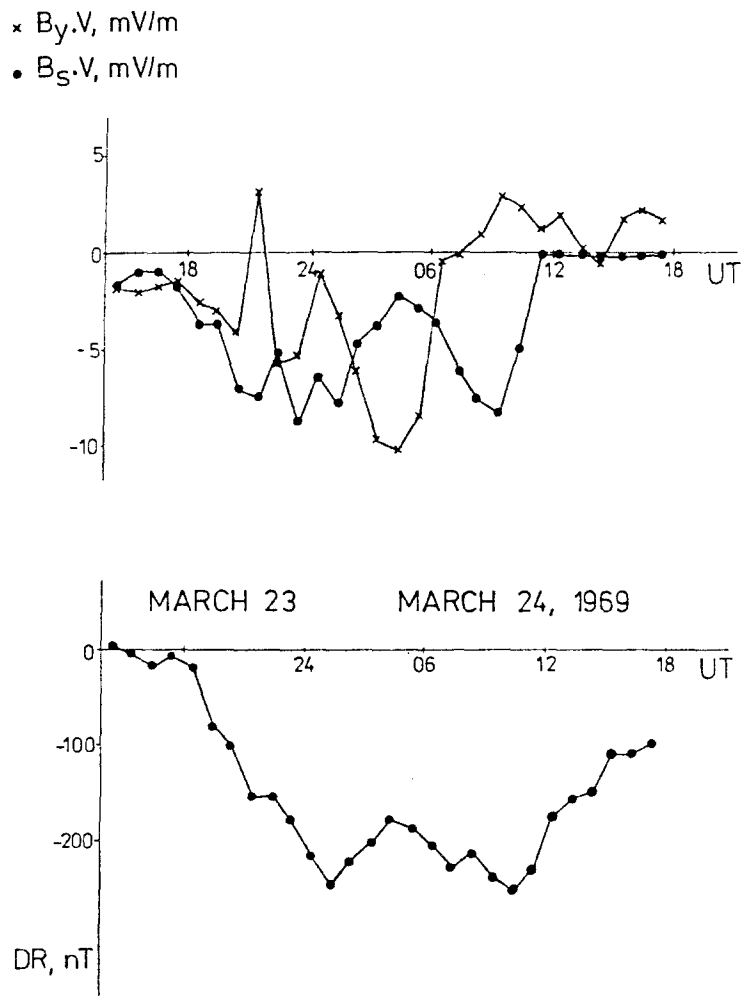

Fig. 31. The parameters of the interplanetary medium and of the ring-current field during an intensive magnetic storm. The hourly values of the E_z and E_y components of the solar wind electric field (*above*). The DR intensity (*below*).

presents the dates of all seven storms, the correlation coefficients $r(D_{st}, B_z)$ and $r(D_{st}, B_y)$ according to (Kovalevsky *et al.*, 1986), and the correlation coefficients of the observed DR_{exp} values and of the DR_{mod} values calculated for the storms in terms of the model (Pisarsky *et al.*, 1989).

The tabulated δ values characterize the standard deviation of DR_{mod} from DR_{exp} related to one-hour interval. From the table it follows that:

(1) the high values of $r(DR_{\text{mod}}, DR_{\text{exp}})$ indicate that the ring-current evolution is controlled by the north–south component of the IMF;

(2) the control is also effective during the storms when $r(D_{st}, B_z) \ll r(D_{st}, B_y)$ and $r(D_{st}, B_z)$ differs but slightly from zero;

(3) individual storms with very similar patterns of the D_{st} and B_y variations can

TABLE IV

Correlation coefficients $r(D_{st}, B_z)$ and $r(D_{st}, B_y)$ according to Kovalevsky *et al.* (1986) and $r(DR_{exp}, DR_{mod})$

No.	Interval	$r(D_{st}, B_z)$	$r(D_{st}, B_y)$	$r(DR_{mod}, DR_{exp})$	δ, nT
1	March 31–Apr. 2, 1973	0.37	0.91	0.97	12.8
2	Jan. 13–14, 1967	0.01	0.87	0.98	20.3
3	Apr. 5–7, 1968	0.03	0.60	0.88	14.7
4	Oct. 31–Nov. 3, 1972	0.25	0.45	–	–
5	Oct. 13–16, 1974	0.64	0.47	–	–
6	Feb. 16–17, 1967	–	–	0.96	15.3
7	March 6–7, 1972	–	–	0.94	14.3

Note

The values of $r(D_{st}, B_z)$ and $r(D_{st}, B_y)$ for storms Nos. 6 and 7 were not presented by Kovalevsky *et al.* (1986).

always be selected among a great number of storms. However, even during the selected storms is the ring-current evolution controlled by the B_z, rather than the B_y, component of the IMF.

7. Ion Energy in Ring Current Relevant to Ground-Based Magnetic Disturbances

The magnetic disturbance intensity on the Earth's surface was noted above to relate directly to the integral ion energy in ring current. Therefore, as early as the initial ion measurements in the inner magnetosphere at energies of dozens of keV made it possible to juxtapose the total charged-particle energy with the respective magnetic effects on the Earth's surface (Hoffman and Bracken, 1965, 1967; Frank, 1967a, b). The measurements of that type were continued by Kovtyuh *et al.* (1981) who estimated the magnetic effect of quiet ring current, $DR_q = -8.1 \pm 2.2$ nT. Feldstein and Porchkhidze (1983) used the values of the magnetic effects of quite ring currents inferred elsewhere from satellite measurements of charged particles and juxtaposed them with the magnetic effects obtained by ground-based observations of the geomagnetic field variations (the D_{st} index). The similar values of the magnetic field of quiet ring current obtained by the two methods indicate a nearly-zero value of $DR^0 + DCF^0 \sim 0$ nT. This means that the value of the H-component at low-latitude observatories during the quite intervals when the ring-current magnetic field (DR^0) is approximately compensated for by the fields of the currents on the magnetopause (DCF^0) is taken to be the reference value when calculating the D_{st}-index. The measurements of the total energy of the ring-current protons during magnetic storms demonstrated also a fairly good agreement between the expected and observed geomagnetic field variations (Frank, 1967a). The pioneer studies, however, measured the ion energies within a fairly narrow energy range and failed to yield information on the ion composition of the ring current. The measurements of such a type were carried out during magnetic storms in the framework of the AMPTE project (Gloeckler *et al.*, 1985; Hamilton *et al.*, 1988). The most complete data on the

ring-current energy were obtained during the magnetic storm which began on February 6, 1986, enhanced sharply late on February 8, and reached $D_{st} \sim -312$ nT at the first hour of February 9. The energy densities on the L-shells from 2 to 7 were found for the first time in all the basic ion components of ring current in the 1–310 keV e^{-1} range. The storm-time ring current was shown to consist of solar wind ions and of ionospheric-origin ions. The H^+ ions carry the major fraction of energy in the ring current almost throughout the storm, but the O^+ ions prevail near the maximum of the main phase. The situation near the maximum of the main phase of the given intensive storm differs from that observed usually during moderate storms when protons constitute the major fraction of the ring current. Hamilton *et al.* (1988) juxtaposed the total energy of ring-current ions (E) and the expected magnetic effects ΔB on the Earth's surface with the D_{st} variation observed on the respective satellite orbits. Table V presents

TABLE V

Ring-current ion energy content, observed, and predicted values of the magnetic field

Pass	Total E 10^{30} keV $L = 2$–7	Predicted ΔB, nT	Observed D_{st}, nT	Observed DR nT	$2/3DR$	Predicted Observed
1 in	3.67	−14.6	+0.7	–	–	–
1 out	3.33	−13.2	+2.7	–	–	–
2 in	3.98	−15.9	−7.2	–	–	–
2 out	3.59	−14.3	+1.2	–	–	–
3 in	8.68	−20	−83	−90	−60	0.33
3 out	22.1	−74	−88	−128	−86	0.8
4 in	12.4	−36	−115	−125	−84	0.4
4 out	12.4	−36	−131	−141	−94	0.3
5 in	47.6	−175	−257	−285	−190	0.86
5 out	41.5	−151	−244			
6 in	25.2	−86	−131	−147	−98	0.88
6 out	21.8	−73	−133	−133	−86	0.85
7 in	17.2	−54	−112	–	–	–
7 out	16.9	−53	−106	–	–	–
8 in	14.8	−45	−92	−83	−56	0.8
8 out	12.6	−36	−73	−76	−50	0.72

the values of E, ΔB, and D_{st} according to Hamilton *et al.* (1988). It is seen that the expected ΔB values are substantially below the D_{st}-index throughout, in practice, the entire storm. This means that the magnetic field decrease on the Earth's surface is associated but partly with the motion of energetic ions around the Earth, i.e., with the ring-current generation. Should this conclusion be correct, it would be indicative of a fundamental difficulty in explaining the reason for the ΔB intensity observed during the storm. Additional mechanisms would have been used for generating the field directed in opposite phase with the geomagnetic dipole field.

However, the conclusion that the ΔB and D_{st} values disagree during the intensive storm in February, 1986 proves to be incorrect if allowance is made for the fact that

the D_{st} field on the Earth's surface is composed of fractions of external and internal (induction) origins. The external fraction of the D_{st} field is about 2 times as intensive as the internal fraction. In view of this circumstance, Table V contains the DR and $\frac{2}{3}DR$ columns and the ratio of the predicted value of magnetic field to its observed allowing for the induced fraction. The values of DR from (7) and of $\frac{2}{3}DR$ were calculated using the data (King, 1989) on the solar wind plasma density and velocity during the storm of February. The allowance for only the external fraction of the DR field gives the ratio $DR_{\text{pred}}/\frac{2}{3}DR_{\text{exp}} \sim 0.85$ during the main phase maximum and in the initial stage of the recovery phase. During a later stage, the ratio decreases down to 0.7–0.8. The possible explanations of the given disagreement include the necessity of allowing, during the energy studies, for the contribution of the L-shells which are external to $L = 7$ and the necessity of allowing for ions with energies ≥ 310 keV e^{-1}. Even with these restrictions, however, from the measurements of the total ion energy for the given storm it follows that the energy near the main phase maximum on already L-shells between 2 and 7 is sufficient for the geomagnetic field DR variations observed on the Earth's surface to be explained. Therefore, we should not seek for any alternative energy sources or any alternative generation mechanisms of the magnetic disturbance which accounts for the decrease of the geomagnetic field horizontal component in low latitudes during magnetic storms.

Significant discrepancies in the values of DR_{pred} and $\frac{2}{3}DR_{\text{exp}}$ at the commencement of the main phase can be a consequence of the great D_{st} asymmetry (and consequently DR_{exp}) in this interval. In connection with the essential longitudinal asymmetry in the ion energy density distribution during the magnetic storm main phase, the comparison with $\frac{2}{3}DR_{\text{exp}}$ requires the ion energy density measurements made simultaneously by several satellites at different MLT.

The comparison between ΔB predicted and ΔB observed must be made allowing in (3) for the self-energy E_{RC} of the ring current (Olbert *et al.*, 1968). Hamilton *et al.* (1988) have estimated that such an allowance improves the agreement between E and D_{st} in maximum of the storm main phase but is insufficient in case of the recovery phase. Undoubtedly, the determination of ΔB from the relation (3) must allow for E_{RC} which, however, requires that the E_{RC} values should be estimated more accurately. The replacement of E by $E + \frac{1}{2}E_{RC}$ in (3) can probably yield an even better agreement between the observed and predicted DR values compared with the data of Table V.

The data of Hamilton *et al.* (1988) make it possible to estimate the magnetic effect of the quiet ring current more accurately than earlier, thereby estimating the reference level of the D_{st} variation field ($DR^0 + DCF^0$). Assuming, according to Hamilton *et al.* (1988) that $DR_q = -14$ nT, $DCF_q = 18$ nT, and $D_{st} = 1$ nT during the prestorm quiet interval of 08:00–10:00 UT on February 6 (the fields of external sources without the fraction induced by the Earth are presented), we get the reference level $DR^0 + DCF^0 = 3$ nT. This value agrees, within the errors in determining DR_q, DCF_q, and D_{st}, with the result $DR^0 + DCF^0 = 0$ obtained by Feldstein and Porchkhidze (1983). If the DCF^0 value is assumed to be 12–18 nT, the magnetic field of quiet ring current on the Earth's surface is -12–18 nT.

8. Conclusion

Magnetic storms belong to the natural phenomena which have been known for centuries. However, the factors defining the magnetic storm generation in the Earth's magnetosphere were established safely only during the recent years. The formation of the ring current in the inner magnetosphere proved to be the main consequence of the magnetic storms. The models proposed by now make it possible to predict the intensity of the magnetic field and the character of its variations relevant to the ring current. The major fraction of the variations are associated directly with the interplanetary medium parameters because the function of energy injection into the ring curent is controlled by both the solar wind electric field intensity (the main term under the IMF southward component) and the solar wind velocity (the additional term describing the injection as relevant to the high-velocity flux flow around the magnetosphere). The injection into the ring current is permanent and occurs under any IMF orientation, thereby maintaining the ring current even during magnetically-quiet intervals.

The estimates based on the total energy of the ions which constitute the ring current yield the values $DR^0 + DCF^0 \sim 0 \pm 3$ nT for the quiet intervals adopted to be the D_{st} variation reference level. This means that the ring-current field intensity on the Earth's surface from the outer source is $-9 \sim -15$ nT during very quiet periods.

The ring-current magnetic field variation controlled directly by the geoeffective characteristics of interplanetary medium and tracing the changes of the characteristics constitute the driven fraction of the field variations. This main fraction of the field variations is superposed in low and middle latitudes with the shorter-term *DR* variations produced by the injections into the inner magnetosphere during magnetospheric substorms. The injections are associated with the explosion-like processes in the magnetospheric tail and constitute the unloading fraction of the *DR* field variations.

The direct measurements of ion energy in the inner magnetosphere, which are, however, still restricted, have shown that the total energy is sufficient for the low-latitude magnetic field observed during the magnetic storm main phase to be generated. The reasons for the occurrence of a diversity of magnetic storms relevant to their ionic and energy compositions are still to be found. The available data on the differences in the *DR* behaviour during weak and strong magnetic storms reflect more profound features of the ring current. The pending accumulation of the data of direct measurements in the ring current is expected to permit the features of the ionic and energy compositions of the ring-current plasma to be related to certain situations in interplanetary medium. This concerns the solar wind plasma supplied to the ring-current and the ionospheric plasma accelerated and trapped in the inner magnetosphere. The aim of the further studies of the ring current must also be to find the proportion between the solar and ionospheric plasmas in the ring current and to determine the factors controlling the proportion.

The small values of τ during the magnetic storm main phase, which are much lower than the τ value inferred from the theoretical concepts concerning the charge exchange with the geocoronal hydrogen, must be explained in terms of other mechanism for the ring-current ion loss. Such mechanisms may include the interactions of the ring-current

ions with the waves generated in the inner magnetosphere near the plasmapause (Cornwall *et al.*, 1970; Solomon and Picon, 1981). We are of the opinion that this problem has not been solved yet and must be solved by a more thorough analysis of the processes occurring in the ring current.

Bespalov *et al.* (1989) have examined some problems relevant to diagnozing the asymmetric ring current; in particular, they studied the ~ 100 keV proton motions as controlled by 0.1–10 Hz hydromagnetic waves as a function of a given L-shell and of the background plasma density. The ion-cyclotron instability in the ring-current region was examined taking account of the effects of azimuthal magnetic drift of energetic ions. The effectiveness condition for the ion-cyclotron coupling is $v > v_A$ (v_A is the Alfvén velocity) and is satisfied only in the region with a sufficiently high plasma density. The relevant estimations have shown that, in case of the 100 keV protons on $L \sim 4$–5, the cyclotron instability is likely to occur inside the plasmapause. The dusk-side plasmaspheric buldge is the most probable cyclotron relaxation region of the ring-current protons. In this case the time scale of the decay of the ring current (of its asymmetric fraction) is defined by the time-scales of magnetic drift and of injection which are of the order of one or few hours. The given examination seems still to be much simplified, but has yielded correct estimates of the parameter τ in the main phase of a storm during injection periods.

Senatorov (1989) has examined the scattering of ring-current particles by hydromagnetic waves in the range of the P_c 1, 2, 3 geomagnetic pulsations. The calculated H^+ and O^+ ion lifetimes vary from fractions of an hour to dozens of hours. This means that the parameter τ of ring-current decay during a magnetic storm must be estimated making allowance for the ion-MHD wave interactions.

The equatorward motions of electrojets in the course of ring-current evolution make it necessary that the data from the subauroral observatories should be used to determine the *AE*, *AU*, and *AL* indices of geomagnetic activity. The commonly-adopted standard indices have been much underestimated for the magnetic storm intervals, so the scientific conclusions drawn from them have to be very carefully treated. The necessity seems to have become imminent that either the indices of auroral electrojets for the storm intervals should be determined anew using the data from the network of subauroral observatories or that they should be calculated on the basis of the close relationship of the auroral indices to the geoeffective characteristics of interplanetary medium.

Determining the function of injection into the ring current has make it possible to estimate the energy fraction supplied to the ring-current relative to ε, i.e., to the solar wind energy fraction supplied into the magnetosphere. The relevant estimates have shown that $F \sim 0.15\varepsilon$ which is much below the estimates adopted elsewhere (Gonzalez *et al.*, 1989a).

Acknowledgements

The author is indebted to his colleagues B. A. Belov, L. A. Dremuhina, A. Grafe, A. E. Levitin, V. Yu. Pisarsky, A. Prigantseva, N. M. Rudneva, and P. V. Sumaruk who took an active part in developing the ring-current model and in numerous discussions of the problem. The author acknowledge Dr J. Heppner and Dr K. Snyder for providing with the data on the solar wind plasma and IMF during the magnetic storm of March 23–24, 1969. The data are obtained by OGO-5 and Explorer 35 through NSSDC R and S.

References

Akasofu, S.-I.: 1968, *Polar and Magnetospheric Substorms*, D. Reidel Publ. Co., Dordrecht, Holland.
Akasofu, S.-I.: 1977, *Physics of Magnetospheric Substorms*, D. Reidel Publ. Co., Dordrecht, Holland.
Akasofu, S.-I.: 1981a, *Planetary Space Sci.* **29**, 1151.
Akasofu, S.-I.: 1981b, *Space Sci. Rev.* **28**, 121.
Akasofu, S.-I.: 1981c, *J. Geophys. Res.* **86**, 4820.
Akasofu, S.-I.: 1986, *Planetary Space. Sci.* **34**, 563.
Akasofu, S.-I. and Chapman, S.: 1972, *Solar-Terrestrial Physics*, Clarendon Press, Oxford.
Akasofu, S.-I. and Meng, C.-I.: 1969, *J. Geophys. Res.* **74**, 293.
Akasofu, S.-I. and Yoshida, S.: 1966, *J. Geophys. Res.* **71**, 231.
Akasofu, S.-I., Ahn, B. H., Kamide, Y., and Allen, J. H.: 1983, *J. Geophys. Res.* **88**, 5769.
Akasofu, S.-I., Chapman, S., and Venkatesan, D.: 1963, *J. Geophys. Res.* **68**, 3345.
Allen, J. H., Abston, C. C., and Morris, L. D.: 1974, *Auroral Electrojet Magnetic Activity Indices AE (11) for 1969*, WDSA, Report AGU-31.
Axford, W. I.: 1967, *Space Sci. Rev.* **41**, 149.
Baker, D. N., Zwickl, R. D., Bame, S. J., Hones, E. W., Tsurutani, B. T., Smith, E. J., and Akasofu, S.-I.: 1983, *J. Geophys. Res.* **88**, 6230.
Bargatze, L. F., McPherron, R. L., and Baker, D. N.: 1986, in Y. Kamide and J. A. Slavin (eds.), *Solar Wind-Magnetosphere Coupling*, Terrapublication, Tokyo, p. 101.
Bespalov, P. A., Demekhov, A. G., Trakhtengerts, V. Yu., and Grafe, A.: 1989, *Fifth Symposium KAPG on Solar-Terrestrial Physics*, Samarkand, October, 1989, Abstracts, p. 107.
Bobrov, M. S.: 1977, *Astron. Mag.* **54**, 1335.
Bobrov, M. S.: 1981, *Geomagnetizm i Aeronomiya* **21**, 1048.
Burton, R. K., McPherron, R. L., and Russell, C. T.: 1975, *J. Geophys. Res.* **80**, 4204.
Chapman, S.: 1962, *J. Phys. Soc. Japan* **17**, Suppl. A-1, p. 6.
Chistoserdov, B. M.: 1983, *Geomagnetizm i Aeronomiya* **23**, 685.
Cladis, J. B. and Francis, W. E.: 1985, *Adfv. Space Res.* **5**, 415.
Clauer, C. R. and McPherron, R. L.: 1980, *J. Geophys. Res.* **85**, 6747.
Cornwall, J. M., Coroniti, F. V., and Thorne, R. M.: 1970, *J. Geophys. Res.* **75**, 4699.
Dremuhina, L. A.: 1986, in A. E. Levitin (ed.), *Solar Wind and Near-Earth Processes*, Nauka, Moscow, p. 121.
Fejer, B. G., Gonzalez, C. A., Farley, D. T., Kelley, M. C., and Woodman, R. F.: 1979, *J. Geophys. Res.* **84**, 5797.
Feldstein, Ya. I.: 1976, *Space Sci. Rev.* **18**, 777.
Feldstein, Ya. I. and Porchkhidze, Ts. D.: 1983, *Bull. Acad. Sci. Georgian SSR* **112**, 301.
Feldstein, Ya. I., Goncharova, E. E., Shashunkina, V. M., and Yudovich, L. A.: 1984, *Investigations of F Region and Outer Ionosphere*, IZMIRAN, Moscow, p. 318.
Feldstein, Ya. I., Pavlovich, L. K., and Puolokainen, T. P.: 1967, *Geomagnetizm i Aeronomiya* **7**, 364.
Feldstein, Ya. I., Pisarsky, V. Yu., Rudneva, N. M., and Grafe, A.: 1984, *Planetary Space Sci.* **32**, 975.
Frank, L. A.: 1967a, *J. Geophys. Res.* **72**, 1905.
Frank, L. A.: 1967b, *J. Geophys. Res.* **72**, 3371.
Friis-Christensen, E. and Wilhjelm, J.: 1975, *J. Geophys. Res.* **80**, 1248.
Friis-Christensen, E., Lassen, K., Wilhjelm, J., Wilcox, J. M., Gonzalez, W., and Colburn, D. C.: 1972, *J. Geophys. Res.* **77**, 3371.

Fukushima, N.: 1969, *Rep. Ionosph. Space Res. Japan* **23**, 219.
Ghielmetti, A. G., Johnson, R. G., Sharp, R. D., and Shelley, E. G.: 1978, *Geophys. Res. Letters* **5**, 59.
Gloeckler, G., Wilken, B., Studemann, W., Ipavich, F. M., Hovestadt, D., Hamilton, D. C., and Kremser, G.: 1985, *Geophys. Res. Letters* **12**, 325.
Gonzalez, W. D.: 1986, in Y. Kamide and J. A. Slavin (eds.), *Solar Wind-Magnetosphere Coupling*, Terra, Tokyo, Japan, p. 315.
Gonzalez, C. A., Kelley, M. C., Fejer, B. G., Vickrey, J. F., and Woodman, R. F.: 1979, *J. Geophys. Res.* **84**, 5803.
Gonzalez, C. A., Kelley, M. C., Behnke, R. A., Vickrey, J. F., Wand, R., and Holt, J.: 1983, *J. Geophys. Res.* **88**, 9135.
Gonzalez, W. D., Tsurutani, B. T., Gonzalez, A. L. C., Smith, E. J., Tang, F., and Akasofu, S.-I.: 1989a, *J. Geophys. Res.* **94**, 8835.
Gonzalez, W. D., Gonzalez, A. L. C., and Tsurutani, B. T.: 1989b, *J. Geophys. Res.* **94**, 1547.
Grafe, A.: 1988, *Planetary Space Sci.* **36**, 765.
Grafe, A. and Best, A.: 1966, *Pure Applied Geophys.* **64**, 59.
Hamilton, D. C., Gloeckler, G., Ipavich, F. M., Studemann, W., Wilken, B., and Kremser, G.: 1988, *J. Geophys. Res.* **93**, 14343.
Harel, M., Wolf, R. A., Spiro, R. W., Reiff, P. H., Chen, C.-K., Burke, W. J., Rich, F. J., and Smiddy, M.: 1981, *J. Geophys. Res.* **86**, 2242.
Hoffman, R. A. and Bracken, P. A.: 1965, *J. Geophys. Res.* **70**, 3541.
Hoffman, R. A. and Bracken, P. A.: 1967, *J. Geophys. Res.* **72**, 6039.
Ivanov, K. G. and Mikerina, N. V.: 1970, *Geomagnetizm i Aeronomiya* **10**, 1075.
Iyemori, T., Maeda, H., and Kamei, T.: 1979, *J. Geomag. Geoelectric* **31**, 1.
Kamide, Y.: 1974, *J. Geophys. Res.* **79**, 49.
Kamide, Y.: 1979a, in S.-I. Akasofu (ed.), *Dynamics of the Magnetosphere*, D. Reidel Publ. Co., Dordrecht, Holland, p. 425.
Kamide, Y.: 1979b, 'Relationship between Substorms and Storms', preprint KSU/ICS 79–03.
Kamide, Y. and Fukushima, N.: 1971, *Rep. Ionosphere Space Res. Japan* **25**, 125.
Kawasaki, K., Akasofu, S.-I., Yasuhara, F., and Meng, C.-I.: 1971, *J. Geophys. Res.* **76**, 6781.
Khorosheva, O. V.: 1986, *Geomagnetizm i Aeronomiya* **26**, 447.
Khorosheva, O. V.: 1987, *Geomagnetizm i Aeronomiya* **27**, 804.
King, J.: 1977, *Interplanetary Medium Data Book, Appendix*, NSSDC-A-R-S-04a, GSFC.
Kisabeth, J. L.: 1979, in W. P. Olson (ed.), *Geophys. Monograph*, AGU, Washington, Vol. 21, p. 473.
Kovalevsky, I. V., Levitin (ed.), *Geomagnetic Variations and Currents in the Earth's Magnetosphere*, IZMIRAN, Moscow, p. 5.
Kovtyuh, A. S., Sizova, L. Z., and Shevnin, A. D.: 1981, *Geomagnetizm i Aeronomiya* **21**, 755.
Levitin, A. E., Feldstein, Y. I., Afonina, R. G. *et al.*: 1984, *Model of Large-Scale Electric Fields and Currents in High-Latitude Ionosphere*, Parts 1–6, Hydrometeorological Service, Moscow.
Liu, Z. X., Lee, L. C., Wei, C. Q., and Akasofu, S.-I.: 1988, *J. Geophys. Res.* **93**, 7366.
Loginov, G. A. and Starkov, G. V.: 1972, in S. I. Isaev (ed.), *Geophysical Investigations in the Auroral Zone*, Apatity, p. 87.
Lyatsky, V. B.: 1978, *Current System of Magnetosphere-Ionosphere Disturbances*, Publ. House Nauka, Leningrad.
Lyons, L. R. and Williams, D. J.: 1980, *J. Geophys. Res.* **85**, 523.
Mauk, B. H. and Meng, C.-I.: 1987, *Phys. Scripta* **18**, 128.
Maynard, N. C., Aggson, T. L., Herrero, F. A., and Liebrecht, M. C.: 1988, *J. Geophys. Res.* **93**, 4021.
McPherron, R. L. and Manka, R. H.: 1985, *J. Geophys. Res.* **90**, 1175.
McPherron, R. L., Fay, R. A., Garrity, C. R., Bargatze, L. F., Clauer, C. R., Baker, D. N., and Searls, C.: 1984, *Achievements of the IMS*, ESA, p. 161.
Meng, C.-I.: 1983, *J. Geophys. Res.* **88**, 137.
Murayama, T.: 1982, *Rev. Geophys. Space Phys.* **20**, 623.
Murayama, T.: 1986a, in Y. Kamide and J. Slavin (ed.), *Solar Wind-Magnetosphere Coupling*, Terrapublication, Tokyo, p. 119.
Murayama, T.: 1986b, private communication.
Nishida, A.: 1968a, *J. Geophys. Res.* **73**, 1795.

Nishida, A.: 1968b, *J. Geophys. Res.* **73**, 5549.
Nishida, A.: 1971, *Planetary Space Sci.* **19**, 205.
Nishida, A., Iwasaki, N., and Nagata, T.: 1966, *Ann. Geophys.* **22**, 478.
Obayashi, T. and Jacobs, J. A.: 1957, *J. Geophys. Res.* **62**, 589.
Ochabova, P.: 1989, *Studia Geophys. Geod.* **33**, 362.
Olbert, S., Siscoe, G. L., and Vasyliunas, V. M.: 1968, *J. Geophys. Res.* **73**, 1115.
Onwumechili, A., Kawasaki, K., and Akasofu, S.-I.: 1973, *Planetary Space Sci.* **21**, 1.
Patel, V. L.: 1978, *J. Geophys. Res.* **83**, 2137.
Perreault, P. and Akasofu, S.-I.: 1978, *Geophys. J. Roy. Astron. Soc.* **54**, 547.
Pisarsky, V. Yu., Rudneva, N. M., Feldstein, Y. I., and Grafe, A.: 1986a, *Geomagnetizm i Aeronomiya* **26**, 454.
Pisarsky, V. Yu., Rudneva, N. M., Feldstein, Y. I., and Grafe, A.: 1986b, *Geomagnetizm i Aeronomiya* **26**, 461.
Pisarsky, V. Yu., Feldstein, Y. I., Rudneva, N. M., and Prigancova, A.: 1989, *Studia Geophys. Geod.* **33**, 61.
Porchkidze, Tc. D., Kiziria, L. V., Pisarsky, V. Yu., Vorfolomeeva, N. G., Rivin, Yu. R., and Feldstein, Y. I.: 1989, in A. E. Levitin (ed.), *Large-Scale Variations of Geomagnetic Field*, Academy of the Sciences USSR, Moscow, p. 51.
Pudovkin, M. I. and Semenov, V. S.: 1986, *Geomagnetizm i Aeronomiya* **26**, 1026.
Pudovkin, M. I., Grafe, A., Zaitseva, S. A., Sizova, L. Z., and Usmanov, A. V.: 1988, *Gerlands Beitr. Geophys.* **97**, 523.
Pudovkin, M. I., Zaitseva, S. A., and Sizova, L. Z.: 1985a, *Planetary Space Sci.* **33**, 1097.
Pudovkin, M. I., Zaitseva, S. A., Sizova, L. Z., and Orlova, N. M.: 1985b, *Geomagnetizm i Aeronomiya* **25**, 812.
Rangarajan, G. K.: 1984, *Proc. Indian Acad. Sci. (Earth Planetary Sci.)* **93**, 343.
Rastogi, R. G.: 1977, *Nature* **268**, 422.
Rastogi, R. G. and Chendra, H.: 1974, *J. Atmospheric Terrest. Phys.* **36**, 377.
Rastogi, R. G. and Patel, V. L.: 1975, *Proc. Indian Acad. Sci.* **A82**, 121.
Reddy, C. A., Devasia, C. V., and Somayajulu, V. V.: 1980, *Low Latitude Aeron. Processed, Proc. Symp.*, Oxford, p. 39.
Reddy, C. A., Somayajulu, V. V., and Devasia, C. V.: 1979, *J. Atmospheric Terrest. Phys.* **41**, 189.
Reddy, C. A., Somayajulu, V. V., and Viswanathan, K. S.: 1981, *J. Atmospheric Terrest. Phys.* **43**, 817.
Reiff, P. H., Collin, H. L., Craven, J. D., Burch, J. H., Winningham, J. D., Shelley, E. C., Frank, L. A., and Friedman, M. A.: 1988, *J. Geophys. Res.* **93**, 7441.
Rezhenov, B. V., Vorobjev, V. G., and Feldstein, Y. I.: 1979, *Planetary Space Sci.* **27**, 699.
Roelof, E. C. and Williams, D. J.: 1988, *JHAPL, Technical Digest*, Vol. 9, No. 2, p. 144.
Roelof, E. C., Mitchell, D. G., and Williams, D. J.: 1985, *J. Geophys. Res.* **90**, 10991.
Russell, C. T.: 1971, *Cosmic Electrodynamics* **2**, 184.
Russell, C. T., PcPherron, R. L., and Burton, R. K.: 1974, *J. Geophys. Res.* **79**, 1105.
Schadrina, L. P. and Plotnikov, I. Ya.: 1988, *Abstract of International Symposium Polar Geomagnetic Phenomena*, May 25–31, Souzdal, USSR, Apatity.
Schielge, J. P. and Siscoe, G. L.: 1970, *J. Atmospheric Terrest. Phys.* **32**, 1819.
Sckopke, N.: 1966, *J. Geophys. Res.* **71**, 3125.
Senatorov, N. V.: 1989, SibIZMIR, Preprint Nos. 23–89, Irkutsk, p. 6.
Sharp, R. D., Johnson, R. G., and Shelley, E. G.: 1975a, *J. Geophys. Res.* **81**, 3283.
Sharp, R. D., Johnson, R. G., and Shelley, E. G.: 1975b, *J. Geophys. Res.* **81**, 3292.
Shelley, E. G., Klumpar, D. M., Peterson, W. K., Ghielmetti, A., Balsiger, H., Geiss, J., and Rosenbauer, H.: 1985, *Geophys. Res. Letters* **12**, 321.
Shevnin, A. D.: 1973a, *Geomagnetizm i Aeronomiya* **13**, 122.
Shevnin, A. D.: 1973b, *Geomagnetizm i Aeronomiya* **13**, 330.
Siscoe, G. and Crooker, N.: 1974, *Geophys. Res. Letters* **1**, 17.
Siscoe, G. L.: 1982, *J. Geophys. Res.* **87**, 5124.
Sizova, L. Z. and Shevnin, A. D.: 1979, *Geomagnetizm i Aeronomiya* **19**, 703.
Sizova, L. Z. and Shevnin, A. D.: 1983, in A. D. Shevnin (ed.), *Physics of Ionosphere and Magnetosphere*, IZMIRAN, Moscow, p. 84.
Sizova, L. Z. and Zaitseva, S. A.: 1984, in A. I. Laptuhov (ed.), *Geomagnetic Variations and Solar Wind*, IZMIRAN, Moscow, p. 108.

Smith, P. and Bewtra, N. K.: 1978, *Space Sci. Rev.* **22**, 301.
Smith, P. H., Bewtra, N. K., and Hoffman, R. A.: 1981, *J. Geophys. Res.* **86**, 3470.
Solar-Geophysical Data, No. 296, April 1969, U.S. Department of Commerce.
Solomon, J. and Picon, O.: 1981, *J. Geophys. Res.* **86**, 3335.
Somayajulu, V. V., Reddy, C. A., and Viswanathan, K. S.: 1985, *Geophys. Res. Letters* **12**, 473.
Somayajulu, V. V., Reddy, C. A., and Viswanathan, K. S.: 1987, *Geophys. Res. Letters* **14**, 876.
Starkov, G. V. and Feldstein, Y. I.: 1967, *Geomagnetizm i Aeronomiya* **7**, 71.
Stern, D. P.: 1984, *Space Sci. Rev.* **39**, 193.
Sumaruk, P. V. and Feldstein, Y. I.: 1973, *Cosmic Investigations* **11**, 155.
Sumaruk, P. V., Feldstein, Y. I., and Porchkidze, Tc. D.: 1980, *Phys. Solariterrest.* **12**, 70.
Sumaruk, P. V., Feldstein, Y. I., and Belov, B. A.: 1989, *Geomagnetizm i Aeronomiya* **29**, 110.
Sun, W., Ah, B.-H., Akasofu, S.-I., and Kamide, Y.: 1984, *J. Geophys. Res.* **89**, 10881.
Tinsley, B. A.: 1981, *J. Atmospheric Terrest. Phys.* **43**, 617.
Tinsley, B. A. and Akasofu, S.-I.: 1982, *Planetary Space Sci.* **30**, 733.
Troshichev, O. A., Pudovkin, M. I., Pegov, L. A., and Grafe, A.: 1974, *Gerlands Beit. Geophys.* **83**, 275.
Tverskaya, L. V. and Khorosheva, O. V.: 1983, *Geomagnetizm i Aeronomiya* **23**, 605.
Vasiliev, F. P.: 1980, *Numerical Methods of Extreme Problems Solutions*, Publ. House Nauka, Moscow.
Vasiliunas, V. M.: 1987, *Geophys. Res. Letters* **14**, 1183.
Vasiliunas, V. M., Kan, J. R., Siscoe, G. L., and Akasofu, S.-I.: 1982, *Planetary Space Sci.* **30**, 359.
Woodman, R. F. and Hagfors, T.: 1969, *J. Geophys. Res.* **74**, 1205.
Zwickl, R. D., Bargatze, L. F., Baker, D. N., Clauer, C. R., and McPherron, R. L.: 1987, in A. T. Y. Lui (ed.), *Magnetotail Physics*, Johns Hopkins University Press, Baltimore, p. 155.